

UNCLASSIFIED

AD NUMBER

ADB088771

NEW LIMITATION CHANGE

TO

**Approved for public release, distribution
unlimited**

FROM

**Distribution authorized to U.S. Gov't.
agencies and their contractors; Critical
Technology; MAR 1984. Other requests shall
be referred to Air Force Rocket Propulsion
Lab, Attn: TSTR[STINFO], Edwards AFB, CA
93523.**

AUTHORITY

**Air Force Rocket Propulsion Lab ltr dtd 6
Dec 1985**

THIS PAGE IS UNCLASSIFIED



AFRPL TR-83-067

AD:

Final Report
for the period
3 March 1983 to
21 September 1983

Alternate Propulsion Energy Sources

December 1983

Author:
Dr. R. L. Forward

Forward Unlimited
34 Carriage Square
Oxnard, California 93030

AD-B088 771

FILE COPY
MFC

Subject to Export Control Laws

This report contains a summary of the non-proprietary technical results of the referenced contract. Additional material can be found in the Final Program Review Data Package obtainable through AFRPL/LKDH, Edwards AFB, CA 93523. *US Government agencies and their contractors*
~~Report distribution limited to DOD and DOD contractors only, Critical Technology, 17 Nov 1983 — Mar 8~~
Other requests for this document must be referred to AFRPL/TSTR (Stop 24), Edwards AFB, California 93523

prepared for the: **Air Force
Rocket Propulsion
Laboratory**

Air Force Space Technology Center
Space Division, Air Force Systems Command
Edwards Air Force Base,
California 93523

7 1985

84 12 28 199

NOTICE

When government drawings, specifications, or other data are used for any purpose other than in connection with a definitely government-related procurement operation, the United States Government incures no responsibility or obligation whatsoever. The fact that the government may have formulated or in any way supplied the said drawings, specifications, or other data, is not to be regarded by implication, or otherwise in any manner construed, as licensing the holder, or any other person or corporation; or as conveying any rights or permission to manufacture, use, or sell any potential invention that may in any way be related thereto.

FORWARD

The work described herein was performed for the Air Force Rocket Propulsion Laboratory under Contract Number F04611-83-0013. The project manager was Mr Franklin B. Mead, Jr. The program was carried out by Dr Robert L. Forward. This report has been reviewed and is released in accordance with the distribution statement on the cover and on the DD Form 1473.

Franklin B. Mead, Jr.
FRANKLIN B. MEAD, Jr.
Project Manager

James B. Ellledge
JAMES B. ELLEDGE, Capt, USAF
Chief, Advanced Propulsion Branch

FOR THE DIRECTOR

Clark W. Hawk
CLARK W. HAWK
Chief, Liquid Rocket Division

REPORT DOCUMENTATION PAGE		READ INSTRUCTIONS BEFORE COMPLETING FORM
1 REPORT NUMBER AFRPL-TR-83-067	2 GOVT ACCESSION NO AD-B088771	3 RECIPIENT'S CATALOG NUMBER
4 TITLE (and Subtitle) ALTERNATE PROPULSION ENERGY SOURCES		5 TYPE OF REPORT & PERIOD COVERED Final Technical Report 3 Mar 83 - 21 Sep 83
7 AUTHOR(s) Dr. Robert L. Forward	6 PERFORMING ORG REPORT NUMBER F04611-83-C-0013	
9 PERFORMING ORGANIZATION NAME AND ADDRESS Forward Unlimited 34 Carriage Square Oxnard, California 93030 USA	10 PROGRAM ELEMENT, PROJECT, TASK AREA & WORK UNIT NUMBERS	
11 CONTROLLING OFFICE NAME AND ADDRESS Air Force Rocket Propulsion Laboratory LKDH Edwards AFB, CA 93523	12 REPORT DATE Dec 1983	13 NUMBER OF PAGES 134
14 MONITORING AGENCY NAME & ADDRESS (if different from Controlling Office)	15. SECURITY CLASS. (of this report) Unclassified	
	16. DECLASSIFICATION/DOWNGRADING SCHEDULE	
16. DISTRIBUTION STATEMENT (of this Report) Report Distribution Limited to DoD and DoD Contractors Only , Critical Technology 17 Nov 1983 ^{Mar 84} . Other requests shall be referred to: AFRPL/TSTR(Stinfo), Stop 24, Edwards AFB, CA 93523		
17. DISTRIBUTION STATEMENT (of the abstract entered in Block 20, if different from Report) Abstract Approved for Public Release		
18. SUPPLEMENTARY NOTES Interim Report: AFRPL-TR-33-039 (AD: A131 939) June 1983		
19. KEY WORDS (Continue on reverse side if necessary and identify by block number) Propulsion energy, metastable helium, free-radical hydrogen, solar pumped plasmas, antiproton annihilation, ionospheric lasers, solar sails, perforated sails, microwave sails, quantum fluctuations, antimatter rockets		
20. ABSTRACT (Continue on reverse side if necessary and identify by block number) 'This report contains a summary of the non-proprietary technical results of the referenced contract. Additional material consisting of proprietary technical information, budgetary recommendations, and sensitive program evaluations and recommendations, can be found in the Final Program Review Data Package obtainable through AFRPL/LKDH, Edwards AFB, CA 93523. The objective of the contract was to survey the entire field of		

advanced propulsion to uncover and carry out a technical assessment of any concept that showed promise of leading to a major advance in available energy sources for space power and propulsion in the next century. In general, any concept that might derive energy from the space environment was to be considered, as well as any unconventional methods of storing energy in a compact form that may have applicability to space power and propulsion. In Phase 1, 64 concepts were uncovered and preliminary technical assessments were carried out on 28 of the more promising concepts. For Phase 2, it was recommended that further studies be carried out on solid metastable helium, solar heated plasmas, perforated solar sails, and antiproton annihilation propulsion. Of these, the Air Force selected two concepts to receive the major portion of the Phase 2 effort, solar heated plasmas and antiproton annihilation. As time permitted, studies were to also continue on free radical hydrogen, quantum dynamic energy, and ionospheric lasing. At the conclusion of the technical effort it was determined that six concepts had the potential to provide a new alternate propulsion energy source and it was recommended that the Air Force sponsor further research in those areas. The recommended concepts were: Antiproton annihilation propulsion; where antiprotons would be manufactured by a large special-purpose particle accelerator, converted into antihydrogen ice, stored using electric and magnetic fields, then used to heat large amounts of hydrogen to provide thrust. Perforated solar sails; where holes smaller than a wavelength of sunlight are made in solar sails to decrease the mass to area ratio and the atmospheric drag without reducing reflectivity. Solar heated plasmas; where sunlight is used to heat and sustain an alkali metal plasma discharge which captures the solar energy and transfers it at high efficiency to a hydrogen working fluid. Lasing the ionosphere; where mirrors are used to extract laser energy from large volumes of the upper atmosphere. Solid metastable helium; where excited helium molecules are induced to form a stable solid by a combination of laser light and magnetic fields. Electromagnetic vacuum fluctuation energy; where electric fields are used to extract electrical energy from the attractive Casimir vacuum fluctuation force that is known to exist between any two conductors.

1	
2	
3	
4	
5	
6	
7	
8	
9	
10	
11	
12	
13	
14	
15	
16	
17	
18	
19	
20	
21	
22	
23	
24	
25	
26	
27	
28	
29	
30	
31	
32	
33	
34	
35	
36	
37	
38	
39	
40	
41	
42	
43	
44	
45	
46	
47	
48	
49	
50	
51	
52	
53	
54	
55	
56	
57	
58	
59	
60	
61	
62	
63	
64	
65	
66	
67	
68	
69	
70	
71	
72	
73	
74	
75	
76	
77	
78	
79	
80	
81	
82	
83	
84	
85	
86	
87	
88	
89	
90	
91	
92	
93	
94	
95	
96	
97	
98	
99	
100	
101	
102	
103	
104	
105	
106	
107	
108	
109	
110	
111	
112	
113	
114	
115	
116	
117	
118	
119	
120	
121	
122	
123	
124	
125	
126	
127	
128	
129	
130	
131	
132	
133	
134	
135	
136	
137	
138	
139	
140	
141	
142	
143	
144	
145	
146	
147	
148	
149	
150	
151	
152	
153	
154	
155	
156	
157	
158	
159	
160	
161	
162	
163	
164	
165	
166	
167	
168	
169	
170	
171	
172	
173	
174	
175	
176	
177	
178	
179	
180	
181	
182	
183	
184	
185	
186	
187	
188	
189	
190	
191	
192	
193	
194	
195	
196	
197	
198	
199	
200	
201	
202	
203	
204	
205	
206	
207	
208	
209	
210	
211	
212	
213	
214	
215	
216	
217	
218	
219	
220	
221	
222	
223	
224	
225	
226	
227	
228	
229	
230	
231	
232	
233	
234	
235	
236	
237	
238	
239	
240	
241	
242	
243	
244	
245	
246	
247	
248	
249	
250	
251	
252	
253	
254	
255	
256	
257	
258	
259	
260	
261	
262	
263	
264	
265	
266	
267	
268	
269	
270	
271	
272	
273	
274	
275	
276	
277	
278	
279	
280	
281	
282	
283	
284	
285	
286	
287	
288	
289	
290	
291	
292	
293	
294	
295	
296	
297	
298	
299	
300	
301	
302	
303	
304	
305	
306	
307	
308	
309	
310	
311	
312	
313	
314	
315	
316	
317	
318	
319	
320	
321	
322	
323	
324	
325	
326	
327	
328	
329	
330	
331	
332	
333	
334	
335	
336	
337	
338	
339	
340	
341	
342	
343	
344	
345	
346	
347	
348	
349	
350	
351	
352	
353	
354	
355	
356	
357	
358	
359	
360	
361	
362	
363	
364	
365	
366	
367	
368	
369	
370	
371	
372	
373	
374	
375	
376	
377	
378	
379	
380	
381	
382	
383	
384	
385	
386	
387	
388	
389	
390	
391	
392	
393	
394	
395	
396	
397	
398	
399	
400	
401	
402	
403	
404	
405	
406	
407	
408	
409	
410	
411	
412	
413	
414	
415	
416	
417	
418	
419	
420	
421	
422	
423	
424	
425	
426	
427	
428	
429	
430	
431	
432	
433	
434	
435	
436	
437	
438	
439	
440	
441	
442	
443	
444	
445	
446	
447	
448	
449	
450	
451	
452	
453	
454	
455	
456	
457	
458	
459	
460	
461	
462	
463	
464	
465	
466	
467	
468	
469	
470	
471	
472	
473	
474	
475	
476	
477	
478	
479	
480	
481	
482	
483	
484	
485	
486	
487	
488	
489	
490	
491	
492	
493	
494	
495	
496	
497	
498	
499	
500	
501	
502	
503	
504	
505	
506	
507	
508	
509	
510	
511	
512	
513	
514	
515	
516	
517	
518	
519	
520	
521	
522	
523	
524	
525	
526	
527	
528	
529	
530	
531	
532	
533	
534	
535	
536	
537	
538	
539	
540	
541	
542	
543	
544	
545	
546	
547	
548	
549	
550	
551	
552	
553	
554	
555	
556	
557	
558	
559	
560	
561	
562	
563	
564	
565	
566	
567	
568	
569	
570	
571	
572	
573	
574	
575	
576	
577	
578	
579	
580	
581	
582	
583	
584	
585	
586	
587	
588	
589	
590	
591	
592	
593	
594	
595	
596	
597	
598	
599	
600	
601	
602	
603	
604	
605	
606	
607	
608	
609	
610	
611	
612	
613	
614	
615	
616	
617	
618	
619	
620	
621	
622	
623	
624	
625	
626	
627	
628	
629	
630	
631	
632	
633	
634	
635	
636	
637	
638	
639	
640	
641	
642	
643	
644	
645	
646	
647	
648	
649	
650	
651	
652	
653	
654	
655	
656	
657	
658	
659	
660	
661	
662	
663	
664	
665	
666	
667	
668	
669	
670	
671	
672	
673	
674	
675	
676	
677	
678	
679	
680	
681	
682	
683	
684	
685	
686	
687	
688	
689	
690	
691	
692	
693	
694	
695	
696	
697	
698	
699	
700	
701	
702	
703	
704	
705	
706	
707	
708	
709	
710	
711	
712	
713	
714	
715	
716	
717	
718	
719	
720	
721	
722	
723	

TABLE OF CONTENTS

SECTION

0. INTRODUCTION AND SUMMARY	0-1
1. ANTIPIRON ANNIHILATION PROPULSION	1-1
2. SOLAR HEATED PLASMA PROPULSION	2-1
3. PERFORATED SOLAR SAILS	3-1
4. LASING THE IONOSPHERE	4-1
5. SOLID METASTABLE HELIUM	5-1
6. VACUUM FLUCTUATION ENERGY SOURCE	6-1
7. OTHER PROPULSION ENERGY SOURCE CONCEPTS	7-1
Laser thermal propulsion	7-1
Laser electric propulsion	7-2
Beamed microwave thrusters	7-2
Laser pushed lightsails	7-3
Microwave pushed sails	7-4
Tethers	7-5
Free-radical hydrogen	7-6
Metallic hydrogen	7-7
Unconventional nuclear propulsion concepts	7-8
Quark catalyzed fusion	7-8
Imploded micropellet fusion	7-9
Muon catalyzed fusion	7-10
Ultracold neutron fission	7-11
Magnetic monopole catalyzed fusion	7-12

APPENDICES

- | | |
|---|-----|
| A. Extracting electrical energy from the vacuum
by cohesion of charged foliated conductors | A-1 |
| B. Light-levitated geostationary cylindrical orbits
using perforated solar sails | B-1 |
| C. Starwisp (Microwave-pushed wire mesh
interstellar probe) | C-1 |

SECTION 0

INTRODUCTION AND SUMMARY

The objective of the contract effort was to identify new sources of propulsion energy or new propulsion concepts for known energy sources, study the problems still remaining that prevent the concept from being feasible, and recommend a program of research and development to solve those problems. Since the purpose of the contract was to produce "quantum breakthroughs in energy storage and propulsion", I deliberately spent little time investigating well-studied subjects such as airbreathing propulsion, chemical propellants, electric propulsion, advanced chemical batteries, or conventional nuclear reactor propulsion concepts.

The work on the contract was greatly aided by a number of prior surveys of advanced propulsion. If a topic is adequately covered in one of these surveys and no new information was found, then the topic is only covered briefly, if at all, in this final report. In the text of this final report, these prior reports will be referred to as:

[AFRPL 1972]: AFRPL-TR-72-31, "Advanced Propulsion Concepts - Project Outgrwth", F.B. Mead, Jr, Air Force Rocket Propulsion Laboratory, Edwards AFB, CA 93523 (1972)

[JPL 1975]: JPL-TM-33-722, "Frontiers in Propulsion Research", D.D. Papailiou, Jet Propulsion Laboratory, Pasadena, CA 91109 (1975)

[Boeing 1981]: Boeing, "Advanced Propulsion Systems - Concepts for Orbital Transfer Study", Final Report on Contract NAS8-33935 with NASA/Marshall Space Flight Center by Dr. Dana G. Andrews, Boeing Aerospace Company, Seattle, Washington 98124 (July 1980 to July 1981).

[JPL 1982]: JPL Report 715-151, "Ultra High Performance Propulsion for Planetary Spacecraft", FY81 Final Report, P.W. Garrison, R.H. Frisbee, M.F. Pompa, Jet Propulsion Laboratory, Pasadena, California (January 1982).

PHASE 1 ACTIVITIES

The Phase 1 activities on the contract were to consist of a preliminary survey of all possible propulsion energy concepts, including those that might violate the presently known laws of physics. A condensed version of the Phase 1 Statement of work follows:

Phase 1: Technical Assessment

The contractor shall conduct a thorough literature search and carry out an intense technical assessment of the latest concepts in science and engineering that show promise of leading to a major advance in available energy sources for space power and propulsion in the next century. In general, the contractor shall study any physical concept that might derive energy from the space environment, as well as any unconventional methods of storing energy in a compact form that may have applicability to space power and propulsion.. The best of these shall be investigated in Phase 2.

A literature search combined with a large number of personal contacts with people involved in the field of advanced propulsion insured that as many new concepts as possible were uncovered. Although some time was spent on detailed analysis when the concept warranted it, most of the activities in Phase 1 were of the data collection type rather than data analysis. This effort resulted in the uncovering of 64 propulsion energy concepts, of which 28 were well defined enough to be selected for preliminary technical assessment.

CONCEPTS RECEIVING PRELIMINARY TECHNICAL ASSESSMENT

metallic hydrogen	microwave sails
free-radical hydrogen	tether power systems
metastable helium	tether propulsion
mass drivers	dynamic structures
lightweight lenses	high temperature radiators
solar heated plasmas	nuclear fission pulsejet
beamed microwave thrusters	imploded micropellet fusion
ionospheric laser	monopole catalyzed fusion
laser heated thrusters	quark catalyzed fusion
laser electric thrusters	ultracold neutron fission
solar sails	muon catalyzed fusion
perforated light sails	metastable excited nuclei
laser sails	antiproton annihilation
quantum dynamic energy	anisotropic radiator thruster

The remaining 36 concepts were, for one reason or another, not felt to show sufficient promise of leading to a major advance in available energy sources for space power and propulsion in the next century. Those concepts are listed below. In this list, when I use the word "drive" in the description of the concept, that means that the concept proposes a mechanism that violates one or more of the laws of conservation of mass-energy, linear momentum, or angular momentum. The "drive" concepts are not on this list because they violate conservation laws, but because of the lack of hard evidence (working models) to base any assessment on. (Indeed, the real breakthrough in propulsion will come when we can find a "drive" that somehow gets around the momentum conservation laws, just as the last breakthrough came when Einstein and Fermi found a way around the law of conservation of mass by demonstrating how to convert mass into energy.)

CONCEPTS NOT RECEIVING PRELIMINARY TECHNICAL ASSESSMENT

black hole thermal energy source	negative matter
sodium heat engine	Alfvén propulsion
fission fragment rocket	gravity propulsion
e-beam activated radioactivity	space warps
induced dipole microwave thruster	time machines
stimulated K capture	spin annihilation drive
solar heat collector prime power	antigravity
inertia cancellation drive	flywheels
inertia redistribution drive	fusion ramjet
microwave phase drive	psychokinetics (PK)
oscillating proton drive	water flow drive
momentum annihilation drive	rotary launcher
electromagnetohydrodynamic drive	scissors launcher
hyperfield resonance drive/warp	high speed pellet beam
unbalanced rotor (Dean) drive	gravity shielding
magnetic levitator and thruster	tachyons
cold-gas turbine thruster	radioisotope sail
cryogenic oscillator	beta-decay battery

PHASE 1 RESULTS

Of the 28 concepts that received technical assessment in Phase 1, I recommended that four be considered for more detailed study in Phase 2. The concepts recommended were solid metastable helium, solar heated plasmas, perforated solar sails, and antiproton annihilation propulsion. Of these, the Air Force selected two concepts to receive the major portion of the Phase 2 effort, solar heated plasmas and antiproton annihilation. As time permitted, studies were to also continue on free radical hydrogen, quantum dynamic energy, and ionospheric lasing.

PHASE 2 ACTIVITIES

The Phase 2 activities consisted of a more intensive analysis of the selected topics leading to a recommended program of research and development to advance those concepts. A condensed version of the Phase 2 Statement of Work follows:

Phase 2: Concept Definition

The contractor shall identify the problems that still exist in making the selected concepts feasible, and identify the people or groups of people that can best analyze and propose solutions for those remaining problems. The contractor shall then assemble that team of investigators to attack the remaining problems in the selected technologies and put together a program plan that will be proposed to the Air Force Rocket Propulsion Laboratory. This program plan will outline the steps required for full development of the selected concepts.

Antiproton annihilation received most of the effort in Phase 2. In this concept antiprotons are manufactured by a large special-purpose particle accelerator, converted into antihydrogen ice, stored using electric and magnetic fields, then used to heat large amounts of hydrogen to produce thrust. There are at least 17 significant problems that must be solved to make this concept feasible. The three major problems are the efficiency of production of antiprotons, identification of the annihilation products of an antiproton in a heavy nucleus, and the conversion efficiency of the annihilation products into thrust. I can see solutions to all the major problems and most of the minor problems. As a result, I believe that antiproton annihilation propulsion is feasible, although expensive, and will provide the Air Force with a significant advance in propulsion technology in the coming century. I have identified the people that can best tackle the remaining problems and have recommended a research program to the Air Force.

Early in Phase 2 it was found that a program on solar heated plasma propulsion was underway at the University of Washington. In this concept, sunlight is used to heat and sustain an alkali metal plasma discharge which captures the solar energy and transfers it at high efficiency to a hydrogen working fluid. The University of Washington work on solar pumped plasma propulsion is in addition to studies on solar pumped plasmas for lasers and prime power carried out at a number of other institutions. The major problems are maximizing the absorption of sunlight, sustaining the plasma, and transferring the energy to the hydrogen working fluid at high temperature while minimizing the

window damage, reradiation and wall losses, and amount of alkali metal used. It was relatively easy to identify those groups of people that could best analyze and propose solutions to the remaining problems in solar heated plasma propulsion. Only three weeks were found necessary for this task.

I expected to spend less than a week on both quantum dynamic energy and ionospheric lasing since my initial opinion was that both concepts were not feasible. An extensive literature search uncovered ongoing proprietary work in ionospheric lasing that showed that it may indeed be possible to make the ionosphere lase and that the power levels could be significant. Two weeks were spent on this topic. My look at extracting energy from quantum fluctuations started out with a great deal of skepticism. A reading of the extensive body of literature in the field, however, uncovered a well-known, experimentally verified force, called the Casimir force, that is due to the electromagnetic fluctuations in the vacuum. I invented methods for using this force to increase the energy in a stored electric field, thus converting the electromagnetic vacuum fluctuation energy into usable electric energy. Three weeks were spent studying this completely new energy source. As a result, no time was left for the study of free radical hydrogen.

CONCEPTS UNCOVERED THAT HAVE POTENTIAL PROPULSION ENERGY PAYOFF

During both Phase 1 and Phase 2 of the contract I identified six new concepts for alternate propulsion energy sources that had not been known, or had been deemed unfeasible or too far off in the future by the prior surveys of advanced propulsion. These are each discussed in detail in the following sections of this report.

1. **Antiproton Annihilation** - Mentioned in many previous advanced propulsion studies but thought to be unfeasible or limited to interstellar missions in the far distant future when technology has advanced further. I have determined that antiproton annihilation propulsion is probably feasible with reasonable extrapolations of present day technology, although the engineering development effort will be difficult and expensive. Antiproton annihilation is certainly worth further intensive study as a high risk/high payoff concept.
2. **Solar Heated Plasmas** - An approach to a solar thermal rocket that can obtain an exhaust temperature close to the sun's temperature. Concentrated sunlight is used to heat and sustain a plasma discharge in a mixture of alkali metal and hydrogen gas. This is a near-term advanced propulsion concept suitable for the follow-on phase of the existing AFRPL solar thermal rocket program.

3. Perforated Solar Sails - A concept for an improved performance solar or laser sail invented during Phase 1 of this contract. The sail is perforated with holes smaller than a wavelength of light to reduce mass and atmospheric drag without reducing the reflectivity. This concept was not studied in detail in Phase 2 because other topics had higher priority.

4. Lasing the Ionosphere - Methods for extracting energy from solar pumped molecules in the ionosphere by laser action.

5. Solid Metastable Helium - A new approach to making stable excited helium by using lasers and magnetic fields to form it into a ferromagnetic room-temperature solid. This concept was not studied in Phase 2 because AFRPL was already supporting the work.

6. Vacuum Fluctuation Energy Source - A concept invented during this contract for extracting electrical energy from the electromagnetic fluctuations of the vacuum.

In addition to these six concepts chosen for detailed study on this contract because of their promise and novelty, I identified a number of other propulsion energy concepts that are either good advanced propulsion concepts already being intensively studied (laser propulsion, tethers), or are a promising concept that has some fundamental problem with no solution available yet (metallic hydrogen, magnetic monopole catalyzed fusion). These are briefly discussed in Section 7.

SECTION 1

ANTIPROTON ANNIHILATION PROPULSION

In this section I discuss a new high specific impulse, high thrust propulsion system based on the generation, storage, and utilization of antiprotons. I will first summarize how I think the first antiproton annihilation propulsion system will operate, all the way from the production of the antiprotons to the conversion into propulsive thrust. I will then discuss each of the steps in more detail in separate paragraphs that follow.

The antiprotons will be generated by antiproton "factories" especially designed for the purpose that use extrapolations of the antiproton production facilities at IHEP in the USSR, CERN in Switzerland, and Fermilab in the USA. The antiprotons are generated by the collision of high energy protons with multiple arrays of thin metal targets. The high energy antiprotons emanating from the targets are collected by arrays of magnetic lenses leading to stacks of holding rings, each designed to handle antiprotons in different energy bands. There, using stochastic cooling, the energy spread of the captured antiprotons is narrowed, allowing the multiple beams to be decelerated to a common subrelativistic speed, transferred to another holding ring and cooled again using electron cooling. With the aid of laser interactions, the antiprotons are combined with positrons to form first atomic hydrogen, then molecular hydrogen beams. The molecular hydrogen beams are then further cooled and decelerated using resonant light from a molecular hydrogen laser, then brought to a stop and trapped as milligram sized balls of antihydrogen ice using a combination of laser light, magnetic bottles, and electrostatic fields. If kept below 2 K, the lifetime will be limited by the quality of the vacuum of the storage container rather than sublimation. The storage containers containing the few milligrams of antihydrogen "fuel" are then transferred to the using vehicle. When propulsive energy is desired, the antiprotons are extracted from the antihydrogen ice ball by strong localized electric fields and directed by electric and magnetic fields to the "magnetic bottle" reaction chamber of the rocket. In the rocket chamber, the antiprotons interact at low energies with a reaction mass made of heavy nuclei. The annihilation of the antiproton with a proton or neutron in the heavy nucleus will produce a number of high energy pions. The pions will immediately transfer their kinetic energy to the rest of the nucleus, which will break up into alpha particles (along with a small number of neutrons, protons, and larger fragments). The isotropic kinetic energy of the charged particles is then channeled into unidirectional thrust by a rocket nozzle made of magnetic fields.

THRUST FROM ANTIMATTER ANNIHILATION

It has long been realized that antimatter would be a valuable propulsion energy source because it allows for the complete conversion of mass to energy. Early studies of the concept [Sanger, 1953] assumed that the antimatter would be antielectrons or positrons, which interact with electrons to produce 0.511 MeV gamma rays. Sanger unsuccessfully tried to invent electron-gas mirrors to direct these short wavelength gamma rays to produce a photon rocket. The antiproton is much more suitable for propulsion systems. The annihilation of an antiproton by a proton does not produce gamma rays immediately. Instead the products of the annihilation are from three to seven pions. On the average there are 3.2 charged pions and 1.6 neutral pions [Agnew 1960]. The neutral pions have a lifetime of only 90 attoseconds and almost immediately convert into two high energy gamma rays. The charged pions have a normal half-life of 26 nanoseconds, but because they are moving at 94% the speed of light, their lives are lengthened to 70 nanoseconds. Thus, as is shown in Figure 1-1, they travel an average of 21 meters before they decay. This time and interaction length is easily long enough to collect the charged pions in a thrust chamber constructed of magnetic fields and direct the isotropic microexplosion into directed thrust. Even after the charged pions decay, they decay into energetic charged muons, which have even longer lifetimes and interaction lengths for further conversion into thrust. Thus, if sufficient quantities of antiprotons could be made, captured, and stored, then present known physical principles show that they can be used as a highly efficient propulsion fuel [Forward 1982].

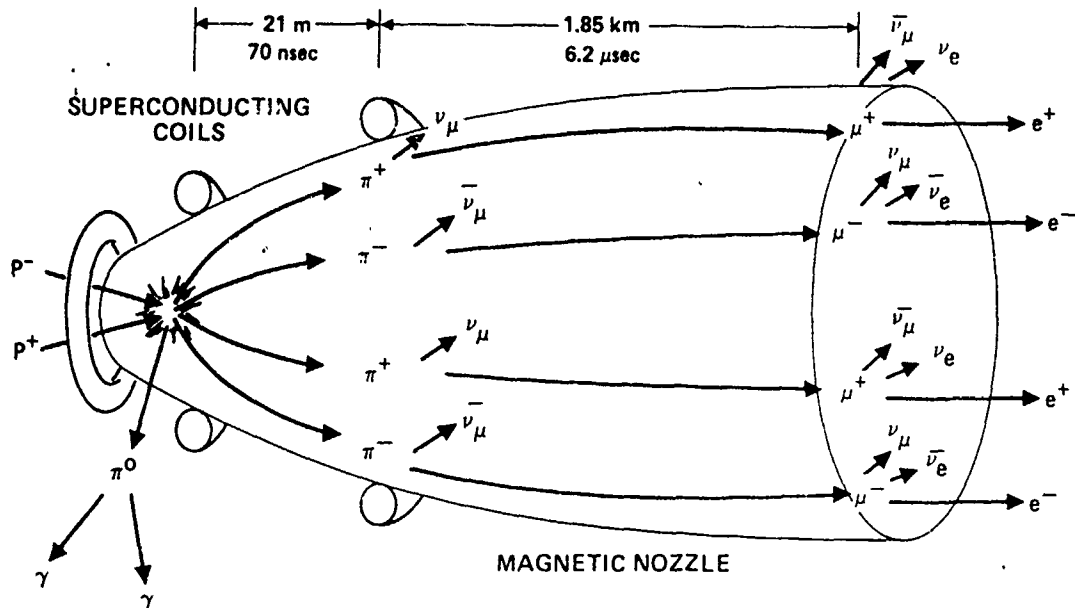


Figure 1-1
Thrust from antiproton annihilation

Because of the extreme difficulty in obtaining significant quantities of antimatter, the idea of an antimatter rocket has usually remained in the "science fiction" category. Any papers before 1980 [see 27 references in section 02.01 of bibliography by Mallove, et al. 1980] were usually concerned with interstellar missions and glossed over the problems of generating, storing, and using the antimatter. Recent progress in particle physics on methods for obtaining intense antiproton beams, however, have caused those in the space propulsion community to take another look at the concept of antimatter propulsion and see if the concept can be removed from the "science fiction" category to the "engineeringly difficult and very costly" category, at which point the military services or NASA could begin considering its use. The last five years has seen the presentation of a number of papers on antimatter propulsion [Forward 1980, Cassenti 1983, Zito 1983, Vulpetti 1983a and b], including a special issue of the Journal of the British Interplanetary Society on the subject of antimatter propulsion [Massier 1982, Forward 1982, Cassenti 1982, Morgan 1982, Zito 1982, Chapline 1982].

A typical scenario for the proposed antiproton annihilation propulsion system [Forward 1982, Morgan 1982] is that antiprotons will be generated by high energy particle beams, the antiprotons will be collected, cooled, and decelerated to sub-relativistic speeds using a combination of electron and stochastic cooling. With the aid of lasers, the antiprotons will be combined with positrons to produce antihydrogen atoms and then antihydrogen molecules. These molecular beams will be further cooled and decelerated using lasers, then trapped and condensed into balls of antihydrogen ice by a combination of laser beams and magnetic fields. The antihydrogen ice will be transferred to high-vacuum cryogenic storage containers that use a combination of passive magnetic levitation and active electrostatic levitation to handle low and high acceleration environments with minimum energy input to the antihydrogen ice. The "fuel tanks" with their antihydrogen ice "fuel" will be transferred to the using vehicle. The antiprotons will be extracted from the antihydrogen ice pellet at a few eV by strong localized fields and directed by electric and magnetic fields to the reaction chamber of the rocket. The antiprotons will be mixed at low energy with a beam of heavy atoms. They will be electrostatically attracted to the positive heavy nuclei producing a high capture cross-section and after a brief time as an antiprotonic atom, the antiproton will annihilate with a proton or neutron in the heavy nucleus. Nearly all the energy in the resultant annihilation process, including the energy in the short-lived neutral pions will be transmitted to the remainder of the heavy nucleus breaking it up into alpha particles plus larger and smaller chunks. Most of the fragments will be charged and their kinetic energy can be transferred into directed thrust by either a magnetic nozzle [Morgan 1975, 1976, 1982] or by interaction with a flowing wall of hydrogen gas protecting a material nozzle [Chang and Fisher 1983].

The problems to be solved in making the antiproton annihilation scenario feasible can be listed as:

Antiproton Generation
Antiproton Capture
Cooling at Relativistic Velocities
Deceleration from Relativistic to Subrelativistic Velocities
Cooling at Subrelativistic Velocities
Conversion of Antiproton Beam to Antihydrogen Beam
Cooling of Antihydrogen Beam
Conversion of Antihydrogen Atoms to Antihydrogen Molecules
Cooling of Molecular Antihydrogen Beam
Stopping of Antihydrogen Molecules
Trapping of Antihydrogen Molecules
Conversion of Antihydrogen Gas to Antihydrogen Ice
Long Term Storage of Antihydrogen Ice
Extraction of Antihydrogen from Ice
Annihilation of Antihydrogen
Transfer of Annihilation Energy to Working Fluid
Conversion of Working Fluid Energy to Thrust

I have looked at these problems one at a time. Some, like generation, capture, relativistic cooling, deceleration, and subrelativistic cooling have already been demonstrated. I can see solutions to most of the rest of the problems, although not all of them. In the remainder of this section we will see what is the present state of the art, what are the problems yet to be solved, and how one might approach a solution to those problems.

COMPARISON OF PRESENT ANTIPIRON PRODUCTION FACILITIES

Antimatter in the form of antiprotons is being made and stored today, albeit in small quantities. The two major producers are IHEP in the USSR and CERN in Europe. Fermilab in the US has started construction of their antiproton facility and expects to be in operation in 1985. In these facilities, the antiprotons are generated by sending a high energy beam of protons into a dense tungsten target. When the relativistic protons strike the dense metal nuclei, their kinetic energy, which is many times their rest-mass energy, is converted into a spray of particles, some of which are antiprotons. A magnetic field focuser and selector separates the antiprotons from the resulting debris and directs it to a storage ring.

When the antiprotons are generated, they have a wide spread of energies. This makes it difficult to decelerate them to subrelativistic velocities, so it is necessary to "cool" the beam so that all the antiprotons have the same energy. Two techniques for reducing the velocity spread have been successfully demonstrated. In the stochastic cooling scheme, the radio noise generated by fluctuations in the beam are detected. This noise is amplified, phase shifted, then transmitted across the diameter of the ring to an electromagnetic kicker that suppresses the

fluctuation [Herr and Rubbia 1980, van der Meer 1981, Kells 1981]. In the electron cooling scheme a beam of monoenergetic electrons is inserted in the ring with the antiprotons. Those antiprotons moving too slow will be sped up by the electrons and those moving too fast will be slowed down [Budker and Skrinskii 1978, Cline, et al 1979, Krienen 1980, Young 1980, Forster, et al., 1981, Kells, et al. 1981, Bell, et al. 1981, Hütten, Poth and Wolf 1982]. These cooled antiprotons could then go through another stage of deceleration and cooling to bring them down to speeds suitable for capture, control, and cooling by other techniques. The accelerator at CERN has generated 3.5 GeV antiprotons with a 26 GeV proton beam and has stored as many as a trillion antiprotons for up to four days in their magnetic ring "racetrack" antiproton accumulator [Physics Today 1979, Scientific American 1982].

The characteristics of the three antiproton production facilities in the world are shown in Figure 1-2 [Vsevolozskaja, et al. 1980]. The CERN data [Gareyte 1980, Robinson 1981] and IHEP data [Aqeyev 1980] describe operational systems, while the FNAL (Fermilab) data [Physics Today 1979, Young 1981] describe the characteristics of their latest plans for the facility they expect to have operational in 1985. In general, the higher the proton energy, the more efficient the proton is at generating antiprotons, so the IHEP and FNAL beams generate more antiprotons per proton, while the CERN facility partially makes up for that with higher beam currents. The major factor in system efficiency is the efficiency of the antiproton collector. The CERN collector has the best angular acceptance (it can capture a 100 mrad beam from a 1 mm target), while the IHEP can capture a wider spread in momentum (velocity). Still, both of these capture efficiencies are very low and only a small fraction of the antiprotons that are generated are ever captured.

	CERN (EUROPE)	FNAL (USA)	IHEP (USSR)
PROTON ENERGY (GeV)	28	120	70
PROTON RATE (10^{12} p/cycle)	10	3	7
CYCLE DURATION (sec)	2.6	2	7
ANTIPROTON ENERGY (GeV)	3.5	8	5.5
ANGULAR CAPTURE (mm - mrad)	100π	20π	60π
MOMENTUM CAPTURE ($\Delta P/P$)	$\pm 0.75\%$	$\pm 3\%$	$\pm 3.2\%$
ANTIPROTON PROD. ($10^6 \bar{p}/\text{cycle}$)	25	70	320
ACCUMULATION RATE ($10^6 \bar{p}/\text{sec}$)	10	35	47
NUMBER EFFICIENCY ($10^{-6} \bar{p}/p$)	2.5	23	46
ENERGY EFF ($10^{-6} 2m\bar{p} c^2/E_p$)	0.2	0.4	1.3

Figure 1-2
Comparison of antiproton production facilities

The plans at all these facilities are to run each machine as an antiproton generator for the order of a day until about 10^{12} to 10^{13} antiprotons are captured, cooled, and stored in an antiproton accumulator ring. Then these antiprotons are reinserted back into the main ring going in the opposite direction to the proton beam. The two beams intersect in one or more experiment areas that have detectors to study the exotic particles created by the proton-antiproton collisions [Physics Today 1979, Robinson 1981, Cline et al. 1982].

To give some scale to what has already been accomplished at these research facilities, 10^{13} antiprotons have a mass of 17 picograms. When this amount of antimatter is annihilated with an equivalent amount of normal matter, it will release 3 kilojoules, an engineeringly significant quantity of energy. To obtain this "firecracker" amount of annihilation energy required the use of billion dollar machines that used an enormous amount of electric energy. Yet it is important to recognize that scientists working in basic physics, using research tools not designed for the job, have produced and continue to produce significant quantities of annihilation energy.

PRESENT ANTIPIRON PRODUCTION RATES

The literature on the production of antiprotons by the impact of a proton beam on a metal target is in a state of flux. The absolute production rate is unknown to a factor of two or more [Krienen and MacLachlan 1981], and there is no agreement between the various papers on the spread in energy and momentum [Chirikov, et al. 1977, Kirk 1980, Krienen and MacLachlan 1981, Vsevolozskaya 1981, Möhring and Ranft 1982, Hojvat and van Ginneken 1983]. For example, in the simple matter of the variation of the production in angle (or transverse momentum), there is no agreement in the literature even in the exponent of the transverse momentum much less the scaling factor. The reason for this lack of agreement is probably due to two causes. First, the experimental data is sparse and usually at lower energies than are being contemplated for the antiproton production facilities, so rough fits can be obtained with any reasonable function. Second, due to the angular limitations of the antiproton collecting lenses, most of the collection takes place near zero transverse momentum where discrepancies in exponents and scaling factors are not important. As we consider higher efficiency production, however, we will have to design lens systems to collect those antiprotons with larger transverse momentum, and it would be desirable to know how the distribution falls off with angle.

The present capture efficiencies of the antiproton facilities are abysmally low. The situation is best summarized by Figure 1-3 from a recent Fermilab publication [Hojvat and van Ginneken 1983]. The upper part of the figure shows the total number of antiprotons generated per GeV of antiproton momentum per

steradian of solid angle at the central portion of the antiproton beam. Integrating the curve over the antiproton momenta shows that each proton produces 7.7 antiprotons per steradian. In the paper, the number of antiprotons per GeV of antiproton momentum is estimated assuming that the antiproton collector can only accept those antiprotons with an angular spread off the axis of 30 mrad (0.0028 steradians). When this curve is integrated over the antiproton momenta we find only 0.014 antiprotons per proton in this narrow angular acceptance. Then, of this small angular spread the Fermilab collector is only able to capture those with a momentum (velocity) spread of $\pm 3\%$ or 0.5 GeV around 8.9 GeV. Thus, ideally, they would expect to capture only about 3.5×10^{-4} antiprotons per proton, with an estimated actual efficiency of 2.3×10^{-5} antiprotons per proton (See Figure 1-2).

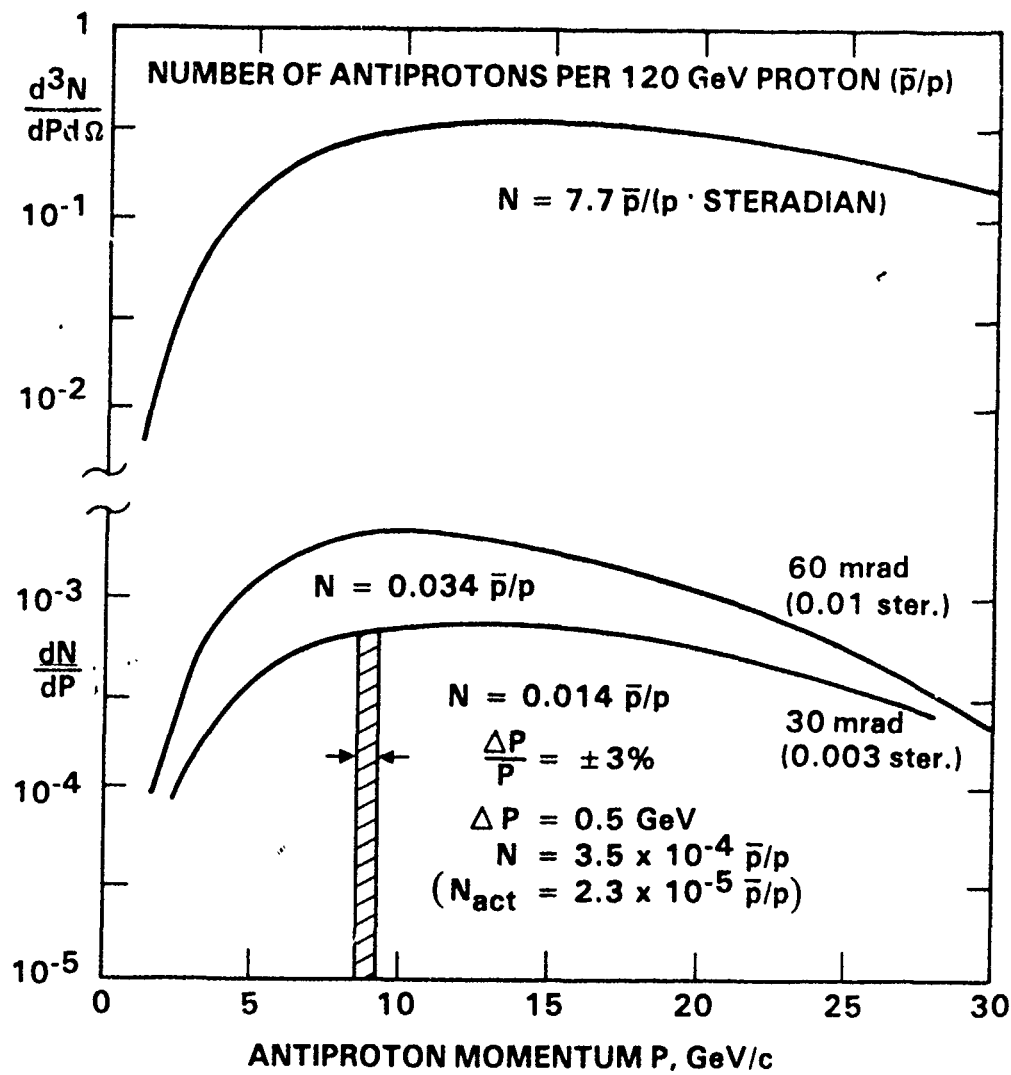


Figure 1-3
Present antiproton capture efficiencies

ESTIMATED FUTURE ANTIPIRON PRODUCTION RATES

The last collection of experimental data on total antiproton production rates was done over a decade ago [Antinucci, et al. 1973]. Many of the measurements were made using colliding beams of protons, so the data is only partially relevant to the problem of colliding protons with heavy nuclei, which is known to give a higher antiproton production rate. As is shown in the first three columns in Figure 1-4, the number of antiprotons produced per proton rises with increased center-of-mass energy. At 200 GeV proton kinetic energy, the colliding beams produce 0.3 antiprotons per proton with an energy efficiency (antiproton annihilation energy divided by proton kinetic energy) of 0.16%. (There are roughly 5 K mesons, 50 pi mesons, and large numbers of positrons and electrons produced for each antiproton generated.)

A more recent estimate [Hojvat and van Ginneken 1983] for the antiproton production spectra has the limitation that the authors were only interested in calculating the production rate on the Fermilab machine. Their magnetic lenses have an angular cutoff of 45 mrad, so the calculations were cut off at 60 mrad, even though the production rate was still increasing with increasing collection angle. As is shown in Figure 1-4, the energy efficiency for 60 mrad cutoff shows a broad peak around 200 GeV. If we increase the assumed collection angle to 200 mrad, then I estimate that we can get collection rates and energy efficiencies for a proton beam into a heavy metal target that are comparable to the Antinucci data for colliding beams. As is shown in Figure 1-4, I estimate that at a proton beam energy of 200 GeV we can obtain a production rate of 0.2 antiprotons per proton at an energy efficiency of 0.2%.

ENERGY OF PROTON BEAM(S) E (GeV)	COLLIDING BEAMS* 4π PRODUCTION		BEAM INTO TARGET			
			60 mrad CUTOFF†		200 mrad CUTOFF (est)	
	n (\bar{p}/p)	$\epsilon(m/E\%)$	n (\bar{p}/p)	$\epsilon(2m/E\%)$	n (\bar{p}/p)	$\epsilon(2m/E\%)$
25	0.09	0.16	0.006	0.04	0.02	0.14
100	0.20	0.18	0.03	0.06	0.09	0.17
200	0.31	0.16	0.07	0.07	0.21	0.20
400	0.45	0.11	0.13	0.06	0.39	0.18
1000	—	—	0.21	0.04	0.63	0.12

Figure 1-4
Estimated antiproton production rates

ANTIPROTON FACTORY

In Figure 1-5 I show a conceptual design for an antiproton factory which would utilize the technologies being developed at CERN, Fermilab, and IHEP, but on a much larger scale and with the design optimized for energy efficiency. There would be more than one proton beam with each beam operated at the optimum beam current. Each proton beam would strike a thin liquid metal target and the resulting particles would be sorted by an array of wide-angle collecting lenses to extract the antiprotons and positrons. The main proton beam would go on to a beam cooler that would reduce the beam spread due to small angle scattering before the next target. The positrons with the right energy would be picked off and sent to the antihydrogen generator, while all the antiprotons possible would be sorted by energy and sent to a stack of stochastic coolers, each optimized for a particular central antiproton momentum. After stochastic cooling, the stack of beams at different energies would go to a decelerator stack that would reduce all the antiproton energies to the same subrelativistic energy (200 MeV). The combined beam would then be sent to an electron cooling ring before being further decelerated and sent on to the antihydrogen generator where the antiprotons are combined with the positrons to make antihydrogen atoms.

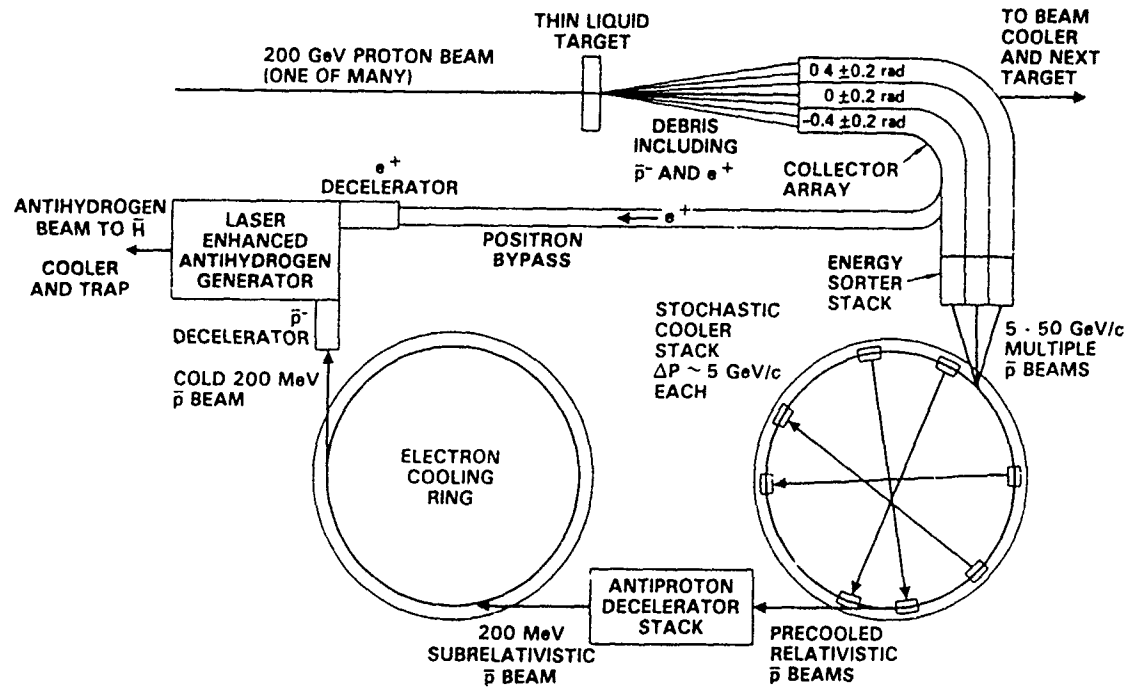
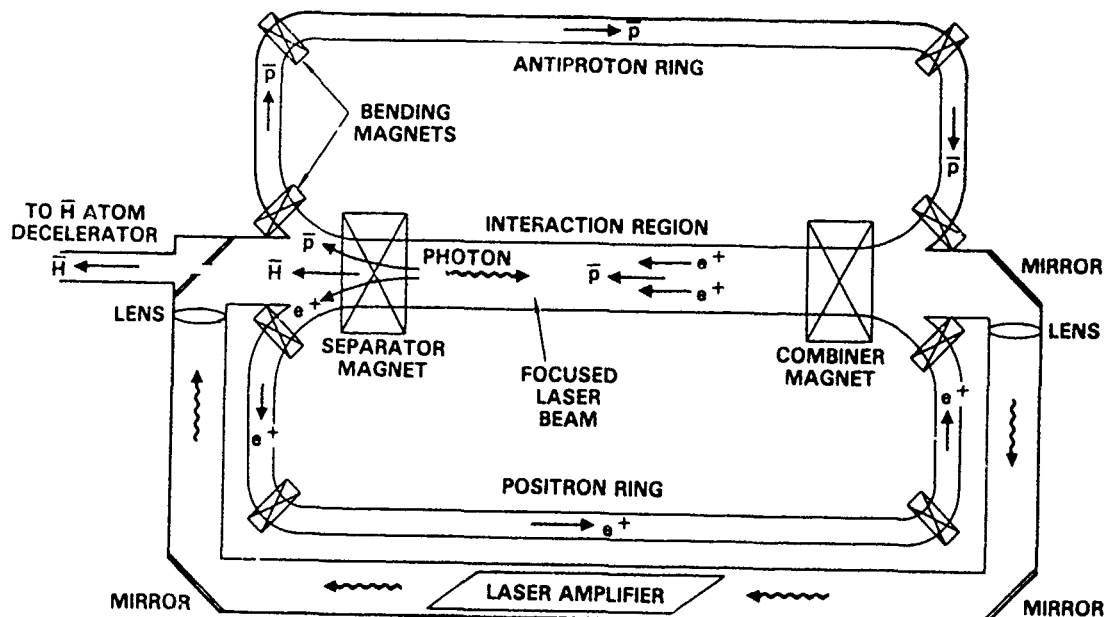


Figure 1-5
Antiproton factory (one segment)

LASER ENHANCED ANTIHYDROGEN FORMATION

The antihydrogen generator would follow the general concepts described in a recent research publication at CERN [Neumann, Poth, Winnacker, and Wolf 1983]. As is shown in Figure 1-6, if a beam of positrons are traveling at the same speed with a beam of antiprotons they will ultimately attract one another and recombine to form antihydrogen. This natural process can be enhanced by factors of 100 or more by stimulating the capture process with photons at the right wavelength. If the laser beam is traveling in the opposite direction to the particles, a visible laser can be used since the laser frequency will be shifted to the desired ultraviolet frequency by the relativistic doppler shift.



PARTICLE MOTION SHIFTS PHOTONS INTO UV
CAPTURE ENHANCED BY >100

Figure 1-6
Laser enhanced antihydrogen formation

COOLING, SLOWING, AND TRAPPING ANTIHYDROGEN

Once an antihydrogen beam has been formed, there are a number of techniques available for cooling the antihydrogen down, slowing it to a stop, and storing it in a trap. Traps for atoms were first proposed by Letokov [1968, 1977, 1980, 1981] and Ashkin [1970, 1976, 1978, 1979]. Deflection focusing, trapping, and cooling have been demonstrated many times [Wineland et al. 1978, Bjorkholm, et al. 1978, Balykin et al. 1979, 1980, Gordon and Ashkin 1980, Phillips and Metcalf 1982, Prodan, Phillips, and Metcalf 1982]. The activities in the field of cooling and trapping atoms has progressed to the point where a Workshop on laser cooling and trapping was held recently at the National Bureau of Standards [Phillips 1983]. In one paper [Phillips, Prodan and Metcalf 1983] reported that they slowed and cooled a neutral beam of sodium atoms using a near resonant, counterpropagating laser. To keep the laser line tuned to the doppler-shifted atomic resonance frequency, they used a spatially varying magnetic field to vary the transition frequency using the Zeeman shift. An alternate approach to compensating for the Doppler shifted transition frequency is to "chirp" the frequency of a tunable laser. Both NBS, Gaithersburg [Prodan and Phillips 1983], NBS, Boulder [Blatt, Ertmer, and Hall 1983], and CUNY [Lubell and Rubin 1983] are looking at this approach.

There are many concepts for traps for atoms. One can use passive electric fields if the atoms exhibit a positive Stark energy so that they concentrate at the minimum of an electric field. Although the $2^2S_{1/2}$ state of atomic hydrogen (and antihydrogen) has this property [Wing 1980, 1983a], the short lifetime makes it of little use for long term storage. The depth of most atomic traps is quite shallow, so even gravitational effects have to be considered [Wing 1983b]. Yet in a final trapping system, gravitational or centrifugal effects might be useful in the final trapping steps, since it provides yet another way to add or subtract energy from an atom without touching it. One is not limited to simple traps. One could use combinations of forces such as the hybrid laser-magnet trap for spin-polarized atoms [Stwalley 1983] which uses a solenoidal magnetic field for trapping in one direction and a "doughnut mode" laser beam along the magnetic field axis for trapping in the orthogonal directions. Evanescent radiation fields can also interact with neutral atoms to form traps [Cook and Hill 1982].

Although it might be possible to store antihydrogen as an atomic gas [R.W. Cline, et al 1980, Sprik, Walraven and Silvera 1983], the atomic form of antihydrogen is more difficult to control, cool, and trap than sodium. The fundamental problem is that while one Lyman alpha photon will excite an antihydrogen atom, if a second photon arrives before the atom has decayed back into its ground state, the second photon may ionize the antihydrogen atom. Although proprietary ideas exist for overcoming these problems, it is likely that it will be found necessary to convert the antihydrogen atoms into artihydrogen molecules, then store it as

antihydrogen ice. The conversion of antihydrogen atoms to antihydrogen molecules takes place naturally (with the release of lots of energy, that is why spin-polarized normal hydrogen is being looked at as a potential rocket fuel). A large number of the molecules remain in a metastable orthohydrogen state. Left to itself, cold antihydrogen molecules will ultimately all convert to parahydrogen, the ground state of the molecule, but unless a catalyst is used, the process takes many days. Research is needed on the use of lasers and magnetic fields with high gradients to convert the antihydrogen atoms into antihydrogen molecules. These antihydrogen molecules can then be further cooled and trapped using lasers operating on a molecular hydrogen line [Breusova, et al. 1979], then turned into antihydrogen ice in the preferred parahydrogen state.

PASSIVE MAGNETIC FIELD ANTIHYDROGEN ICE TRAP

Since antihydrogen ice, like hydrogen ice, is diamagnetic, a simple passive trap for a ball of antihydrogen ice could be made of magnetic fields [Metcalf 1983]. There are a number of different ways to configure permanent magnets and coils to produce a magnetic field minimum that would attract a diamagnetic material such as graphite [Waldron 1966] or hydrogen. The simple example shown in Figure 1-6 consists of two superconducting coils spaced so that there is a magnetic minimum midway between them [Letokhov and Minogin 1980]. This kind of trap would be completely stable and require no power. It is not very deep, however, and although quite suitable for storage of antihydrogen ice in free fall, could not levitate the antihydrogen ice at high acceleration levels.

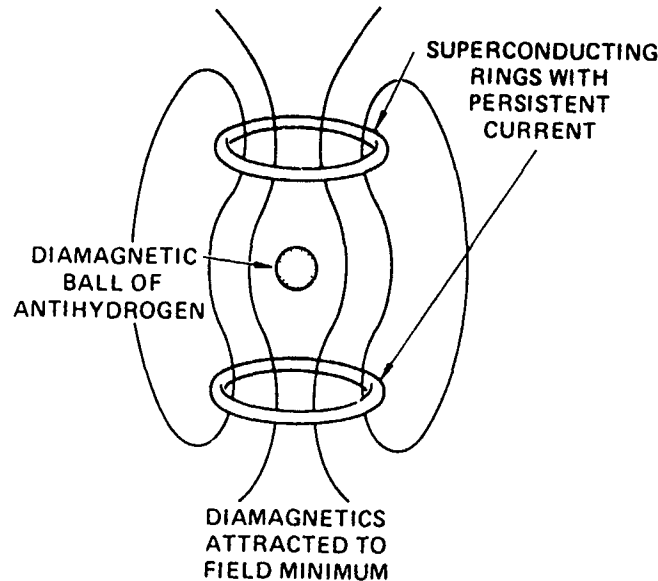


Figure 1-6
Stable magnetic levitation of antihydrogen ice

ACTIVE ELECTRIC LEVITATION AND CONTROL OF ANTIHYDROGEN ICE

For high acceleration levels, a more suitable trap would be a servo controlled dc voltage electrostatic levitation trap such as that shown in Figure 1-7. Such traps have been made at JPL and have levitated large spheres with the density of antihydrogen ice (0.0763 g/cc) in the earth's field [Rhim, Saffren, and Elleman 1982]. Since the antihydrogen ice will be formed at millidegrees or below, and the heat input from the electric levitator will be low, the sublimation pressure of the antihydrogen will be so low that the antihydrogen ice ball should last for years. The antiprotons are extracted from the ice ball by irradiating the ice with ultraviolet, driving off the positrons, extracting the excess antiprotons by field emission with a high intensity electric field, then directing them to the thrust chamber [Morgan 1982].

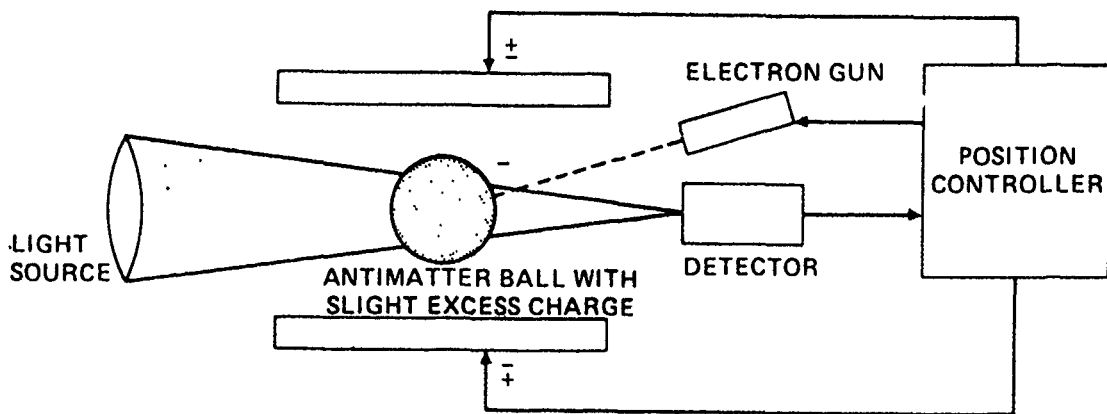


Figure 1-7
Electrostatic levitation of antihydrogen ice

MORGAN MAGNETIC NOZZLE

The plasma created by the interaction of antiprotons with protons may be too hot to be contained and directed by thrust chambers and nozzles made of solid material. Fortunately, most of the particles generated are charged and can be contained and directed by strong magnetic fields. One example of a design for a magnetic field rocket engine is shown in Figure 1-8 [Morgan 1982]. With dimensions in the order of meters, it is about as large as a Shuttle main engine. Note the path of a particular positive or negative pion traced out in the diagram. Even though the pion starts out from the annihilation point in a direction that is opposite to the desired thrust direction, its direction is reversed by the converging magnetic field lines and it is redirected into the proper direction to provide thrust. The magnetic fields required are high, 50 T (500,000 gauss), and will require superconducting magnetic coils that are adequately shielded from the gamma rays and neutrons generated by the reactions.

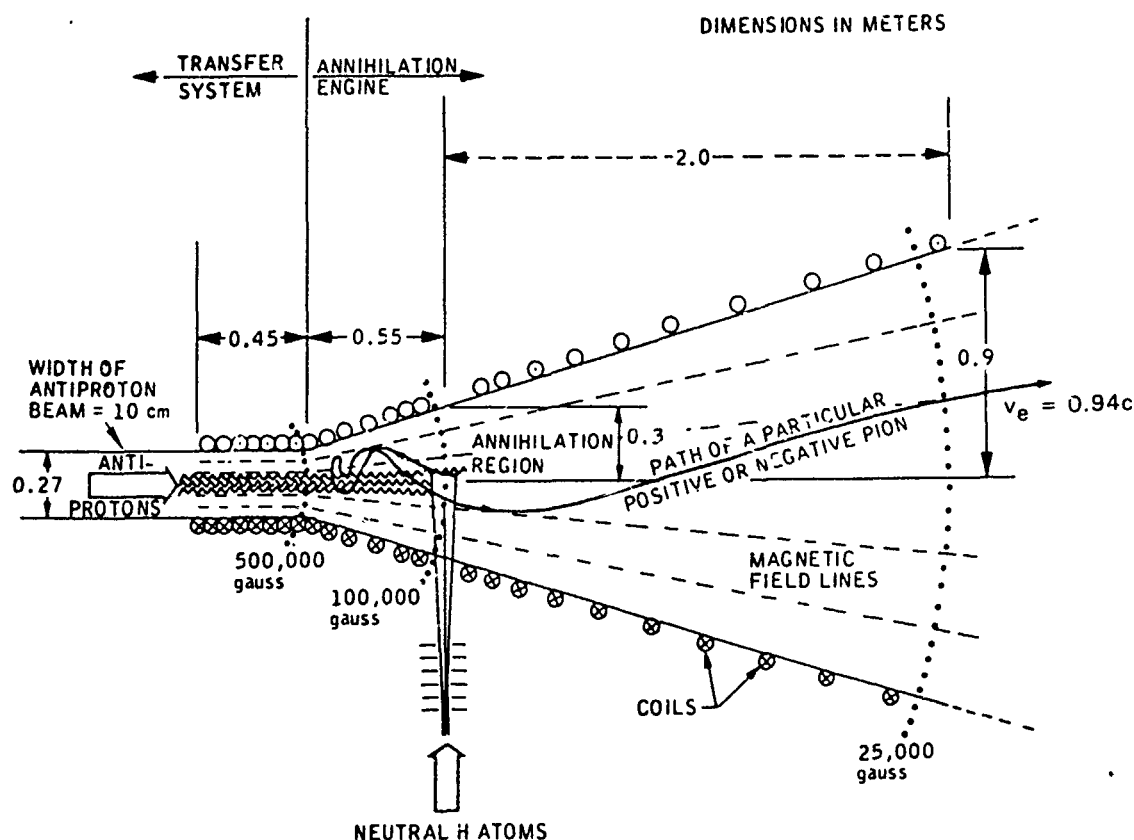


Figure 1-8
Morgan magnetic nozzle for antimatter propulsion

MINIMUM ANTIMATTER OPTIMIZATION

When antiprotons interact with protons (hydrogen), the resultant annihilation products are 400 MeV pions, which translates into an exhaust velocity of 94% of the speed of light. Thus, pure antimatter rockets are best suited for relativistic missions. In an important paper [Dipprey 1975], it was shown that in order to use the minimum amount of antimatter for the mission, the best way to use the antimatter is not to use equal amounts of matter and antimatter. Instead, the antimatter should be used to heat a much larger amount of propellant. The analysis comes to the conclusion that except for extreme relativistic spacecraft speeds ($>0.5 c$), the reaction mass needed is always four times the spacecraft payload mass, or an overall ratio of launch mass to payload mass of 5:1. The mass of the antimatter needed increases as the square of the mission "delta vee", but is always a negligible fraction of the total mass. Dipprey's work has been expanded by Cassenti [1982], who basically confirmed the 5:1 mass ratio and showed that heating liquid hydrogen with antimatter reaction products should produce an energy efficiency of about 44%.

It may turn out to be difficult to transmit the energy of the charged pions to hydrogen because of the long interaction length and the short pion lifetime. This interaction needs to be calculated. It has been suggested that we use heavy nuclei instead of protons [Morgan 1975, 1982]. The antiprotons would be attracted to the heavy nucleus and annihilate with one of the protons or neutrons. The pions would immediately transfer their energy to the rest of the nucleons, lowering the specific impulse and increasing the efficiency for subrelativistic missions. This approach has the advantage that the energy in the neutral pions is not lost, but the disadvantage that any energetic neutrons generated will be lost and will add to the shielding problem. This interaction needs to be calculated and perhaps checked by experiments with antiprotons interacting with heavy nuclei.

CASSENTI ANALYSIS OF ANTIMATTER POWERED MISSION

In some very preliminary studies of an antihydrogen/hydrogen rocket, Cassenti has estimated some of the parameters in an antimatter powered orbit transfer mission. The mission was to take a 10 ton spacecraft from LEO to GEO back to LEO (using aeroassist). The mission delta vee was assumed to be 5.5 km/sec. Using the Dipprey minimum antimatter optimization, Cassenti found that the optimum exhaust velocity was 3.4 km/sec (specific impulse of only 350 sec), the reaction mass required was 40 tons, and the amount of antihydrogen needed was only 6 mg. The energy efficiency of this model was only 23% and both Cassenti and Morgan think that this can be raised significantly (35 to 50%) by annihilation of the antiprotons in heavy nuclei rather than hydrogen. If the amount of antihydrogen used is raised from 6 mg to 10 mg, then the amount of hydrogen reaction mass drops dramatically, from 40 tons to 15 tons, with the exhaust velocity

rising to 5 km/sec. Thus, in this range of the parameters, an additional 4 mg of antihydrogen saves 25 tons of reaction mass. Whether this trade-off is worth it depends upon the relative cost of antihydrogen per milligram compared to the cost of hydrogen per ton in LEO.

ANTIHYDROGEN FACTORY - ESTIMATED ENERGY EFFICIENCIES

In Figure 1-9 I make a first cut at an estimate for the energy efficiency of a factory for producing antihydrogen fuel for propulsion.

The present dc to RF and RF to beam energy efficiencies of proton accelerators are quite high, especially if superconducting magnets are used. The real losses come in the conversion of the high energy protons into a fraction of an antiproton. The rest of the estimates are purely optimistic guesses as to what a well designed antihydrogen factory should be able to do.

If all these efficiencies hold, then an antihydrogen factory should be able to produce antimatter fuel with an energy efficiency of better than 0.01%.

	<u>EFFICIENCY</u>
DC MAINS TO RF	0.75
RF TO 200 GeV PROTONS	0.95
0.2 \bar{p}/p ($\epsilon = 0.2 \times 0.938 \text{ GeV} \times 2/200 \text{ GeV}$)	0.002
ANTIPROTON CAPTURE - ANGULAR SPREAD	0.50
ANTIPROTON CAPTURE - MOMENTUM SPREAD	0.50
STOCHASTIC COOLER LOSSES	0.90
DECELERATOR LOSSES	0.90
ELECTRON COOLER LOSSES	0.90
CONVERSION TO ANTIHYDROGEN ATOMS	0.90
ATOMIC BEAM SLOWING AND COOLING	0.90
TRAP LOSSES	0.90
EXTRACTION LOSSES	0.90
 TOTAL ENERGY EFFICIENCY	1.7×10^{-4}

Figure 1-9
Estimated energy efficiency of an antiproton factory

ANTIPROTON FUEL COST ESTIMATES

A large prime power plant (Grand Coulee Dam or a modern nuclear plant) generates 5 GW of power, while the designs for the proposed Solar Power Satellites go up to 10 GW. A 10 GW power plant produces the equivalent of 3.5 kilograms of energy per year. If a reasonable fraction of that energy could be converted into antimatter and stored, then one such plant could provide enough antimatter for a large Air Force space program.

If antiproton annihilation turns out to be a viable propulsion technique, it would not be desirable for safety or environmental reasons to have the antiproton production facility or its power plants on the earth. The facility should be out in space, powered by sunlight (probably solar thermal rather than solar photovoltaic) where the high vacuum and low gravity aids in the design of the proton accelerators and the antiproton collectors.

Since the sunlight is free, we can assume that the fuel cost is zero. However, we have to amortize the cost of building the power plant and the antihydrogen factory, which I estimate to cost \$3.5B/year (roughly a billion dollars per kilogram of raw energy).

If the antiproton factory is run at an efficiency of 0.01%, then it will produce about 350 milligrams of antihydrogen per year at roughly 10 million dollars per milligram.

Since hydrogen reaction mass (or any fuel) in space costs on the order of five thousand dollars per kilogram to lift it into LEO, we find that reaction mass costs about five million dollars per ton. Thus, in cost, a milligram of antimatter is equivalent to two tons of fuel, depending upon assumed launch costs. As was seen in the earlier Cassenti study, an additional 4 milligrams (\$40M) of antimatter fuel in the rocket saved 25 tons (\$125M) of reaction mass. Thus, although these cost estimates are far from firm, it looks as though antimatter might be a cost-effective fuel for space propulsion.

ANTIPROTON ANNIHILATION PROPULSION - CONCLUSIONS

Our major conclusion about antiproton propulsion is that the concept is feasible but expensive. Yet, despite the high cost of antimatter, it may be a cost effective fuel in space where any fuel is expensive. There is high risk in the development of antiproton propulsion. The major uncertainties seem to be in the efficient production and capture of the antiprotons to keep the cost of the antimatter down. The storage problems look tractable.

Although initial studies can be done using earth-based machines, the antiproton factory will probably have to be made in space where the vacuum, real-estate, gravity, shielding, and safety

problems are eased. This implies a large, front-end capital investment that can only be sold as part of a large Air Force manned presence in space.

The problems that need working on first are to determine the total antiproton production rate and spectrum versus proton energy, the maximum feasible limits to antiproton capture efficiencies of physically feasible lenses and accumulator rings, and the maximum efficiency of the antimatter rocket that uses the antiproton fuel.

ANTIPROTON ANNIHILATION PROPULSION - RECOMMENDATIONS

It is recommended that the Air Force work with DOE and the various National Laboratories to obtain the data needed to accurately determine the antiproton production spectrum at various proton beam energies and with various targets. In addition, particle accelerator designers should be asked to look at designs for high current machines suitable for an antiproton factory instead of higher voltage designs that are the trend of current elementary particle physics efforts.

Knowledge of the interaction of antimatter with normal matter at very low relative velocities and the type and spectrum of the resulting particles is essential in determining the efficiency of an antimatter rocket. The more efficiently the rocket uses the antimatter, the less antimatter we need to make for a given mission. Research is needed to determine the annihilation cross-sections at low energy and their impact on the design of antimatter rockets.

If the efficiencies of production and utilization of antimatter hold up (or are improved over the present estimates), then research on the other aspects of antimatter propulsion such as trapping and cooling of atoms and molecules should be supported. Research on control of hydrogen atoms and molecules should replace the present research on easy-to-control alkali metal atoms as soon as feasible.

ANTIPROTON ANNIHILATION BIBLIOGRAPHY

A.I. Ageyev, et al., "The IHEP accelerating and storage complex (UNK) status report", pp. 60-70, Proc. 11th Int. Conf. High Energy Accelerators, Geneva (1980).

L.E. Agnew, Jr., et al., "Antiproton interactions in hydrogen and carbon below 200 MeV", Phys. Rev., 118, 1371 (1960).

M. Antinucci, et al., "Multiplicities of charged particles up to ISR Energies", Lett. Nuovo Cimento 6, 121-127 (1972).

R. Armenteros and B. French, "Antinucleon-nucleon interactions", in **High Energy Physics - Vol. V**, E. Burhop, ed., Academic Press, New York (1969), pp. 237-410.

A. Ashkin, Phys. Rev. Lett. **25**, 1321 (1970).

A. Ashkin and J.M. Dziedzic, "Optical levitation in high vacuum", Appl. Phys. Lett., **28**, 333-335 (1976).

A. Ashkin, "Trapping of atoms by resonance radiation pressure", Phys. Rev. Lett. **40**, 729-732 (1978).

A. Ashkin and J.P. Gordon, "Cooling and trapping of atoms by resonance radiation pressure", Optics Lett. **4**, 161-163 (1979).

V.I. Balykin, V.S. Letokhov, and V.I. Mishin, "Observation of the cooling of free sodium atoms in a resonance laser field with a scanning frequency", JETP Lett. **29**, 561-564 (1979).

V.I. Balykin, V.S. Letokhov, and V.I. Mishin, "Cooling of sodium atoms by resonant laser emission", Sov. Phys. JETP **51**, 692-696 (1980).

M.Q. Barton, et al., "Minimizing energy consumption of accelerators and storage ring facilities [panel discussion]", pp. 898-908, Proc. 11th Int. Conf. High Energy Accelerators, Geneva (1980).

B.F. Bayanov, et al., "The antiproton target station on the basis of lithium lenses", pp. 362-368, Proc. 11th Int. Conf. High Energy Accelerators, Geneva (1980).

M. Bell, et al. "Electron cooling in ICE at CERN", Nuc. Inst. Methods **190**, 237-255 (1981).

J.E. Bjorkholm, R.R. Freeman, A. Ashkin, and D.B. Pearson, "Observation of focusing of neutral atoms by the dipole forces of resonance-radiation pressure", Phys. Rev. Lett. **41**, 1361-1364 (1978).

R. Blatt, W. Ertmer, and J.L. Hall, "Cooling of an atomic beam with frequency-sweep techniques", pp. 142-153, **Laser-Cooled and Trapped Atoms**, NBS SP-653, W.D. Phillips (editor) (1983).

L.N. Breusova, et al., "Vacuum ultraviolet H₂ laser with a sealed gas-discharge cell", Sov. J. Quantum Elec. **9**, 1452-1453 (1979).

G.I. Budker and A.N. Skrinskii, "Electron cooling and new possibilities in elementary particle physics", Sov. Phys. Usp. **21**, 277-296 (1978).

D.C. Carey, et al., "Unified description of single-particle production in pp collisions", Phys. Rev. Lett. **33**, 330-333 (1974).

B.N. Cassenti, "Design considerations for relativistic antimatter rockets", J. Brit. Int. Soc., 35, 396-404 (1982).

B.N. Cassenti, "Optimization of relativistic antimatter rockets", AIAA Reprint 83-1343, 19th Joint Propulsion Conf., Seattle, WA (1983).

F.R. Chang and J.L. Fisher, "The hybrid plume plasma rocket", Draper Lab preprint (1983).

G. Chapline, "Antimatter Breeders?" J. Brit. Int. Soc., 35, 423-424 (1982).

B.V. Chirikov, et al., "Optimization of antiproton fluxes from targets using hadron cascade calculations", Nuc. Inst. & Meth. 144, 129-139 (1977).

R.W. Cline, et al., "Magnetic confinement of spin-polarized atomic hydrogen", Phys. Rev. Lett., 45, 2117-2120 (1980).

D.B. Cline, et al., "Initial operation of the Fermilab antiproton cooling ring", IEEE Trans. Nuc. Sci. NS-26, 3158-3160 (1979).

D.B. Cline, "The development of bright antiproton sources and high energy density targeting", pp. 345-361, Proc. 11th Int. Conf. High Energy Accelerators, Geneva (1980).

D.B. Cline, C. Rubbia, and S. van der Meer, "The search for intermediate vector bosons", Scientific American 247, No. 3, 48-59 (March 1982).

R.J. Cook and R.K. Hill, "An electromagnetic mirror for neutral atoms", Optics Comm. 43, 258-260 (1982).

D.F. Dipprey, "Matter-Antimatter Annihilation as an Energy Source in Propulsion", Appendix in "Frontiers in Propulsion Research", JPL TM-33-722, D.D. Papailiou, Editor, Jet Propulsion Lab, Pasadena, CA 91109 (15 March 1975).

R. Forster, et al., "Electron cooling experiments at Fermilab", IEEE Trans. Nuc. Sci. NS-28, 2386-2388 (1981).

R.L. Forward, "Interstellar flight systems", AIAA Reprint 80-0823, AIAA Int. Meeting, Baltimore, MD (1980).

R.L. Forward, "Antimatter propulsion", J. Brit. Int. Soc., 35, 391-395 (1982).

J. Gareyte, "The CERN proton-antiproton complex", pp. 79-90, Proc. 11th Int. Conf. High Energy Accelerators, Geneva (1980).

J.P. Gordon and A. Ashkin, "Motion of atoms in a radiation trap", Phys. Rev. A21, 1606-1617 (1980).

- H. Herr and C. Rubbia, "High energy cooling of protons and antiprotons for the SPS collider", pp. 825-829, Proc. 11th Int. Conf. High Energy Accelerators, Geneva (1980).
- C. Hojvat and A. Van Ginneken, "Calculation of antiproton yields for the Fermilab antiproton source", Nuc. Inst. Methods **206**, 67-83 (1983).
- H. Hora, "Estimates for the efficient production of antihydrogen by lasers of very high intensities", Opto-Electronics **5**, 491-501 (1973).
- L. Hütten, H. Poth and A. Wolf, "The electron cooling device for LEAR", CERN/PS/LI 82-9, LEAR Workshop, Erice, Sicily (9-16 June 1982).
- R. Hyde, L. Wood, and J. Nuckolls, "Prospects for rocket propulsion with laser induced fusion microexplosions", AIAA Paper 72-1063 (Dec 1972).
- W. Kells, "Advanced stochastic cooling mechanisms", IEEE Trans. **NS-28**, 2459-2461 (1981).
- W. Kells, et al. "Electron cooling for the Fermilab antiproton source", IEEE Trans. **NS-28**, 2583-2584 (1981).
- T.B.W. Kirk, "Antiproton production target studies - numerical calculations", Fermilab TM-1011 (14 Nov 1980).
- W. Kolos, D.L. Morgan, D.M. Schrader, and L. Wolniewicz, "Hydrogen-antihydrogen interactions", Phys. Rev. **A11**, 1792-1796 (1975).
- F. Krienen, "Initial cooling experiments (ICE) at CERN", pp. 781ff, Proc. 11th Int. Conf. High Energy Accelerators, Geneva (1980).
- F. Krienen and J.A. MacLachlan, "Antiproton collection from a production target", IEEE Trans. **NS-28**, 2711-2716 (1981).
- G. Lambertson, et al., "Experiments on stochastic cooling of 200 MeV protons", IEEE Trans. Nucl. Sci. **NS-28**, 2471-2473 (1981).
- P. Lefèvre, D. Möhl, G. Plass, "The CERN low energy antiproton ring (LEAR) project", pp. 819-823, Proc. 11th Int. Conf. High Energy Accelerators, Geneva (1980).
- V.S. Letokhov, JETP Lett. **7**, 272 (1968).
- V.S. Letokhov, V.G. Minogin and B.D. Pavlik, "Cooling and capture of atoms and molecules by a resonant light field", Sov. Phys. JETP, **45**, 698-705 (1977).

V.S. Letokhov and V.G. Minogin, "Possibility of accumulation and storage of cold atoms in magnetic traps", Optics Comm., 35, 199-202 (1980).

V.S. Letokhov and V.G. Minogin, "Laser radiation pressure on free atoms", Phys. Reports 73, 1-65 (1981) [review].

M.S. Lubell and K. Rubin, "Velocity compression and cooling fo a sodium atomic beam using a frequency modulated ring laser", pp. 125-136, **Laser-Cooled and Trapped Atoms**, NBS SP-653, W.D. Phillips (editor) (1983).

P.F. Massier, "The need for expanded exploration of matter-antimatter annihilation for propulsion application", J. Brit. Int. Soc., 35, 387-390 (1982).

E. Mallove, R.L. Forward, Z. Paprotny, and J. Lehmann, "Interstellar travel and communication: a bibliography", J. Brit. Int. Soc., 33, 201-248 (1980) [entire issue].

H.J. Metcalf, "Magnetic trapping of decelerated neutral atoms", **Laser-Cooled and Trapped Atoms**, NBS SP-653, W.D. Phillips (editor) (1983).

H.-J. Möhring and J. Ranft, "Antiproton production from extended targets using a weighted Monte Carlo hadron cascade model", Nuc. Inst. & Meth. 201, 323-327 (1982).

D.L. Morgan and V.W. Hughes, "Atomic processes involved in matter-antimatter annihilation", Phys. Rev. D2, 1389-1399 (1970).

D.L. Morgan and V.W. Hughes, "Atom-antiatom interactions", Phys. Rev. A7, 1811-1825 (1973).

D.L. Morgan, "Rocket thrust from antimatter annihilation", JPL Contractor Report CC-571769, Jet Propulsion Lab, Pasadena, Calif. (1975).

D.L. Morgan, "Coupling of annihilation energy to a high momentum exhaust in a matter-antimatter annihilation rocket", JPL Contract Report JS-651111 (1976)

D.L. Morgan, "Concepts for the design of an antimatter annihilation rocket", J. Brit. Int. Soc., 35, 405-412 (1982).

R. Neumann, H. Poth, A. Winnacker, and A. Wolf, "Laser-enhanced electron-ion capture and antihydrogen formation", Z. Phys. A, 313, 253-262 (1983).

W.D. Phillips and H.J. Metcalf, "Laser deceleration of an atomic beam", Phys. Rev. Lett., 48, 596-599 (1982).

W.D. Phillips (editor), **Laser-cooled and trapped atoms**, NBS Special Publication 653, Proc. Workshop on Spectroscopic Applications of Slow Atomic Beams, NBS Gaithersburg, MD (14-15 April 1983).

W.D. Phillips, J.V. Prodan, and H.J. Metcalf, "Neutral atomic beam cooling experiments at NBS", pp. 1-8, **Laser-Cooled and Trapped Atoms**, NBS SP-653, W.D. Phillips (editor) (1983).

Physics Today, "CERN builds proton-antiproton ring; Fermilab plans one", Search and Discovery Section, Physics Today, 32, No. 3, 17-19 (March 1979).

J.V. Prodan, W.D. Phillips, and H.J. Metcalf, "Laser production of a very slow monoenergetic atomic beam", Phys. Rev. Lett. 49, 1149-1153 (1982).

J.V. Prodan and W.D. Phillips, "Chirping the light -- fantastic?", pp. 137-141, **Laser-Cooled and Trapped Atoms**, NBS SP-653, W.D. Phillips (editor) (1983).

W-K Rhim, M.M. Saffren, and D.D. Elleman, "Development electrostatic levitator at JPL", pp. 115-119 of **Materials Processing in the Reduced Gravity Environment of Space**, G.E. Rindone, ed., Elsevier Science (1982)

A.L. Robinson, "CERN sets intermediate vector boson hunt", Science 213, 191-194 (10 July 1981).

E. Sänger, "The theory of photon rockets", Ing. Arch. 21, 213 (1953) [in German].

R. Sprink, J.T.M. Walraven, and I.F. Silvera, "Compression of spin-polarized hydrogen to high density", Phys. Rev. Lett. 51, 479-482 (1983).

W.C. Stwalley, "A hybrid laser-magnet trap for spin-polarized atoms", pp. 95-102, **Laser-Cooled and Trapped Atoms**, NBS SP-653, W.D. Phillips (editor) (1983).

F.E. Taylor, et al., "Analysis of radial scaling in single-particle inclusive reactions", Phys. Rev. D14, 1217-1242 (1976).

S. van der Meer, "Stochastic cooling in the CERN antiproton accumulator", IEEE Trans. NS-28, 1994-1998 (1981).

T. Vsevolozskaya, et al., "Antiproton source for the accelerator-storage complex, UNK-IHEP", Fermilab Report FN-353 8000.00 (June 1981), a translation of INP Preprint 80-182 (December 1980).

T.A. Vsevolozskaya, "The optimization and efficiency of antiproton production within a fixed acceptance", Nuclear Inst. & Methods 190, 479-486 (1981).

G. Vulpetti, "A propulsion-oriented synthesis of the antiproton-nucleon annihilation experimental results", submitted to J. Brit. Int. Soc. (1983a)

G. Vulpetti, "An approach to the modeling of matter-antimatter propulsion systems", submitted to J. Brit. Int. Soc. (1983b).

R.D. Waldron, "Diamagnetic levitation using pyrolytic graphite", Rev. Sci. Inst. 37, 29-34 (1966).

D.J. Wineland, R.E. Drullinger, and F.L. Walls, "Radiation-pressure cooling of bound resonant absorbers", Phys. Rev. Lett. 40, 1639-1642 (1978).

W.H. Wing, "Electrostatic trapping of neutral atomic particles", Phys. Rev. Lett., 45, 631-634 (1980).

W.H. Wing, "Some problems and possibilities for quasistatic neutral particle trapping", pp. 74-93, **Laser-Cooled and Trapped Atoms**, NBS SP-653, W.D. Phillips (editor) (1983a).

W.H. Wing, "Gravitational effects in particle traps", p. 94, **Laser-Cooled and Trapped Atoms**, NBS SP-653, W.D. Phillips (editor) (1983b).

D.E. Young, "The Fermilab proton-antiproton collider", IEEE Trans. NS-28, 2008-2012 (1981)

D.E. Young, "Progress on beam cooling at Fermilab", pp. 800 ff, Proc. 11th Int. Conf. High Energy Accelerators, Geneva (1980).

R.R. Zito, "The cryogenic confinement of antiprotons for space propulsion systems", J. Brit. Int. Soc., 35, 414-421 (1982).

R.R. Zito, "Chain reactions in a hydrogen-antiproton pile", J. Brit. Int. Soc., 36, 308-310 (1983).

SECTION 2

SOLAR HEATED PLASMA PROPULSION

The space environment is full of sunlight, 1.4 kilowatts per square meter or 1.4 gigawatts per square kilometer at the orbit of the earth. It is a significant source of energy that is free for the taking. All we need to do is find good ways to collect that sunlight and turn it into propulsion energy. One method, already in use in solar electric propulsion, is to convert the sunlight into electricity with solar cells, then use the electricity to power an electric thruster. The low energy conversion efficiencies and the high specific mass of solar cells limit these systems to low thrust levels. Another method of using the sunlight in space is to use large solar sails driven by the photon momentum. Again, these systems are limited to low thrust levels because of the very high (theoretically infinite) specific impulse of the propulsion method. In this section we will discuss various versions of the solar thermal rocket, where sunlight is collected and used to directly heat a working fluid. This solar heated thermal rocket is one subclass of a more general class of rocket, radiation heated thermal rockets. This class of rocket collects propulsion energy in the form of radiation (sunlight, laser light, microwaves, etc.) from some distant source, and uses the energy to heat some working fluid (hydrogen, water, carbon or metal seeded hydrogen) which produces thrust when expanded through a nozzle.

RADIATION HEATED THERMAL ROCKETS - SOLAR vs. LASER

There are two basic types of radiation that can be used to power a radiation heated rocket. One is incoherent radiation such as sunlight. The other is coherent radiation such as microwaves or laser light. Coherent radiation can be brought to an intense focus to create very high temperatures. Focused sunlight can only produce a temperature that is less than or at most equal to the temperature of the sun itself (5800 K). This limits the maximum specific impulse obtainable from a solar heated thermal rocket to about 1500 sec.

Because of this temperature limit, as well as other desirable features of coherent radiation, most of the advanced propulsion efforts on radiation heated thermal rockets have been on laser propulsion systems. Work on the propulsion aspects of this concept is well underway at NASA/Marshall and NASA/Lewis [Jones and Keefer 1982] and work on the high power lasers and the pointing and tracking optics is well underway on a number of DOD and DOE high power laser programs.

Yet, a realistic evaluation of the complexity and cost of a laser thermal rocket system must include the complexity and cost of the laser source and the transmission optics, not just the collecting optics and the laser rocket engine. Laser thermal rockets are certainly worth studying, but it will be many years before they come into being, and they will always be more expensive to operate than a solar thermal rocket. Solar thermal rocket can give a significant improvement in performance over a chemical rocket, the energy source (sunlight) is available now, and the energy is free. These incoherent cousins of the laser rockets deserve more attention by the advanced propulsion community.

SOLAR THERMAL ROCKETS

A generic example of a solar thermal rocket vehicle is shown in Figure 2-1. The collector consists of two large inflatable mirrors with an elliptical cross-section 23 m wide by 40 m long. They rotate about two axes so that they can collect sunlight independent of the relative orientation of the thrust vector and the sun angle. The light is directed to a focus inside the thermal thruster. The type of thermal thruster can vary depending upon the technology used to convert the sunlight into thrust. The vehicle was designed by Rockwell under an AFRPL contract [Etheridge 1979]. The study considered two different types of solar thermal engines. One used hydrogen passed through a black-body metallic heat exchanger that had an estimated specific impulse of 872 sec. The other had a windowed chamber type of thruster and a carbon-particle-laden hydrogen flow with a specific impulse of 1041 sec.

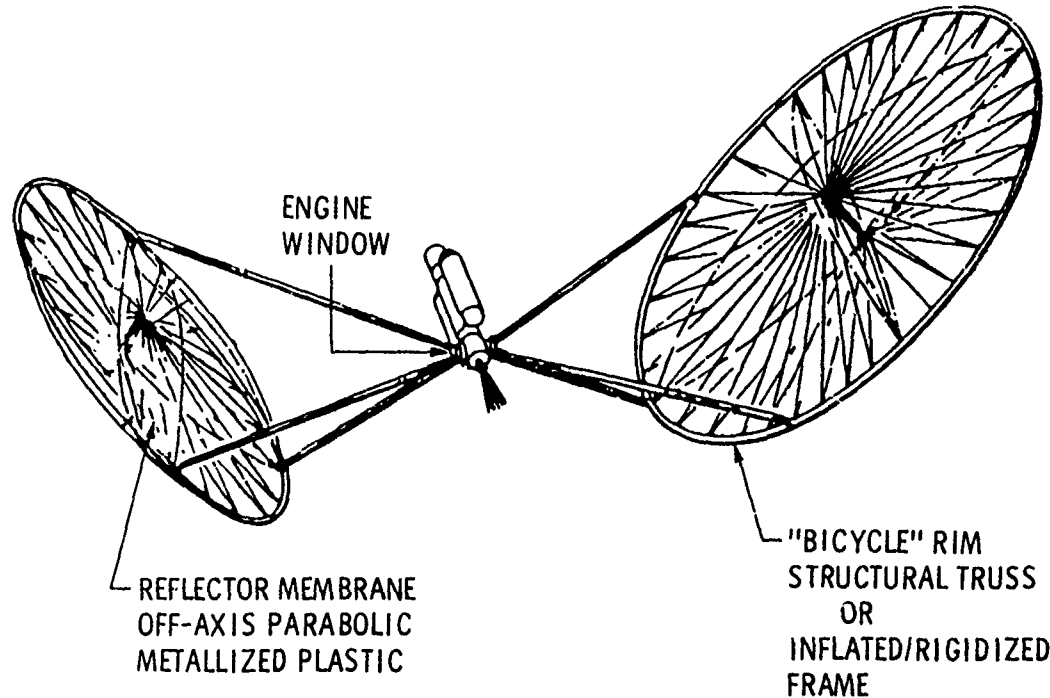


Figure 2-1
Solar thermal rocket [Etheridge 1978]

There are four different types of solar thermal thruster designs that have been looked at.

Heat Exchanger Absorber - In the heat exchanger absorber thruster design, the sunlight is absorbed by a dark heat exchanger made of refractory metal or ceramic which transfers the heat to hydrogen or some other reaction fluid that is expelled to provide thrust. A ground test heat exchanger absorber/thruster system is being fabricated by Rockwell/Rocketdyne for the AFRPL [Shoji 1983]. The thruster will be tested in the new Solar Concentrator Facility at the AFRPL. The melting point of the rhenium tubing used for the heat exchanger limits the operational temperature of the Air Force thermal thruster to 2750 K and the specific impulse to 800 sec.

Particulate Seed Absorber - By seeding hydrogen gas with 0.2 micron carbon particles, the sunlight can be absorbed by the carbon particles and the heat transferred rapidly to the hydrogen. Temperatures of 3900 K can be reached this way, but the mass of the seed keeps the specific impulse down. A Rockwell study indicated that a specific impulse of 1041 sec could be reached [Etheridge 1979], while a later study felt that the specific impulse would be less than 1000 sec [Boeing 1981].

Rotating Bed Absorber - By flowing hydrogen through a bed of 100 micron tantalum carbide particles temperatures of 4000 K can be reached. By retaining the particles using centrifugal force supplied by a rotating chamber, the specific impulse reaches 1100 sec [Boeing 1981]. Although this approach gives the highest specific impulse, it is felt that the complexity and weight of the rotating bed makes this concept less desirable than the solar heated plasma version.

Alkali Metal Plasma Absorber - The most promising solar heated rocket concept and the one recommended for further study is the solar sustained alkali metal plasma thruster. The sunlight is absorbed in a small amount of alkali metal vapor which transfers the energy to hydrogen. Temperatures in excess of 3900 K and specific impulses of 1000 sec are predicted for this system [Rault and Hertzberg 1983]. These performance numbers are only estimates and need to be substantiated by laboratory studies of the interaction of sunlight with alkali metal plasmas and the interaction of the heated plasmas with the hydrogen reaction mass. We need to determine the conversion efficiency of sunlight into thrust taking into account all of the loss processes and the percentage amounts and types of alkali metal seedant needed to absorb the sunlight and the effect of that seedant mass on the specific impulse.

SOLAR HEATED PLASMA THRUSTER

The basic concept of a solar heated plasma thruster is shown in Figure 2-2 [Rault and Hertzberg 1983]. It consists of a main reaction chamber with a sapphire window at one end and the exhaust nozzle at the other. Surrounding the window is a black coated flat disc preheater which absorbs the sunlight falling outside the main high intensity beam. The high intensity sunlight is transmitted through the window which is cooled on its inner face with pure hydrogen which does not absorb the sunlight. The premixed alkali-hydrogen propellant is preheated by regeneration in the chamber walls or the front disc preheater to above 1200 K. This keeps the alkali metal in a "dry" vapor state with no condensate droplets. The heated alkali-hydrogen propellant then enters the core of the reaction chamber where the alkali metal vapor absorbs the sunlight and transfers the energy to the hydrogen reaction mass.

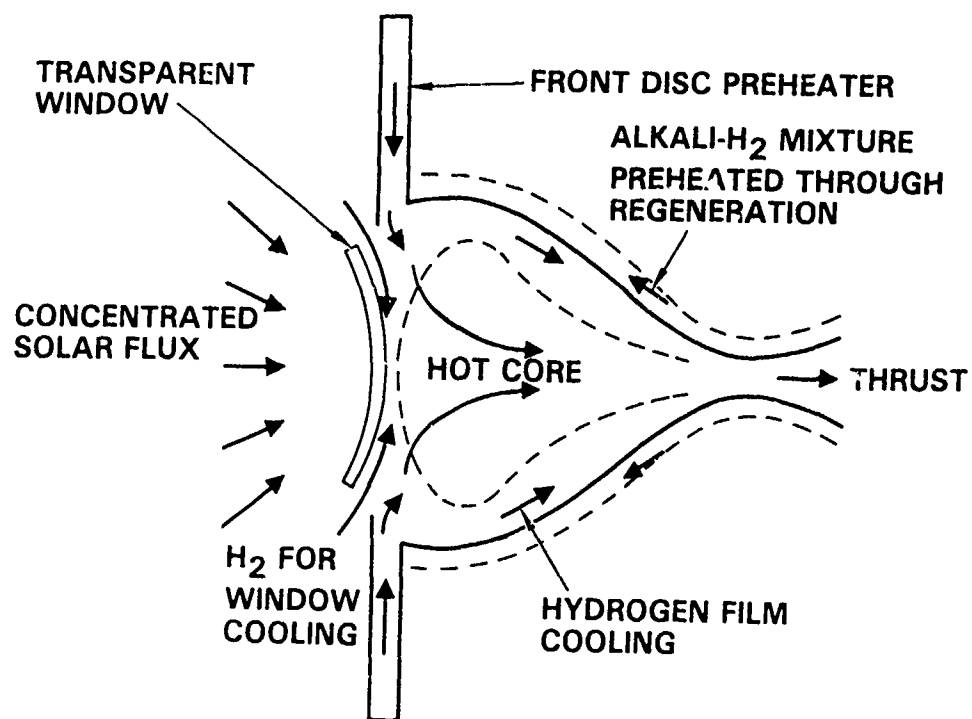


Figure 2-2
Solar heated plasma thruster

In the solar heated plasma thruster the concentrated sunlight is transmitted through a transparent window and absorbed within an internal volume of alkali metal vapor. In this gaseous volume absorber concept, the reradiated infrared energy from the hot gasses downstream is partially reabsorbed by the cooler gases entering the receiver near the front window. As is shown in Figure 2-3, the reradiation losses from this volumetric alkali metal absorber are much lower than the reradiation losses from a blackbody surface absorber [Mattick et al. 1979]. The volumetric absorber can operate at a higher temperature than a blackbody absorber because it is not limited by the melting point of materials. In addition, because the reradiation losses in a volumetric absorber are less, it maintains a high collection efficiency even at very high temperatures where a blackbody radiator is emitting as much energy in the infrared as it is absorbing in the visible.

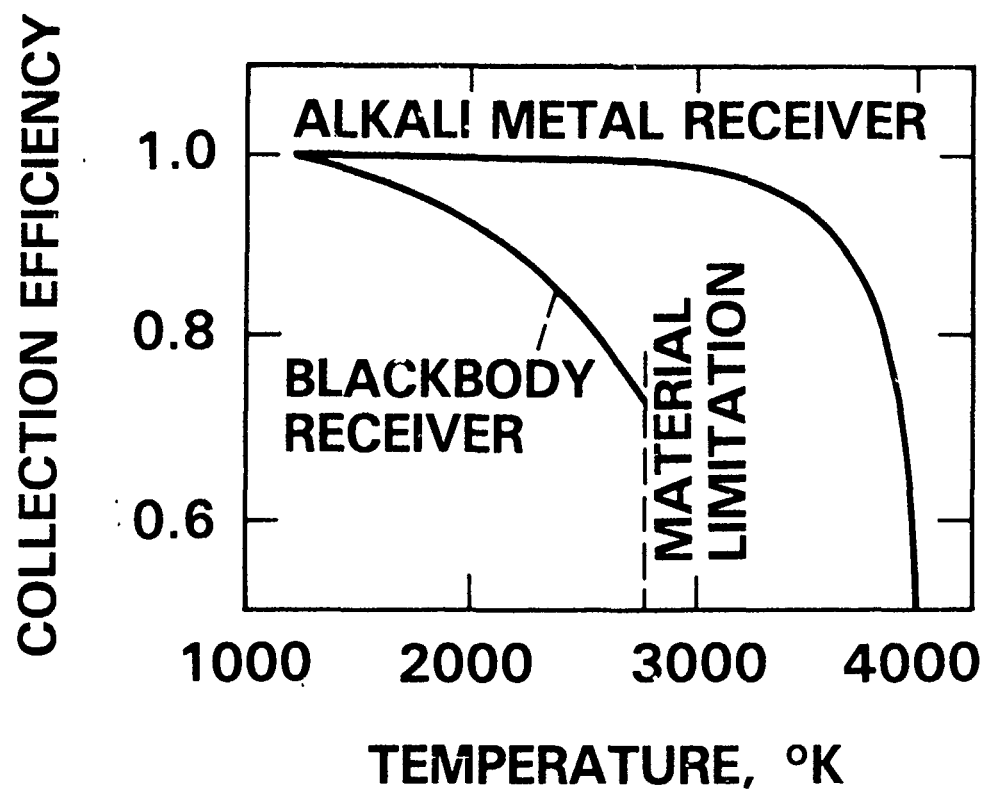


Figure 2-3
Volumetric and blackbody receiver performance

POTASSIUM ABSORPTION SPECTRUM AND SPACE SOLAR SPECTRUM

An example of the predicted absorption of a hot plasma of potassium vapor over the wavelength region covered by the solar emission spectrum is shown in Figure 2-4 [Hertzberg et al. 1978]. As can be seen, there is a transmission band predicted for the green part of the visible spectrum. This prediction has been confirmed by recent work at Columbia and Princeton University, where a stream of hot potassium vapor was found to look green in transmitted light [Ligere 1983, Ligere et al. 1983]. A similar stream of hot sodium vapor did not transmit green light, so a mixture of the two should be quite "black" from the ultraviolet to the long infrared.

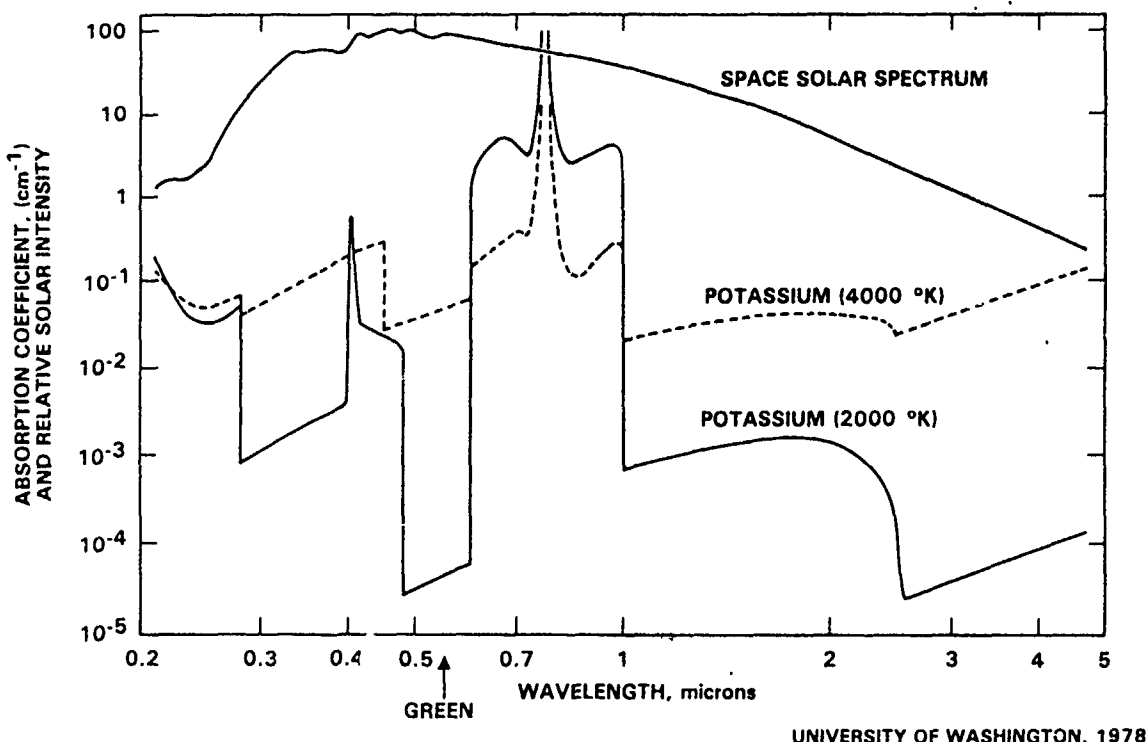


Figure 2-4
Potassium absorption spectrum and space solar spectrum

SOLAR HEATED PLASMAS - CONCLUSIONS

From a review of the literature in solar heated plasmas and discussions with the principal investigators in the field, we have concluded that solar heated plasmas are a promising advanced propulsion research field for the Air Force Rocket Propulsion Laboratory to engage in, both through contract work and in-house efforts. The research is obviously an excellent extension to the ongoing AFRPL solar thermal rocket program. The potential for doubling the specific impulse over chemical rockets while maintaining reasonably high thrust levels gives adequate justification for the research.

A significant advantage of solar heated thrusters is that if the research and development work at the AFRPL produces a good thruster design, then the thruster can be developed into a usable flight propulsion system without having to depend upon concurrent developments elsewhere. This is in contrast to work on laser thrusters where a good thruster design cannot be flight tested until some other branch of DoD or NASA develops the high power laser source and the transmitter optics needed to beam the laser energy to the vehicle optics. Also, unlike R&D in laser thrusters, the characteristics of the radiation source is completely known and the energy costs nothing.

Even if the research in solar heated plasmas uncovers a problem which makes a solar heated plasma thruster unfeasible, the research information will nevertheless be valuable to other programs, such as laser heated thrusters, solar pumped lasers, and solar prime power systems.

SOLAR HEATED PLASMAS - RECOMMENDATIONS

It is recommended that basic research be supported on alkali metal plasmas and their application to solar thermal propulsion. A portion of this work would be done at universities and other research centers, combined with studies carried out in special facilities at the AFRPL.

Alkali metals are dangerous to work with, and when hot alkali metal vapors are combined with hydrogen, the mixture is one that is better handled at the AFRPL than in some basement university laboratory. In addition to the present Solar Concentrator Facility at the AFRPL, it is recommended that the AFRPL consider the construction and operation of a versatile alkali metal research facility, and a alkali metal/hydrogen facility to study the interaction of hot alkali metal plasmas with hydrogen gas at various mixtures and flow rates. All of this will ultimately lead to the design, construction, and bench test of a solar heated plasma rocket.

SOLAR HEATED PLASMAS BIBLIOGRAPHY

Boeing, "Advanced Propulsion Systems - Concepts for Orbital Transfer Study", Final Report, NASA/Marshall Contract NAS8-33935, D.G. Andrews, Boeing Aerospace Company, Seattle, Washington 98124 (July 1980 to July 1981).

G.J. Dunning and A.J. Palmer, "Toward a high-temperature solar electric converter", *J. Appl. Phys.* 52, 7086-7091 (1981).

F.G. Etheridge, "Solar Rocket System Concept Analysis", Final Report on AFRPL Contract F04611-79-C-0007, AFRPL-TR-79-79, Rockwell International, Space Systems Group, Downey, CA 90241 (Nov 1979).

A. Hertzberg, et al, "High temperature solar photon engines", AIAA reprint 78-1177, 11th Fluid and Plasma Dynamics Conf., Seattle, WA (10-12 July 1978).

M.K. Ligare, **Spectroscopy of Dense Potassium Vapors**, Ph.D. Thesis, Columbia University (1983).

M. Ligare, S. Schaefer, J. Huennekens, and W. Happer, "Infrared spectroscopy of a dense potassium vapor jet", Princeton University Physics Department preprint submitted to Optics Communications (1983).

A.T. Mattick, A. Hertzberg, R. Decher, and C.V. Lau, *J. Energy* 3, 30 (1979).

L.W. Jones and D.R. Keefer, "NASA's Laser-Propulsion Project", *Astronautics & Aeronautics*, pp. 66ff (September 1982).

D. Rault, **Radiation energy receiver for high performance energy conversion cycles**, Ph.D. Thesis, Univ. Washington (1983).

D. Rault and A. Hertzberg, "Radiation energy receiver for laser and solar propulsion systems", AIAA reprint 83-1207, 19th Joint Propulsion Conf., Seattle, WA (27-29 June 1983).

R.J. Rodgers, N.L. Krascella, and J.S. Kendall, "Solar Sustained Plasma/Absorber Conceptual Design", Final Report, NASA/Ames Contract NAS2-10010, United Technologies Research Center, East Hartford, Conn. (Feb 1979).

J.M. Shoji, "Performance potential of advanced solar thermal propulsion", AIAA preprint 83-1307, 19th Joint Propulsion Conf., Seattle, WA (27-29 June 1983).

SECTION 3

PERFORATED SOLAR SAILS

One of the known alternate propulsion energy sources in space is sunlight. If the collecting structures are large enough, the amount of power available becomes enormous -- 1.4 GW/km^2 . One way of obtaining thrust from this power is to attach a large, light-reflecting sail to a payload. The light reflecting from the sail will produce a force per unit area F that is proportional to the incident power per unit area P divided by the speed of light c :

$$F = 2P/c .$$

The factor of 2 arises from the double transfer of momentum of the photon to the sail, once as it hits the sail and again as it is reflected from the sail. For a highly reflective sail, the 1.4 GW/km^2 solar flux will produce a force of 9 N/km^2 . This is a reasonable force level considering that the spacecraft requires no fuel and can maintain this thrust level for the life of the spacecraft. To achieve significant accelerations, however, ways must be found to reduce the mass per unit area of the sail without seriously affecting the reflectivity or structural stability.

SOLAR SAILS - PRESENT STATUS

In 1977 a JPL team designed a number of solar sails that would use near term thin film and structures technology to construct a high-performance spacecraft that could reach the very difficult target of the retrograde Halley's Comet [Friedman 1978]. Although many thought that the predicted performance of the solar sails was better than that of a comparable Solar Electric Propulsion System (SEPS), the SEPS was chosen for the mission because the technology was more mature. (The SEPS was later cancelled by Congress.)

The recommended JPL solar sailcraft design used a central mast and booms to spread a square sail 850 meters on a side (1/2 mile) made of 2 micron kapton plastic coated with aluminum. The other side had an emissive coating to improve the thermal performance while the sail was in a "cranking orbit" near the sun to shift from earth orbital coordinates to the retrograde Halley comet orbital coordinates. The sail areal density was 6 grams per square meter and the total sail mass was five tons. Since the sail had to be launched in 1985 to meet the comet in time, no advanced technology was used.

Although improved technologies and designs exist [Drexler 1979] that would make a modern solar sail far exceed an electric propulsion system for many missions, there seems to be no research being supported on these advanced concepts. One small group of engineers [WSF] is attempting to launch a small kapton sail using private funding. Other than that, no activity in solar sail research was found in the United States, and only paper studies in Europe.

The solar sail has a major drawback in that it cannot be launched or operated below about 1000 kilometers. The air drag below this altitude is larger than the solar thrust. On this contract we have invented a version of the solar sail, called a perforated solar sail, that may be able to overcome this problem as well as provide improved performance.

PERFORATED SOLAR SAILS - CONCEPT

It is well known that a microwave reflector does not have to be made of solid metal in order to be a good reflector of microwaves. Many radar dishes, in order to reduce weight and wind loading, are made of wire mesh with holes smaller than the wavelength of the microwave radiation. In the same manner, it should be possible to reduce the mass of a solar sail by fabricating it with holes smaller than a wavelength of most of the light in the solar spectrum. It is also probable that the air drag of a perforated sail will be less than that of a solid sail, especially at high altitudes where the air is in the molecular flow regime. Whether perforated sails can be launched at the upper range of the Shuttle orbital altitude is an unanswered question that can probably only be resolved by a Shuttle flight test.

Techniques exist in the laboratory to make a thin perforated sail. Focused ion beams have already demonstrated the capability to make holes down to 0.1 microns, well below solar light wavelengths. Crossed holographic gratings have already been developed in photosensitive resists and used to make arrays of square posts with 0.2 to 0.5 micron spacing. The use of a positive rather than a negative resist would produce a square grating with similar sized square holes.

A schematic design of a perforated microstructured solar sail is shown in Figure 3-1 [Forward 1983]. The basic concept is to decrease the mass per unit area of an aluminum or aluminum coated kapton sail by making submicron perforations in the sail material. If the holes are significantly smaller than a wavelength of light, the light will be reflected.

Solar sails in earth orbits will not experience high light fluxes, so their normal infrared reradiation will suffice to keep them from melting. If, however, high intensity laser light is

used to push the sail, or the sail is to travel in near the sun during its mission, it will need to have an improved emissivity on the backside to keep the sail temperature below the melting point. The emissivity of a metal surface can be increased over the bulk metal emissivity by constructing microstructures on the backside that have dimensions corresponding to the peak infrared wavelength emitted by the sail at its operational temperature.

In the example shown in Figure 3-1, the microstructures are simple quarter-wave antennas driven at the base by random thermal Nyquist currents. The radiation pattern from these simple spikes is not optimum, being a doughnut shaped pattern with a null in the rearward direction, but there should still be a significant increase in emissivity with these structures. More complicated microstructures such as broadband end-fire antennas or slots may have better emissive properties although they will be more difficult to fabricate.

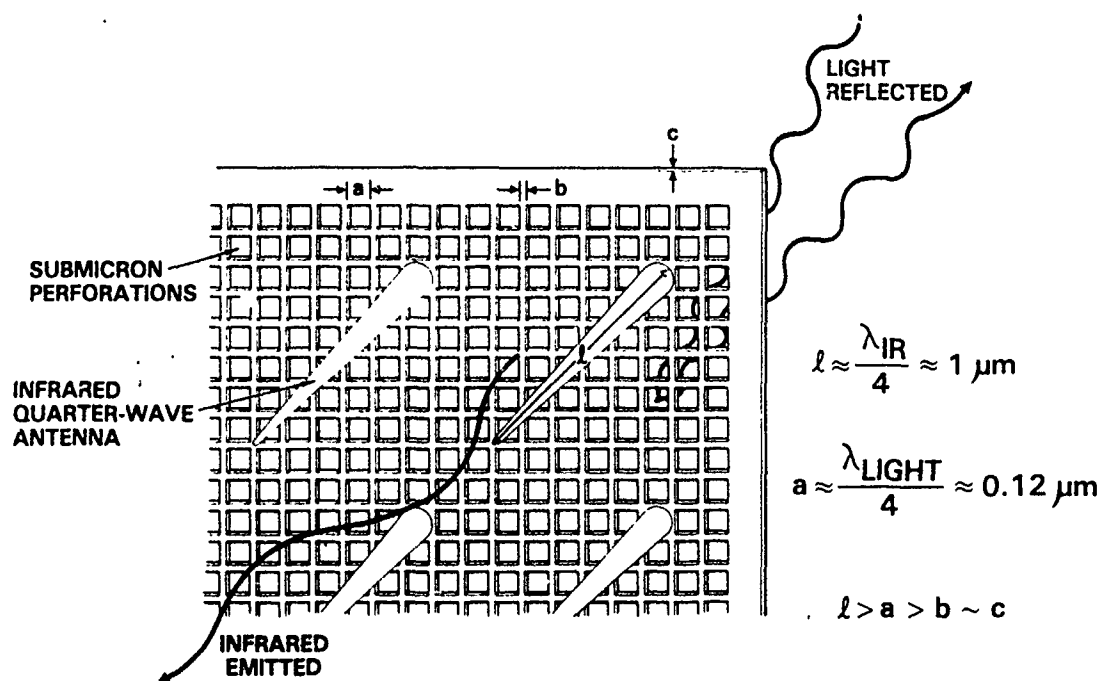


Figure 3-1
Perforated microstructured light sail

PERFORATED SOLAR SAILS - POTENTIAL PAYOFF

If perforated solar sails can be made, then there are significant performance potentials to be gained.

IF the physics cooperates, it may be possible to manufacture and launch perforated solar sails from low earth orbit.

IF the mass of an unfurlable plastic-backed sail can be lowered to 0.1 metric tons per square kilometer by using perforation techniques, then it will have the low mass and performance of an aluminum film sail with the ruggedness and unfurlability of a plastic-backed sail.

IF a perforated aluminum film sail can be made with a 10:1 reduction in mass over a non-perforated film sail, then new missions become possible, such as creating new geostationary orbits that are not on the equator. One such concept is described on the next section.

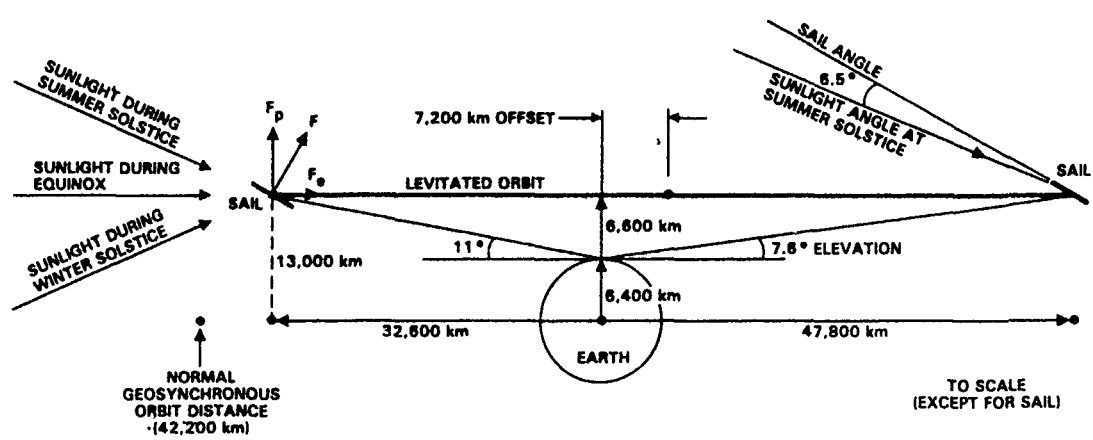
IF microstructures on the backside allow us to make a film that is highly reflective on one side and highly emissive on the other, then this would allow us to operate the sail close to the sun (where the accelerations are higher).

POLAR LEVITATED GEOSTATIONARY ORBITS USING PERFORATED SOLAR SAILS

One of the potential applications of an ultrathin perforated solar sail is to use the light pressure from the sun to levitate the orbit of a geostationary satellite up out of the equatorial plane. At the present time, the only geostationary orbits are those along the equator at 35,800 kilometers altitude (42,200 kilometers from the center of the earth). Although geostationary spacecraft can be seen at the Arctic and Antarctic Circles (depending upon the local horizon topography), they cannot be used by ground stations near the poles.

If a spacecraft were supplied with a lightweight sail, it could use the sunlight to supply a constant force in the poleward direction. This would levitate the orbit out of the equatorial plane and the spacecraft would orbit about a point determined by the relative magnitude of the earth gravity forces and the solar light pressure forces. The amount of displacement above or below the equatorial plane is limited to a few hundred kilometers for unfurlable kapton sails and a few thousand kilometers for very thin aluminum film sails [Forward 1981]. By perforating the sail, however, we can improve the displacement distance significantly. Figure 3-2 shows a geostationary orbit that is levitated by the constant solar pressure 13,000 km northward from the equatorial plane, about twice the radius of the earth. The details of the calculations for this configuration are presented in a paper prepared for journal publication that will be found in Appendix B.

The levitated orbit is noticeably displaced in the direction opposite to the sun. (This effect was noticed on the Echo satellite.) By varying the sail angle with the seasons, the levitated orbit can be kept synchronous with the earth's rotation. The time chosen for Figure 3-2 is at summer solstice, where the sun angle is the worst for providing northward thrust. In this worst case example, the position of the satellite is not truly geostationary. As seen from the north pole, it moves ± 1.7 degrees about its nominal elevation angle of 9.3 degrees. The development of perforated solar sails and their use to create levitated orbits would not only relieve the pressure on the limited number of positions along the equatorial geostationary orbit, but would for the first time provide a true geostationary communications capability to the militarily important polar regions of the earth.



SAIL PARAMETERS

MASS	- 2T (1T PAYLOAD)
DIAMETER	- 12 km
m/A	- 0.013 T/km ²

ORBITAL PARAMETERS

ORBITAL RADIUS	- 40,200 km
ORBITAL OFFSET	- 7,200 km
ORBITAL LEVITATION	- 13,000 km
ORBITAL PERIOD	- 24 hours
POLAR ELEVATION	- 9.3° $\pm 1.7^\circ$ (WORST CASE)

Figure 3-2
Polar levitated geostationary orbits using perforated solar sails

RECOMMENDATIONS

The research tasks that need to be done to check the feasibility of the perforated sails concept are straightforward.

Optical Properties Study - This study would determine how well a perforated light reflector would perform. Using variations on already developed sub-micron microcircuit fabrication techniques, thin self-supported aluminum and aluminum-coated kapton films would be prepared with thicknesses ranging from 10 nm (just below the point where an aluminum film becomes partially transparent) to 5 microns. These films would have holes of varying sizes with differing patterns (square, hexagonal, triangular) and varying thickness of the remaining "wires". The reflectance, emittance, absorptance, and transmittance should then be measured as a function of wavelength, perforation properties, aluminum oxide thickness, and temperature. This data should then provide the basic information needed to determine if perforated solar sails are feasible.

Aerodynamics Study - Along with the optical properties study, it would be desirable to subject the same or similar samples of perforated sail material to atmospheric flows that simulate the range of aerodynamic conditions that are expected to be found at the various shuttle altitudes.

Thermal Properties Study - By using the data obtained from the optical studies, it should be possible to determine the resistance, capacitance, and inductance of the wires and junctions in the perforated structure. Using this information it should be possible to design microstructures to attach to the backside of a perforated sail that will produce a broadband impedance match of the thermal noise currents in the structure to the 377 ohms impedance of space, thus increasing the emissivity of the backside of the perforated sail. Samples of perforated microstructured sails should then be tested under simulated sunlight to determine the improvement in emissivity of the backside and to look for any change in the frontside properties. The thermal studies should also include high temperature tests to measure the agglomeration point of the aluminum as a function of structure and aluminum oxide thickness.

Mechanical Properties Study - A solar sail is not just film. Studies need to be done to design and test truss structures to hold the films that have high strength, low mass, and resistance to catastrophic failure.

Mission Studies - Once we know the optical, thermal, and mechanical properties of the perforated solar sails, then we can finally proceed to studies of the unique missions that these new propulsion systems can perform.

PERFORATED SOLAR SAIL BIBLIOGRAPHY

R.L. Forward, "Light-levitated geostationary cylindrical orbits", J. Astronaut. Sci. 29, 73-80 (1981).

R.L. Forward, "Perforated Microstructured Lightsail", Patent Disclosure F-001, submitted to Air Force under provisions of contract F04611-83-C-0013 (1983).

L. Friedman, et al., "Solar Sailing - The Concept Made Realistic", AIAA Paper 78-82, AIAA 16th Aerospace Sciences Meeting, Huntsville, AL (1978).

K.E. Drexler, "High performance solar sails and related reflecting devices", AIAA paper 79-1418, Fourth Princeton/AIAA Conf. on Space Manufacturing Facilities, Princeton, NJ (14-17 May 1979).

World Space Foundation, Box Y, South Pasadena, California, 91030

(Concluding page of Section 3)

SECTION 4

LASING THE IONOSPHERE

One of the more exotic alternate propulsion energy sources uncovered during the contract is the concept of using large, lightweight mirrors to make the ionosphere lase. In this concept, two mirrors are arranged so that the path between them passes through a region of the atmosphere where some molecular species has a larger number of molecules populating a high energy state than populating a low energy state. This inverted population condition will allow lasing action to take place. As is shown in Figure 4-1, one version of a ionospheric lasing propulsion system would have two spacecraft cooperating with each other, while another would have a ground station cooperating with the using satellite. There could be many variations on this general concept. The standard method of operating a laser is to use a multipass mode, where the resonance gain of the laser mirrors is used to extract energy from a lasing medium with low intrinsic gain. If the lasing medium has a high gain, the laser can operate in a single pass mode to amplify a signal sent from the transmitter to the receiving spacecraft. Other novel proprietary system concepts are described in the Final Program Review Data Package of this contract. Copies can be obtained from the AFRPL address given on the Report Documentation Page.

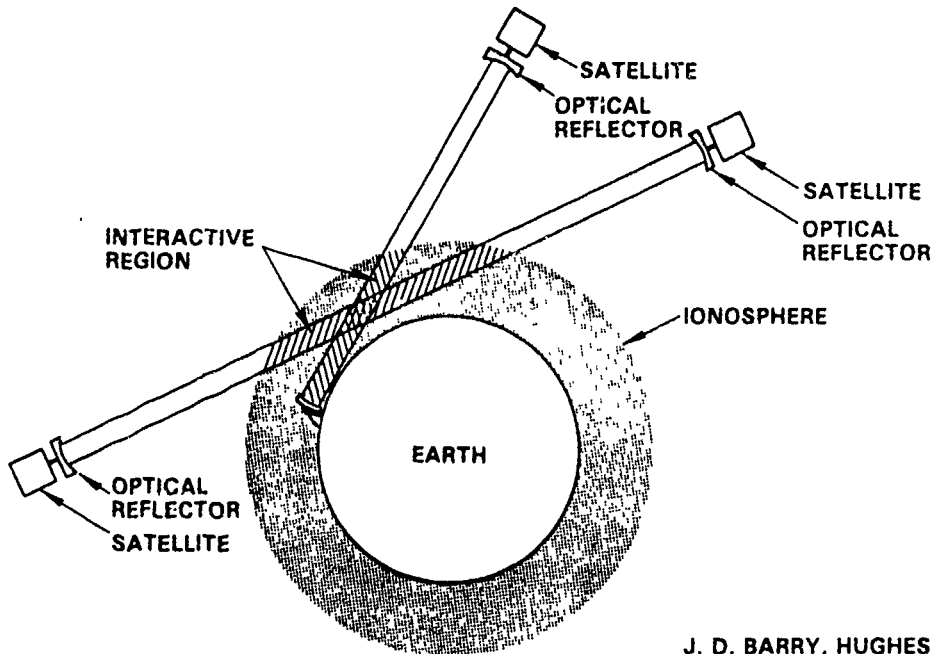


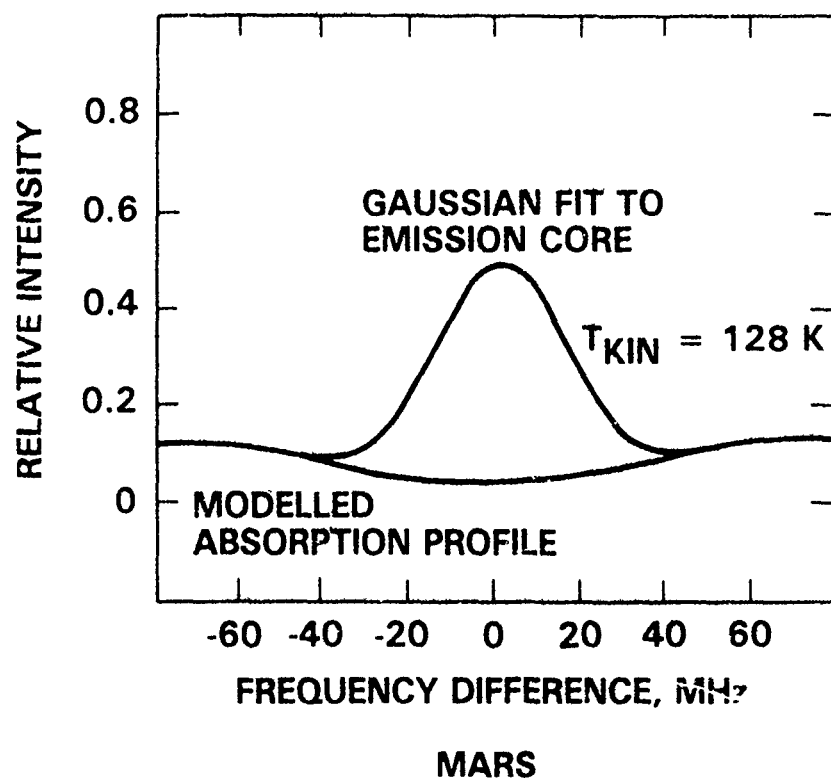
Figure 4-1
Lasing the ionosphere

IONOSPHERIC LASING AT 10 MICRONS - EVIDENCE FROM THE PLANETS

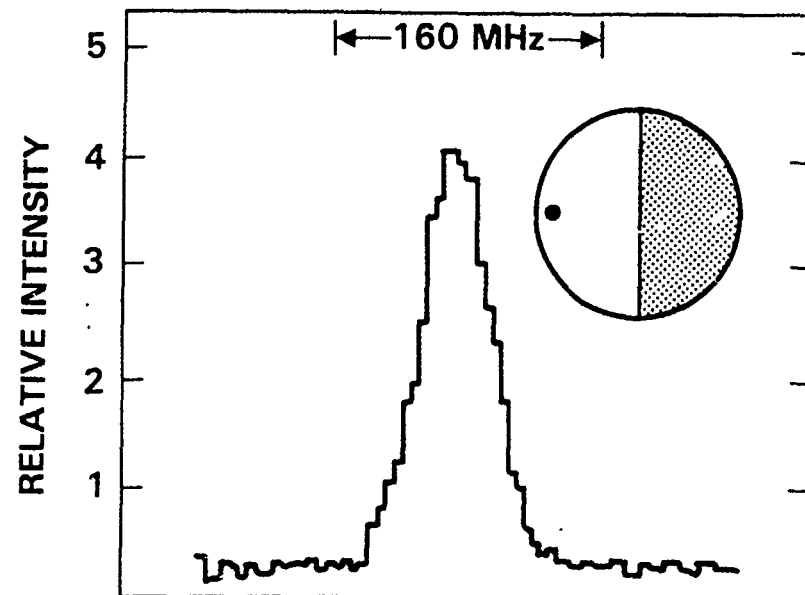
Non-thermal emission has been seen in the cores of the 9.4 and 10.4 micron carbon dioxide bands on Mars and Venus [Mumma et al. 1981, Deming et al. 1983, Deming and Mumma 1983, Gordiyets and Panchenko 1983]. The emission spectra are shown in Figure 4-2. The emission is believed to be excited by absorption of solar energy in the near-IR CO₂ bands, followed by collisional transfer to the 00⁰1 state of CO₂. The observed flux from Mars agrees closely with the predictions of the theoretical model, while the flux observed from Venus is 74% of the predicted flux. The emission from Mars has been identified as a natural atmospheric laser, and it is suspected that the emission from Venus is also due to laser action.

Although the atmosphere of the earth has a high percentage of nitrogen that may inhibit laser action, the number density of CO₂ in the upper atmosphere of earth is comparable to the number density of CO₂ in the lasing regions of Mars and Venus, so there is a possibility that the atmosphere of the earth may emit in the 10 micron region. It would be desirable to carry out a shuttle experiment to look for signs of this inversion. A passive experiment would use a spectrometer on the shuttle to look for infrared emission near the limb. An active experiment would use a tunable infrared laser and telescope on the earth to send a probe beam up to a detector on the shuttle. The detector would look for amplification or line narrowing of the laser beam.

The HILAT satellite was recently launched into a 830-kilometer altitude orbit with an 82.2 degree inclination. It will make radio, visible, and UV observations of the ionosphere, aurora, and airglow [EOS 1983]. The data from this spacecraft may be useful in studies of ionospheric lasing.



MARS



VENUS

Figure 4-2
Evidence for laser action around 10 microns
in the mesospheres of Mars and Venus

ESTIMATE OF POWER OUTPUT

Rasor Associates [Britt 1981] has estimated the power obtainable by extracting energy stored in the solar-pumped ionosphere by a single pass laser system. Although no solar-pumped inverted population is known in the upper atmosphere of the earth, they assumed a lasing species with a nominal number density of 3×10^{10} molecules per cubic centimeter emitting at a nominal energy of 1.3 eV (1 micron wavelength). If the mirrors are one meter in diameter and spaced 1000 km apart, then the volume enclosed is 0.8×10^6 cubic meters. This volume contains 2.4×10^{22} excited molecules (about one gram worth), each with an energy of 1.3 eV (2×10^{-19} J), for a total of 5000 J. A short one microsecond light pulse started at one mirror and collected by the other will sweep the 5000 J of energy out of that volume. As soon as the mirrors have moved one meter, the next pulse will sweep the energy out of the adjacent volume of the atmosphere. The repetition rate depends upon the orbital velocity and the size of the mirrors. For one meter mirrors moving at 8 km/sec, the repetition rate would be 8 kHz. The average power output of this system would be about 40 megawatts. This is a significant power level, both for propulsion and weapons purposes.

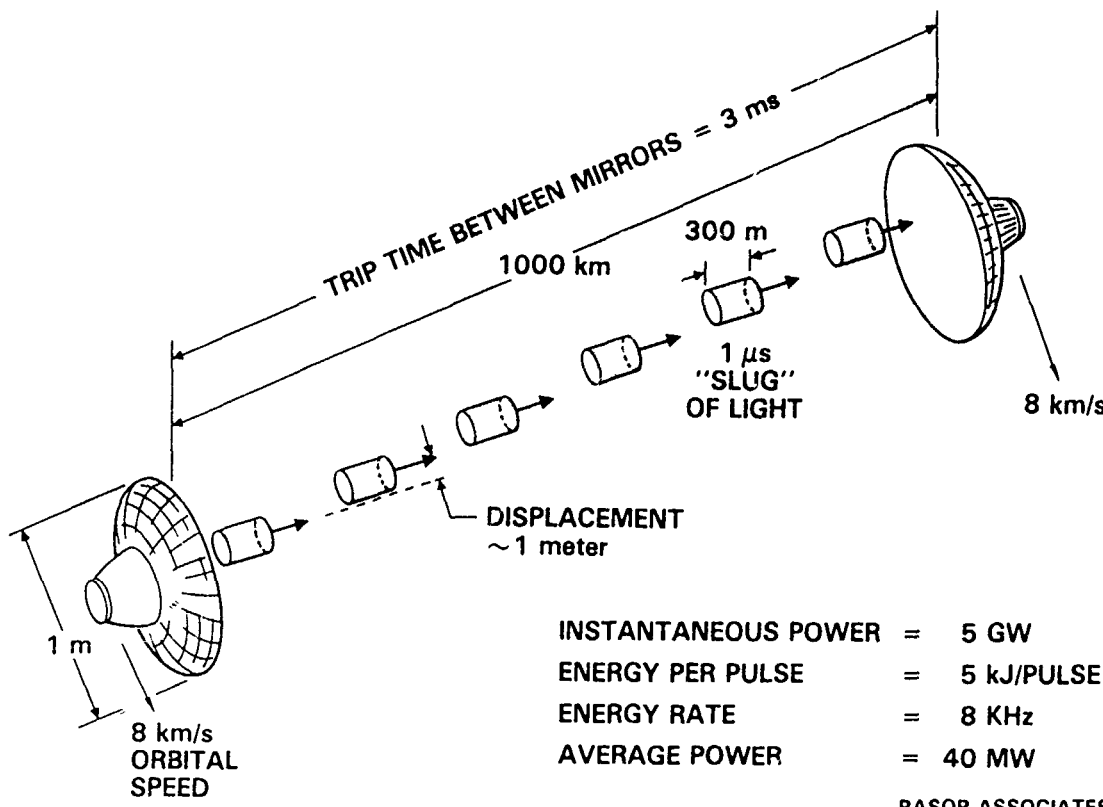


Figure 4-3
Extracting stored ionospheric energy with two orbiting mirrors

CONCLUSIONS

From the information gathered during this contract it seems that the concept of lasing the ionosphere is probably feasible. Since Mars and Venus (and probably Jupiter) have demonstrated natural laser action, it should be possible to design mirror systems around these planets to extract kilowatts of power. This should be of interest to NASA planetary mission planners. We may find that similar natural lasing takes place in the ionosphere of the earth, but it is more likely that one or more of the proprietary ideas discussed in the Final Program Review Data Package will be needed to obtain significant amounts of power. Studies and experiments will be required to determine the feasibility of any of these concepts.

If ionospheric lasing can be made to work, the amount of power available from this concept is significant. Even with the most pessimistic assumptions, as long as any laser action at all is possible, a one meter mirror can collect much more energy than a large solar cell array many times larger and heavier. With more optimistic assumptions the power levels that might be achieved reach gigawatts and terawatts. These power levels are enough to energize the propulsion and weapons systems of large space forts or even supply prime power to large cities in space or on earth.

Although we have identified ionospheric lasing as a new and powerful alternate propulsion energy source, it should be kept in mind by the propulsion community that this energy source comes with some built-in requirements for operation that limit its flexibility in supplying propulsion power for various missions. A mission will always require the cooperation of at least one distant vehicle (as well as the cooperation of the ionosphere), and the output energy is in the form of laser energy, which must be converted into thrust. Yet, keeping in mind that many future Air Force space missions will require weapons power as well as propulsion power, this concept is certainly worth looking into further.

RECOMMENDATIONS

It is recommended that the Air Force fund studies of some of the Rasor Associates proprietary ideas discussed in more detail in the Final Program Review Data Package.

Since laser action is known to take place on Mars and Venus, it is recommended that NASA/JPL conduct studies of the feasibility of obtaining laser energy from planetary atmospheres.

Since observation of 10 micron CO₂ laser action in the earth's ionosphere cannot be seen from the ground, both the Air Force and NASA should consider initiating a shuttle or spacecraft experiment to search for gain or line narrowing of a probe laser beam sent through the ionosphere.

IONOSPHERIC LASING BIBLIOGRAPHY

J.D. Barry, "Auroral energy source", (internal document), Hughes Aircraft Co, El Segundo, CA 90245 (1981?).

A.L. Betz, R.A. McLaren, E.C. Sutton, and M.A. Johnson, "Infrared heterodyne spectroscopy of CO₂ in the atmosphere of Mars", Icarus 30, 650-622 (1977).

C.J. Britt, "Atmospheric laser system (ATLAS) feasibility investigation", Unsolicited proposal RAP-063 to NASA/Lewis, Rasor Assoc., Sunnyvale, CA 94086 (March 1981).

J. Chamberlain, W. Happer, J. Katz, and R. Novick, "Long Path Solar Pumped Lasers", JASON Technical Report JSR-81-07, SRI International, Arlington, VA 22209, AD B060839L (Sept 1981). (Contains proprietary information, distribution limited to US Government Agencies).

A. Dalgarno, "Metastable species in the ionosphere", Ann. Geophys., 26, 601-607 (1970).

D. Deming, F. Espenak, D. Jennings, T. Kostiuk, and M.J. Mumma, "Observations of the 10 micrometer natural laser emission from the mesospheres of Mars and Venus", NASA TM-85044, NASA/Goddard, Greenbelt, MD 20771 (June 1983).

D. Deming and M. Mumma, "Modeling of the 10 micrometer natural laser emission fro the mesospheres of Mars and Venus", NASA TM-85045, NASA/Goddard, Greenbelt, MD 20771 (June 1983).

EOS (news summary), "The HILAT Program", EOS, Trans. AGU 64, 163 (1983)

B.F. Gordiyets and V.Ya. Panchenko, "Infrared radiation and inversion population of CO₂ laser levels in Venusian and Martian atmospheres", NASA TM-85057, NASA/Goddard, Greenbelt, MD 20771 (May 1983).

M.A. Johnson, A.L. Betz, R.A. McLaren, E.C. Sutton, and C.H. Townes, "Nonthermal 10 micron CO₂ emission lines in the atmospheres of Mars and Venus", Astrophysical J. 208, L145-L148 (1976).

G. Meltz, "LITA", (internal proprietary document), United Technology Research Center, East Hartford, CN 06108 (1977?).

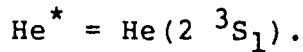
M.J. Mumma, D. Buhl, G. Chin, D. Deming, F. Espenak, T. Kostuik, and D.M. Zipoy, "Discovery of natural gain amplification in the 10-micrometer carbon dioxide laser bands on Mars: a natural laser", Science 212, 45-49 (1981).

M. N. Vlasov, "The photochemistry of excited species", J. Atmospheric and Terr. Physics 38, 807-820 (1976).

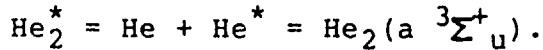
SECTION 5

SOLID METASTABLE HELIUM

Metastable helium is the electronically excited triplet state of a helium atom. When the helium atom decays into the ground state it releases 19.8 eV (480 kJ/gm) of energy. The ideal specific impulse is calculated to be 3150 sec (about six times that of oxygen/hydrogen) and one would expect to get a specific impulse of better than 2000 sec in an operational rocket. Metastable helium comes in two forms. One is atomic metastable helium, which is a single helium atom excited into the lowest level of its orthohelium state or the triplet state:



A metastable helium atom can combine with an unexcited helium atom to form a metastable helium molecule:



Metastable helium atoms are easily produced by electron bombardment, either in a gas (helium-neon lasers use the state) or by sending high energy electrons into superfluid liquid helium [Hill et al. 1971, Watkins et al. 1981]. The process is very efficient, with a 160 keV electron producing of the order of 500 metastable helium molecules at about 12.5% efficiency. The theoretical lifetime of the metastable state is limited by a relativistic spin-orbit coupling mechanism and has been measured to be 2.5 hours in a vacuum, but a typical lifetime in a container is less than a second. Because of the short lifetime, metastable helium is usually not considered to be a suitable propellant.

Recently, however, Dr. Jonas S. Zmuidzinas of JPL has suggested some techniques that might suppress the normal spin-orbit decay of the metastable state. If this decay mode could be suppressed, then according to theory, the next mode of decay is by double-photon emission, and this lifetime is 8 years.

When metastable helium atoms and molecules are formed by electron bombardment of liquid helium, the metastable helium molecules are normally formed with equal numbers in the spin-up and spin-down direction. When two molecules of opposite spin collide, they readily combine to form four unexcited helium atoms and the energy is released as vacuum-ultraviolet (VUV) radiation. This loss process accelerates as the density of metastable helium molecules increases, ultimately limiting the density that can be achieved for a given input of power from the electron beam generating the metastable atoms.

When two excited molecules with the same spin collide, however, the combination has a total spin of two. Since spin conservation forbids the decay into four helium atoms the combination is metastable. The combination of two excited helium molecules also seems to be a chemically bound state. Although no calculations have been done on the chemical binding of spin-aligned excited helium molecules, the binding of spin-aligned excited helium atoms has been calculated [Garrison et al. 1973] and the prediction is that they have a binding energy of about 0.07 eV. The calculated binding energy is shown in Figure 5-1, along with the binding energies of unexcited helium and unexcited xenon. The calculated binding energy of the excited helium molecule is much greater than that of xenon. Since xenon is known to become a solid at 170 K, it is predicted that if enough excited helium molecules can be formed fast enough and at the same time kept in a spin-aligned state, they will form a solid with a melting point of approximately 600 K (300 C).

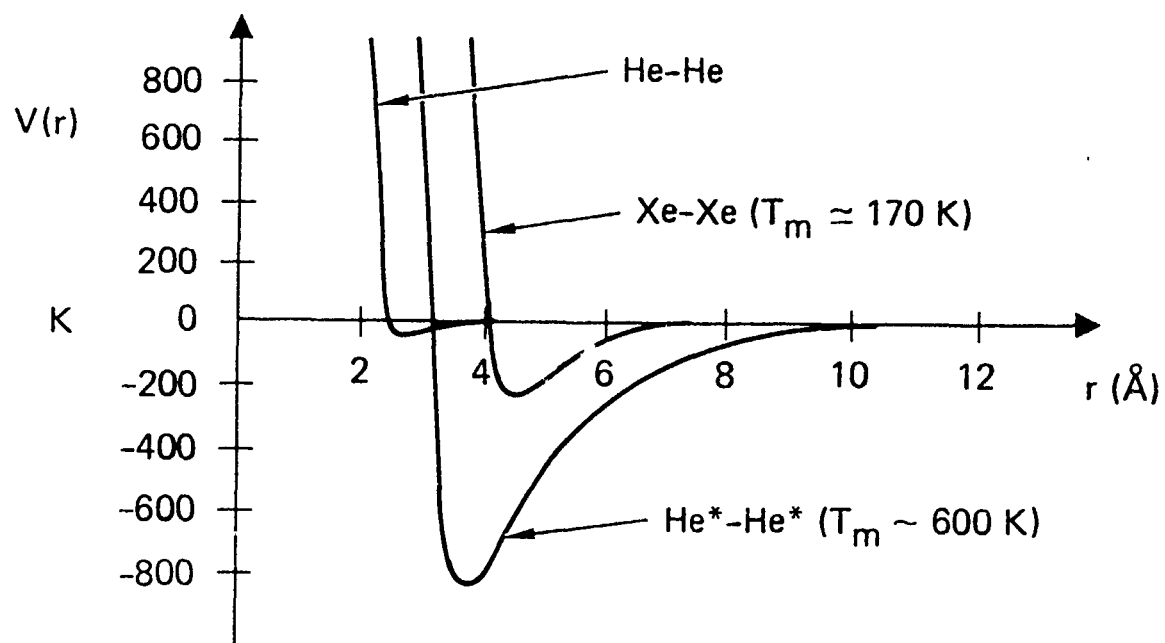
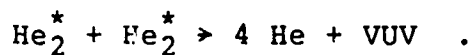


Figure 5-1
Binding energies of helium, xenon, and metastable helium

The JPL approach to making solid spin-stabilized metastable helium will be to produce copious quantities of metastable helium molecules by electron bombardment of liquid helium while at the same time applying a magnetic field and irradiating the liquid helium with right-circularly polarized laser light at 465 nm. As is shown in Figure 5-2, the circularly polarized laser light will optically pump the metastable helium molecules until they are all (99%) in the spin-up state. Preliminary estimates indicate that a number density of 10^{18} excited helium molecules per cubic centimeter can be achieved by this technique. Only experiment will determine if these densities will allow the formation of spin-aligned solid metastable helium. Since the spins are aligned, there are reasons to believe that this new form of excited solid matter could be ferromagnetic. In that case it would have a strong internal magnetic field that would help to keep the spins of the excited helium molecules aligned and suppress the bimolecular decay process:



The JPL group is receiving funding from AFRPL to carry out some experiments to test these predictions.

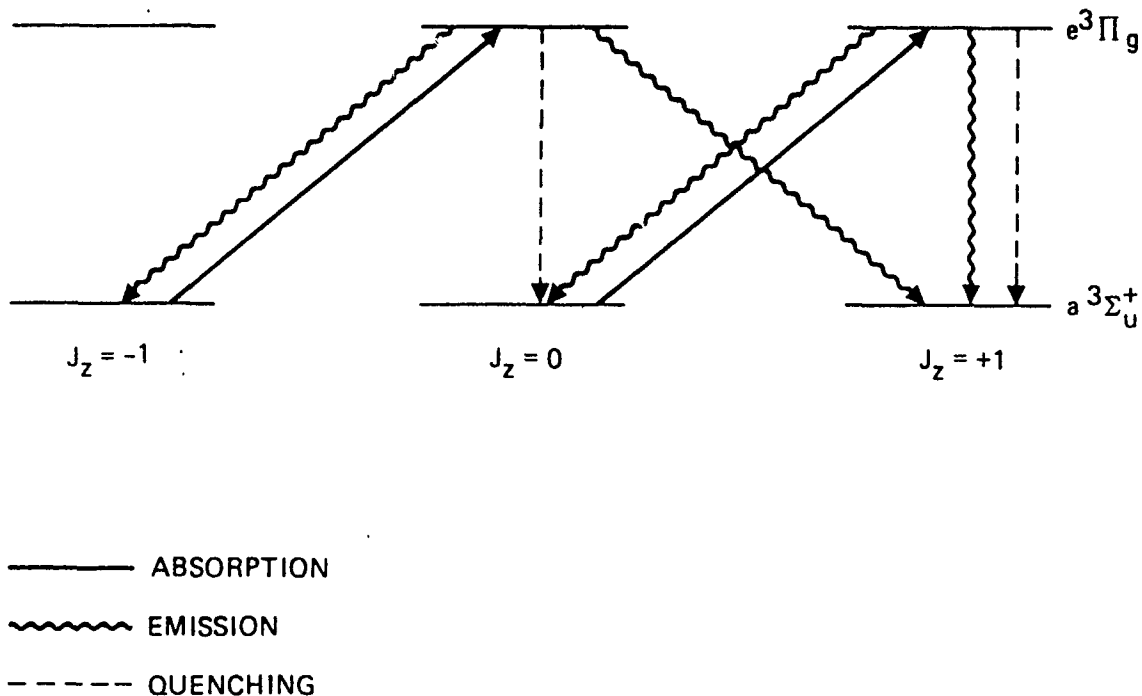


Figure 5-2
Preparing spin-aligned He_2^* by optical pumping

Even if solid metastable molecular helium doesn't exist, there is another possible method to suppress the normal spin-orbit decay. This technique involves irradiating the metastable helium atoms with properly phased coherent laser radiation to inhibit the spin-orbit decay mode [Zmuidzinas 1982]. A simplified model of the process is illustrated by a three-level energy diagram as shown in Figure 5-3. The ground state is level 1, the desired metastable state is level 2, and level 3 is another metastable state with a slightly higher energy than level 2. The atom will be excited as usual by electron bombardment into level 2. The normal decay process is for the atom to return to level 1 by emitting a photon. There is an alternate path from level 2 to level 1 by way of level 3, but this is energetically unfavorable so the decay amplitude by this route is negligible. If, however, a laser is used to pump the transition between level 2 and level 3, then that pathway can compete with the normal decay path directly from level 2 to level 1. If the decay rates are such that $(3 \rightarrow 2) \gg (3 \rightarrow 1) \gg (2 \rightarrow 1)$, and we adjust the frequency, amplitude, and phase of the pump laser to the right values, then the decay amplitude from level 2 through level 3 to level 1 can be made equal in amplitude and opposite in phase to the decay amplitude from level 2 direct to level 1. The two decay amplitudes will interfere destructively and the total decay rate from level 2 to level 1 will vanish, thus stabilizing the metastable atom.

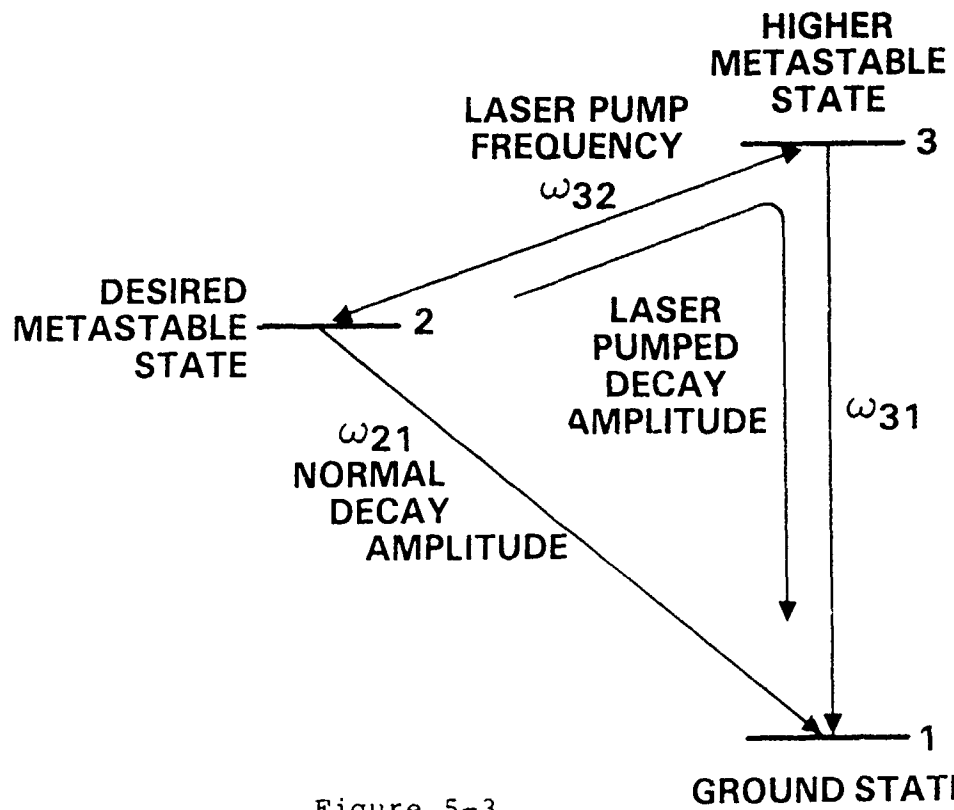


Figure 5-3
Stabilizing a metastable helium atom
by coherent pump inhibition

RECOMMENDATION

It is recommended that the ongoing research on spin-aligned solid metastable helium be continued. IF all the physics breaks the right way, this concept could provide a new, high-energy, chemical propellant many times better than any existing chemical fuel.

SOLID METASTABLE HELIUM BIBLIOGRAPHY

B.J. Garrison, W.H. Miller, and H.F. Schaefer, "Penning and Associative Ionization of Triplet Metastable Helium Atoms", J. Chem. Phys. 59, 3193 (1973).

J.C. Hill, O. Heybey, and G.K. Walters, "Evidence of metastable atomic and molecular bubble states in electron-bombarded superfluid liquid helium", Phys. Rev. Lett. 26, 1213-1219 (1971).

J.L. Watkins, J.S. Zmuidzinas, and G.A. Williams, "Electron beam excitation of the liquid helium surface", Physica 108B, 1313-1314 (1981).

J.S. Zmuidzinas, "Energy storage in solid helium", JPL TM-33-653, Jet Propulsion Lab, Pasadena, CA 91109 (1973).

J.S. Zmuidzinas, "Electronically excited solid helium", Section V of "Frontiers in Propulsion Research", JPL TM 33-722, D.D. Papailiou, Jet Propulsion Lab, Pasadena, CA 91109 (1975)

J.S. Zmuidzinas, "Stabilization of $\text{He}_2(a \ ^3\Sigma^+)$ in Liquid Helium by Optical Pumping", unpublished (1976)

J.S. Zmuidzinas, "Dynamic Stabilization of Metastable Atoms", Applied Physics B28, 107-108 (1982)

(Concluding page of Section 5)

SECTION 6

VACUUM FLUCTUATION ENERGY SOURCE

QUANTUM FLUCTUATIONS OF THE VACUUM

There are two kinds of quantum fluctuations in empty space predicted by theory. In quantum electrodynamics there are quantum fluctuations of the electromagnetic field. The effects of these fluctuations have been experimentally observed. In quantum geometrodynamics there are quantum fluctuations due to the gravitational field. These have yet to be experimentally observed. It is not known [Misner, Thorne, and Wheeler 1973, p. 1202] whether the quantum electrodynamic fluctuations are in addition to the quantum geometricdynamic fluctuations, or whether they are, in some yet unknown way, mere manifestations of them.

As I shall show in more detail later, it is possible to "extract" energy from these energy density fields. We do not get "something for nothing", however, for it seems that these fields are conservative in the sense that they only act as "catalysts" to convert some form of potential energy into some other form of energy. Once you have extracted energy from the system by some mechanism that changes from an initial state to a final state, you must put an equal amount of energy back into the mechanism to move it back to its original state. The vacuum fluctuation fields are therefore not a source of unlimited "free" energy.

QUANTUM FLUCTUATIONS IN THE SPACE-TIME-GRAVITATIONAL FIELD

The presently accepted theory of gravitation, the Einstein general theory of relativity, is a classical theory and does not handle quantum effects. The presently accepted theory of quantum effects, quantum electrodynamics, treats only electrodynamics and does not handle gravitational effects. There have been many attempts to merge the two theories, one example being quantum geometrodynamics [Wheeler 1962]. The Wheeler theory predicts strong fluctuations in the geometry of a vacuum at distances on the order of a Planck length [Misner, Thorne and Wheeler 1973, p.12]:

$$L^* = (\hbar G/c^3)^{1/2} = 1.616 \times 10^{-35} \text{ m}$$

where

$$\begin{aligned}\hbar &= 1.054 \times 10^{-34} \text{ J-sec is Planck's constant} \\ c &= 2.998 \times 10^8 \text{ m/sec is the speed of light} \\ G &= 6.670 \times 10^{-11} \text{ m}^3/\text{kg-sec}^2 \text{ is the gravity constant}\end{aligned}$$

The mass-energy densities associated with this space-time "foam" are of the order of:

$$\hbar/cL^4 = 5 \times 10^{96} \text{ kg/m}^3$$

This high energy density predicted by quantum geometrodynamics has led some to speculate that it might be used as a source of "free" energy [Froning 1980, 1981, Bearden 1980], but except in science fiction [Sheffield 1983], its utilization for propulsion seems distant, if not impossible.

QUANTUM FLUCTUATIONS IN THE ELECTROMAGNETIC FIELD

The theory of quantum electrodynamics is one of the more successful physical theories since it has been checked experimentally many times and found to be accurate. In quantum electrodynamics a region of space is divided up into a large (infinite) number of modes of potential oscillation for the electromagnetic field. The state of the electromagnetic field is defined by counting the number of photons in each mode.. The "vacuum" state is defined as that state where there are no photons in any of the modes. Yet, according to quantum electrodynamics, each mode of oscillation, even when the space is at absolute zero, has in it a zero-point oscillation with an energy $hf/2$. This residual electromagnetic field produces a fluctuating electric field that has observable consequences.

One place where the effects of the electromagnetic fluctuations show up is in the calculation of the energy states in a hydrogen atom. The fluctuating electric fields of the quantum fluctuations cause perturbations to the orbit of the electron around the proton. Even though the electric field perturbations average out over the orbit, the electron moves in a slightly shifted orbit compared to that calculated from the electric field of the proton alone. This produces [Welton 1948, Dyson 1954] most of the shift in the energy levels of the hydrogen atom that is experimentally observed [Lamb and Rutherford 1947].

Since according to quantum electrodynamics, each mode has on the average a zero-point energy of half a photon, and since there are an infinite number of modes, this means that empty space has an infinite amount of energy. Feynman [1965], examining this paradox, tried to put a bound on this infinity by assuming some physically reasonable cutoff for the shortest wavelength mode, such as the Compton wavelength of a proton (2×10^{-16} m). Even this cutoff gives an energy density of 2×10^{18} kg/m³ for the vacuum. This density is comparable to the density of the proton itself.

The paradox remains. Feynman and others found a way around the infinities by a mathematical technique called renormalization, but no one has a good explanation why the extremely high predicted energy densities don't have a large gravitational effect.

In summary, there is a theoretically infinite source of energy in just the electromagnetic fluctuations. The fluctuations definitely exist since they are seen to cause measurable shifts in the electron orbits of the hydrogen atom. It is theoretically possible to interact with the electromagnetic fluctuations and obtain energy. One technique involves the use of small black holes.

BLACK HOLE INTERACTION WITH VACUUM FLUCTUATIONS

According to the theory of quantum mechanics, the vacuum is not empty, but is full of "virtual" particles that are created out of nothing, exist for a while, then merge back into nothing. (See Figure 6-1a.) Most of the particles are low energy photons, but even charged particles like electrons and positrons occasionally appear for a short period of time. If a small black hole were placed in this emptiness full of energy, its powerful gravitational field would swallow the virtual particles if they got too close [Hawking 1977]. (See Figure 6-1b.) With no partner to recombine with, the other member of the virtual particle pair would be promoted to the status of a "real" particle and leave. To an onlooker, it would look as if the black hole had "emitted" the particle. Thus, it would seem that the black hole has extracted energy from the vacuum.

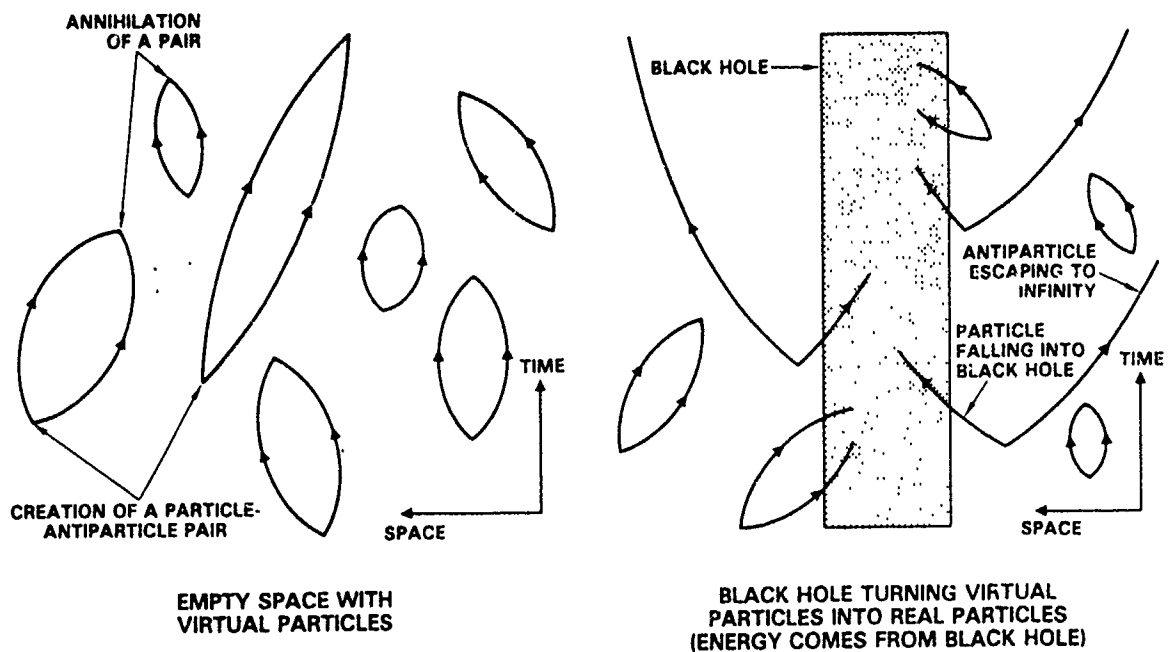


Figure 6-1
Black hole interaction with vacuum fluctuations

In this model of the interaction, the black hole emits radiation and particles as though it had a temperature given by [Hawking 1974, 1975, 1976]:

$$T = \frac{\hbar c^3}{8\pi kGM}$$

where $k = 1.380 \times 10^{-23}$ J/K is Boltzmann's constant and M is the mass of the black hole.

When the mass of the black hole is greater than 10^{14} kg, the temperature is less than 10^9 K so only photons, neutrinos and gravitons are emitted. Such a hole should emit approximately 81% of its mass in neutrinos, 17% in photons and 2% in gravitons [D.N. Page 1976, 1977]. When the mass is less than 10^{14} kilograms, then electrons and positrons are emitted, and when the mass becomes less than 10^{11} kilograms, the temperature now exceeds 10^{12} K and muons, kaons, protons and antiprotons are emitted. The size of a black hole of mass of 10^{11} kilograms is:

$$R = GM/c^2 = 7.4 \times 10^{-17} \text{ m}$$

which is somewhat smaller than a proton. Thus, significant effects are occurring at dimensions many orders of magnitude larger than the Planck length. The lifetime of the black hole is now very short and it essentially "explodes" in a burst of radiation and particles.

In the details of Hawking's theory, however, it is shown that a virtual particle that is swallowed by the black hole has "negative" energy, so the total energy-mass content of the black hole is decreased by the addition of the virtual particle. So, although it looks like the black hole allows us to get something out of the nothing called the "vacuum", in reality the energy came out of the mass of the black hole rather than the vacuum.

THERMODYNAMICS IN THE QUANTUM DOMAIN

The work of Hawking and others on developing relations between black hole physics, quantum theory, and thermodynamics will eventually produce a good theory of thermodynamics in the quantum domain. I suspect that once such a theory is developed we will find out that the vacuum fluctuation energy is unusable because of some quantum version of the second law of thermodynamics.

It is well known that there is plenty of (low grade) energy in the warm waters of the ocean. We would not be violating the first law of thermodynamics by trying to build a boat with an engine that would use this energy for propulsion. But unless we provide the engine with some heat sink that is colder (has less energy density in it) than the ocean, the second law of thermodynamics will see that the engine doesn't work. In the same manner, I suspect that the same type of thing will prevent

the utilization of the vacuum fluctuations as a source of unending "free" energy. We will need to have a "heat sink" for the quantum energy engine, and what can have less energy density in it than the nothing that makes up the vacuum?

QUANTUM FLUCTUATION SPACE DRIVES

Since there is no theory that proves it is impossible to extract energy out of the vacuum, and the example of the "hot" black hole seems to show that it might be possible, there has been a lot of speculation on space drives that somehow use the energy of the vacuum for propulsion. Unfortunately, none of the published work seems to have any substance that would allow a reasonable analysis to be done.

Nuclear Electric Resonance - A "quantum electronic space vehicle" has been proposed [Seike 1969] that uses a concept entitled "nuclear electronic resonance" in materials such as barium strontium titanate to somehow extract power out of the gravitational stress energy in space. Although gravitational stress energy is not exactly the same as vacuum fluctuation energy, this paper was read and an analysis attempted. The abstract of the paper is reproduced below (with a few corrections made to compensate for the poor translation).

Solid state engine of the single-manned space vehicle is presented. It is essentially time reversing motor or inverse (anti-)atomic engine powered by gravitational stress energy in Riemannian space-time in virtue of Nuclear Electric Resonance (NER).

NER is an electric regulation of polar angular momenta of atoms. Under a certain frequency condition of circularly polarized electromagnetic field with ultra high locking magnetic field the quantum seed of ferroxplana and Barium Strontium Titanate is converted into negative eigen state of Dirac's. Negative gravitation in that state is made use of as propulsion of the vehicle. Technological realizations of locking magnetic fields are also examined. A standard output of the single-manned space vehicle with one ton of the quantum seed is about thirty billion horsepower.

The energy source for this system is identified as the stress energy of gravitation given by:

$$W = - g^2 / 8\pi G \sim -5.4 \times 10^{11} \text{ ergs/cc}$$

where G is the Newtonian gravitational constant and g is defined as the gravitational acceleration. If we use a value of the gravitational acceleration near the earth of 9.8 m/sec^2 , we get the above quoted value for the stress energy.

The paper is largely theoretical, but some experimental results are given. They consist of three photographs of sine wave oscillations on an oscilloscope with different amplitude levels. The total wordage associated with the figures is quoted below:

An ordinary broadcasting wave is present in a toroidal coil around the quantum seed of ferroplana and Barium Strontium Titanate when they are not controlled as in the first picture. In accordance with the increase of the negative component of energy that amplitude decreases as in the 2nd picture. It further decreases towards zero as we excite it in negative eigen state of Dirac's as in the third picture. It finally vanishes when $aH_0 + w = 0$, then an inverted electromagnetic wave appears. That peak corresponds with the bottom while the latter with the former, of attenuating electromagnetic wave, respectively, beyond which repulsive gravitation is generated.

The paper defines $a = e/mc$ as the coupling constant of electromagnetic interaction, H_0 as the vertical component of the earth's magnetic field, and w as the frequency of oscillation. For a magnetic field of $H_0 = 0.35$ gauss, $w = 6.3 \times 10^6$ rad/sec. There is no description of the apparatus or the experimental procedures, and no measurement of the "repulsive gravitation". I can guess that what is shown in the figures is a decrease in drive amplitude as the drive frequency reaches a resonance in the crystals, in which case there would be increased coupling of energy to the crystals and we would expect changes in amplitude and phase. But these are well known effects and do not indicate that negative eigen states or repulsive gravitation is generated. Unless something more concrete is published on this concept, there is nothing here solid enough to base any analysis on.

Quantum Interstellar Ramjet - Froning [1980, 1981] has published two similar papers on an interstellar ramjet that utilizes a portion of the quantum fluctuation energy of the vacuum for its energy and reaction mass. Although the papers contain a good deal of information about the quantum fluctuations and detailed calculations of how fast and far the spaceship would fly given the ability to extract a portion of the energy from the vacuum, there is no mention of any ideas for extracting the energy. Indeed, the author admits "our current scientific understanding reveals no way of designing a 'quantum' starship propulsion system".

With nothing in the way of energy extraction methods to analyze, no analysis was done, and until the author comes up with a proposed mechanism to examine, I recommend that no further time be spent looking at this concept.

Hyperspatial Amplifier - One concept that has been proposed for tapping of the zero-point energy of the vacuum to operate a space vehicle is the hyperspatial amplifier [Bearden 1980]. The design and operation of the hyperspatial amplifier is quoted from pages 114-115.

Calculation of the first hyperchannel effect in a multistaged amplifier can be established as shown in [Bearden's] figure 10. The schemna may be visualized as similar to a Class F amplifier using state-of-the-art feedforward and feedback techniques. In the first hyperframe given by $v = c$, all stages of the amplifier appear superposed due to Lorentz-Fitzgerald contraction. For a particle at a particular location in any [amplifier?] stage n the corresponding location in any other stage m will have an exceedingly small but finite probability of having the same energy state, i.e., there is a small but finite and real possibility that the particle exists in both locations simultaneously during a given small increment of time.

Bearden's Figure 10 shows the symbols for n identical amplifiers separated by a distance L in one direction. Above the drawing is the note:

"(At the speed of light, all L's in this direction equal zero.)"

It is difficult to see how one can carry out any reasonable analysis on a concept that requires the violation of special relativity for its operation. (No material object can be made to travel at the speed of light.) I recommend that no further time be spent on this concept.

THE CASIMIR EFFECT

In addition to the Lamb-Rutherford shift in the hydrogen atom, there is another, lesser known, effect of the electromagnetic vacuum fluctuations that has been experimentally verified called the Casimir effect [Casimir and Polder 1946, 1948, Casimir 1948]. Detailed discussion of the Casimir effect is given in Appendix A. Only a short description is included here.

The Casimi. effect is a short range attraction between any two objects caused by the presence of the electromagnetic fluctuations in the vacuum. A calculation of the effect between two conducting plates [Casimir 1948], showed that the conducting plates would restrict the number of normal modes that could exist in the vacuum between them. In a straightforward calculation of the number of normal modes and the zero-point energy in those modes, Casimir predicted that the electromagnetic vacuum fluctuations between the plates would have a negative energy density that was proportional to the third power of the spacing between the plates. There thus would be an attractive force

between the plates that was proportional to the fourth power of the spacing. The force was independent of the material in the conductors.

Later, the analysis was broadened to include dielectrics [Lifshitz 1956]. It was found that any two dielectric plates would experience a similar fourth power force law, but one that was also proportional to the dielectric constant of the plates. The Casimir result is obtained when the dielectric constant of the plates is allowed to go to infinity. The equations describing the Casimir effect are retarded wave solutions and are only valid down to a separation distance proportional to the minimum wavelength at which the plates are still a good conductor or the dielectric constant is not unity. For distances closer than that, a non-retarded equation takes over [Lifshitz 1956]. The attractive force will still increase with decreasing distance, but at a rate proportional to the third power of the separation distance.

Both Casimir and Lifshitz were aware that these forces due to the fluctuations of the vacuum were known previously as "surface tension", "surface energy", and "van der Waals" forces that occur between uncharged atoms and objects.

EXTRACTING ENERGY FROM THE VACUUM USING THE CASIMIR EFFECT

On this contract I invented a way to extract electrical energy out of the electromagnetic fluctuations of the vacuum using the Casimir effect [Forward 1983]. The method is described in a paper prepared for journal publication that can be found in Appendix A. The abstract of the paper follows:

Any pair of conducting plates at close distances ($< 1 \mu\text{m}$) experience an attractive Casimir force that is due to the electromagnetic zero point fluctuations of the vacuum. A "vacuum fluctuation battery" can be constructed by using the Casimir force to do work on a stack of charged conducting plates. By applying a charge of the same polarity to each conducting plate we obtain a repulsive electrostatic force that opposes the Casimir force. If the applied electrostatic force is adjusted to always be slightly less than the Casimir force, the plates will move toward each other and the Casimir force will add energy to the electric field between the plates. A vacuum fluctuation battery made of a multitude of 20-nm-thick metal films brought to 20 nm spacing will have an electrical energy per kilogram equal that of a good chemical battery (100 kJ/kg or 28 W-h/kg). The battery can be recharged by making the electrical forces slightly stronger than the Casimir force to reexpand the foliated conductor.

It would be very desirable to obtain good experimental data on the ultraviolet reflectance of high quality ultrathin electrically-supported aluminum films at wavelengths below 100 nm and to measure the Casimir force between conducting plates of bulk aluminum down to separation distances of 10 nm and below. There is a good chance that high quality aluminum films only 10 nm thick will exhibit a significant fraction of their theoretical Casimir force at 10 nm separation distances. Since the vacuum fluctuation potential energy increases as the third power of the spacing, there is a possibility of obtaining a dramatic improvement in the performance of the "vacuum fluctuation battery" if we can obtain closer spacing with thinner plates.

If the thickness of the aluminum leaves in the foliated structure can be reduced to 10 nm thickness, and if the Casimir force still holds at 10 nm separation distance, and if we can avoid voltage breakdown, then the energy theoretically available from a foliated aluminum "vacuum fluctuation battery" is 1.6 MJ/kg. This is one-third the energy per kilogram of TNT and one-tenth the energy per kilogram of LOX-hydrogen (O_2/H_2) rocket fuel, one of the most potent chemical reactions known.

CONCLUSIONS

Although it was thought impossible at the start of the contract, it now seems that it is indeed possible to extract energy from the quantum fluctuations of the vacuum. We don't get something for nothing, however, and the vacuum is not a source of continuous "free" energy. The electromagnetic vacuum fluctuation field seems to be a conservative field, but there is no known proof of that in the literature. Since the vacuum fluctuation field seems to be the source of what "holds matter together", it is probably limited in energy density to chemical energy levels. Still, I have identified a non-thermodynamic method of extracting that chemical energy, as well as a method for getting chemical energy out of what are normally considered non-reactive chemicals (aluminum foil).

The experimental data on the Casimir force between conductors is of very poor quality. More experimental verification of the Casimir force between conductors needs to be done to prove the feasibility of the vacuum fluctuation battery. The theory of the Casimir force is also in a changing state. There is no general proof that the field is conservative and that you can't just keep on extracting energy if you can think up a clever enough mechanism. In fact, it is easy to imagine perpetual motion machines using variations of the Lifshitz force, but the theory can't prove them wrong yet.

Since the Casimir force produces very high force levels at close spacings, and according to Lifshitz, those force levels vary according to the dielectric or conducting state of the plates, it

is conceivable that the Casimir force could be a significant factor in the operation of microcircuits with sub-micron dimensions. This whole subject area needs further study.

The general conclusion is that on this contract I have uncovered a completely new alternate energy source. Whether it is a new alternate propulsion energy source is still a question.

RECOMMENDATIONS

Despite the fact that the application of electromagnetic vacuum fluctuation energy to propulsion is indirect, it is recommended that further research be done to define the limits of this new energy source.

Accurate experiments need to be done to measure the Casimir force between conductors, between charged conductors, and between plates of different materials before and after they go through phase transitions that change their dielectric constant or state of conductivity. The Lifshitz theory predicts a change in force with a change of state, but it may be that the change of state is inhibited or requires more or less energy. Either result could lead to new effects and/or new devices for extracting or controlling energy. At the same time experiments are taking place, there should be theoretical studies trying to predict or explain the experimental results. This could lead to a new understanding of materials, quantum electrodynamics, and/or quantum gravitation.

VACUUM FLUCTUATION ENERGY BIBLIOGRAPHY

I.I. Abrikosova and B.V. Deriagin, "Direct measurement of molecular attraction of solid bodies. II. Method for measuring the gap. Results of experiments.", Soviet Physics JETP 4, 2-10 (1957) [Zu. Eksp. Teor. Fiz. 31, 3-13 (1957)!]

American Institute of Physics Handbook, McGraw Hill (1972).

W. Arnold, S. Hunklinger, and K. Dransfeld, "Influence of optical absorption on the van der Waals interaction between solids", Phys. Rev. B19, 6049-6056 (1979); Erratum, Phys. Rev. B21, 1713 (1980).

Y.S. Barash and V.L. Ginzburg, "Contribution of electrodynamic theory of van der Waals forces between macroscopic bodies", JETP Lett. 15, 403-407 (1975) [ZhETF Pis. Red. 15, 567-571 (1975)].

Y.S. Barash and V.L. Ginzburg, "Electromagnetic fluctuations in matter and molecular (van der Waals) forces between them", Sov. Phys. Usp. 18, 305-322 (1975) [Usp. Fiz. Nauk 116, 5-40 (1975)] [review of theory - see references therein].

Thomas E. Bearden, "Hyperspace (virtual state) engineering", pp. 102-120 in **UFO Technology; A Detailed Examination**, Mutual UFO Network, Inc., 103 Oldtowne Road, Seguin, Texas 78155. Proceedings MUFON Symposium, Clear Lake, Texas (6-8 June 1980).

P. Candelas, "Vacuum energy in the presence of dielectric and conducting surfaces", *Ann. Phys.* **143**, 241-295 (1982).

W. Black, J.G.V. de Jongh, J.T.G. Overbeek, and M.J. Sparnaay, "Measurements of retarded van der Waals' forces", *Trans. Farad. Soc.* **56**, 1597-1608 (1960).

H.B.G. Casimir and D. Polder, "Influence of retardation on the London-van der Waals forces", *Nature* **158**, 787-788 (1946).

H.B.G. Casimir and D. Polder, "The influence of retardation on the London-van der Waals forces", *Phys. Rev.* **73**, 360-372 (1948).

H.B.G. Casimir, "On the attraction between two perfectly conducting plates", *Proceedings Koninklijke Nederlandse Akademie van Wetenschappen, Amsterdam* **51**, No. 7, 793-796 (1948) [in English] [This reference is hard to obtain. Casimir's result is rederived in an easily readable form in Harris 1972].

D. Chan and P. Richmond, "Van der Waals forces for mica and quartz: calculations from complete dielectric data", *Proc. Royal Soc. A353*, 163-176 (1977).

B.V. Deriagin and I.I. Abrikosova, "Direct measurement of the molecular attraction of solid bodies. I. Statement of the problem and method of measuring forces by using negative feedback", *Soviet Physics JETP* **3**, 819-829 (1957) [*Zh. Eksp. Teor. Fiz.* **30**, 993-1006 (1956)].

B.V. Deriagin and I.I. Abrikosova, "Direct measurements of molecular attraction of solids", *J. Phys. Chem. Solids* **5**, 1-10 (1958).

F.J. Dyson, **Advanced Quantum Mechanics**, mimeographed lecture notes, Physics Department, Cornell University (1954).

J.E. Dzyaloshinskii, E.M. Lifshitz, and L.P. Pitaevskii, "The general theory of van der Waals forces", *Adv. Phys.*, **10**, 165-209 (1961).

R. Eisenschitz and F. London, "Über das Verhältnis der van der Waalsschen Kräfte zu den homopolaren Bindungskräften", *Z. Phys.* **60**, 491-527 (1930).

R.P. Feynman and A.R. Hibbs, **Quantum Electrodynamics**, McGraw-Hill, NY (1965).

R.L. Forward, "Foliated conductor vacuum fluctuation battery", Patent Disclosure F-002, Air Force contract F04611-83-C-0013 (1983).

H.D. Froning, Jr., "Propulsion requirements for a quantum interstellar ramjet", J. Brit. Interplanetary Soc. 33, 265-270, (1980).

H.D. Froning, Jr., "Investigation of a quantum ramjet for interstellar flight", AIAA paper 81-1533, AIAA/SAE/ASME 17th Joint Propulsion Conference, Colorado Springs (27-29 July 1981).

H. Hamaker, "The London-van der Waals attraction between spherical particles", Physica 4, 1058 (1937).

Edward G. Harris, A Pedestrian Approach to Quantum Field Theory, Wiley-Interscience, New York (1972). [Harris gives the wrong volume number for the Casimir 1948 paper.]

S.W. Hawking, "Black hole explosions?" Nature 248, 30 (1 March 1974).

S.W. Hawking, "Particle creation by black holes", Comm. in Math. Physics 43, 199-220 (1975).

S.W. Hawking, "Black holes and thermodynamics", Phys. Rev. D13, 191 (1976).

S.W. Hawking, "The quantum mechanics of black holes", Sci. American, 236, 34-40 (January 1977).

S.W. Hawking, "Spacetime foam", Nucl. Phys. B144, 349-362 (1978).

S.W. Hawking, D.N. Page, and C.N. Pope, "The propagation of particles in spacetime foam", Phys. Letters 86B, 175-178 (1979).

S. Hunklinger, H. Geisselmann, and W. Arnold, "A dynamic method for measuring the van der Waals forces between macroscopic bodies", Rev. Sci. Instrum. 43, 584-587 (1972).

J.N. Israelachvili and D. Tabor, "Measurement of van der Waals dispersion forces in the range 1.5 to 130 nm", Proc. Roy. Soc. A331, 19 (1972).

J.N. Israelachvili, "Van der Waals dispersion force contribution to works of adhesion and contact angles on the basis of macroscopic theory", J. Chem. Soc. Faraday II 69, 1729 (1973).

J.N. Israelachvili and G.E. Adams, "Direct measurement of long range forces between two mica surfaces in aqueous KNO_3 solutions", Nature 262, 774-776 (1976).

J.A. Kitchener and A.P. Prosser, "Direct measurement of the long-range van der Waals forces", Proc. Royal Soc. A242, 403-409 (1957).

W.E. Lamb and R.C. Rutherford, "Fine structure of the hydrogen atom by a microwave method", Phys. Rev. 72, 241-243 (1947).

E.M. Lifshitz, "The theory of molecular attractive forces between solids", Soviet Physics JETP 2, 73-83 (1956) [Zh. Eksp. Teor. Fiz. 29, 94 (1955)].

J. Mahanty and B.W. Ninham, **Dispersion Forces**, Academic Press, New York (1976).

C.W. Misner, K.S. Thorne, and J.A. Wheeler, **Gravitation**, Freeman and Co., San Francisco (1973), p. 1202.

D.J. Mitchell, B.W. Ninham, and P. Richmond, "On black body radiation and the attractive force between two metal plates", A.J.P. 40, 675-678 (1971).

J.T.G. Overbeek and M.J. Sparnaay, "London-van der Waals attraction between macroscopic objects", Disc. Faraday Soc., 18, 12 (1954).

D.N. Page, "Particle emission rates from a black hole: Massless particles from an uncharged, nonrotating hole", Phys. Rev. D13, 198 (1976).

D.N. Page, "Particle emission rates from a black hole. II. Massless particles from a rotating hole", Phys. Rev. D14, 3260 (1976).

D.N. Page, "Particle emission rates from a black hole. III. Charged leptons from a nonrotating hole", Phys. Rev. D16, 2402 (1977).

G.C.J. Rouweier and J.T.G. Overbeek, "Dispersion forces between fused silica objects at distances between 25 and 350 nm", Trans. Farad. Soc. 67, 2117 (1971).

Shinichi Seike, "Quantum electronic space vehicle", Proceedings of the 8th Symposium on Space Technology and Science, Tokyo (1969).

Charles Sheffield, "All the colors of the vacuum", Analog Science Fiction/Science Fact (1981); Third Chronicle [pp. 72-112] in **The McAndrew Chronicles**, TOR/Pinnacle Books, New York (1983). [see also pp. 234-235.]

J. Schwinger, L.L. DeRaad, Jr., and K.A. Milton, "Casimir effect in dielectrics", Ann. Phys. 115, 1-23 (1978).

A. van Silfhout, "Dispersion forces between macroscopic objects.", Proceedings Koninklijke Nederlandse Akademie van Wetenschappen B69, "Part I", 501-515; "Part II", 516-531; "Part III", 532-541 (1966).

M.J. Sparnaay, "Attractive forces between flat plates", Nature 180, 334-335 (1957).

M.J. Sparnaay, "Measurements of attractive forces between flat plates", *Physica* **24**, 751-764 (1958).

D. Tabor and R.H.S. Winterton, "The direct measurement of normal and retarded van der Waals forces", *Proc. Royal Soc.* **A312**, 435-450 (1969).

J.H. van der Waals, *Ph.D. Thesis, University of Leiden* (1873).

T.A. Welton, "Some observable effects of the quantum-mechanical fluctuations of the electromagnetic field", *Phys. Rev.* **74**, 1157-1167 (1948).

J.A. Wheeler, *Geometrodynamics*, Academic Press, New York (1962).

F. Wittmann, H. Splitgerber, and K. Ebert, "Studium der van der Waals-Kraft im Bereich kleiner Abstände (A study of the van der Waals force at small distances)", *Z. Phys.* **245**, 354-360 (1971) [in German].

SECTION 7

OTHER PROPULSION ENERGY SOURCE CONCEPTS

In the previous sections of this report I described those propulsion energy sources that I felt would have significant potential for providing an alternate propulsion energy source in the next century. In this section, I briefly treat a number of other propulsion concepts of possible future interest. Some of the concepts, such as laser thermal propulsion, are certainly important advanced propulsion technologies, but are not discussed in detail in this report because they are already receiving significant recognition and support. The other concepts are either well-known older concepts where new ideas are needed to move them on, or new concepts that are not found in the previous surveys of advanced propulsion [AFRPL 1972, JPL 1975, Boeing 1981, JPL 1982].

LASER THERMAL PROPULSION

Laser thermal propulsion is a concept for obtaining propulsion energy by beaming laser energy to the spacecraft to heat a working fluid. Since the energy source is separate from the reaction mass, the reaction mass can be chosen to have a low molecular weight (hydrogen), and the specific impulse can be tailored to the mission by varying the amount of laser energy supplied per gram of reaction mass.

Little contract time was spent on this concept because work on the propulsion aspects is well underway at NASA/Marshall and NASA/Lewis [Jones and Keefer 1982], and work on the high power laser sources and the pointing and tracking optics is well underway on a number of DOD and DOE high power laser programs.

Recommendation:

Laser thermal propulsion can give high specific impulse and high thrust and is a definite candidate for an advanced propulsion system. The research work should continue at its present level and expand into systems studies as large amounts of laser energy becomes available.

References:

L.W. Jones and D.R. Keefer, "NASA's laser-propulsion project", *Astronautics & Aeronautics*, 66 (September 1982).

LASER ELECTRIC PROPULSION

Another form of beamed laser propulsion is to convert the laser light to electricity first, then use the electricity to power an electric thruster. Studies of this concept have been done [Forward 1975] and the results of those studies are still valid. The advantage of laser electric propulsion over laser thermal propulsion is that the electric ion thrusters are well tested devices, and the laser to electric photovoltaic conversion process is well known, scalable, and should reach conversion efficiencies of greater than 50% (42% efficiency has been demonstrated in the lab). Also, the laser light collector does not have to be of optical quality since it will be distributing the laser light to a large area of photovoltaic cells. Any mission studies involving beamed laser power should consider this option as it may lead to better system performance and reliability.

Recommendation:

It is recommended that further studies be made of the laser electric propulsion option, and that research be carried out on optimizing the efficiency of multilayer semiconductor cells for specific laser frequencies.

References:

R.L. Forward, "Advanced Propulsion Concepts Study - Comparative Study of Solar Electric Propulsion and Laser Electric Propulsion", Final Report, JPL Contract 954085, Hughes Research Labs, Malibu, CA 90265 (June 1975).

BEAMED MICROWAVE THRUSTERS

The basic concept proposed here is to assume that we will use the existing thruster designs that use microwave power to create and heat a plasma to produce thrust. Instead of generating the microwaves on board, however, the microwaves will be beamed to the spacecraft and sent directly to the thruster. The advantage of this approach is that the high mass penalty of the prime power source and the microwave generator will be replaced by the (hopefully) more modest mass of the collector for the microwaves. It is very likely the thruster designs will have to be modified to optimize the total system performance (i.e. making them operate at high microwave frequencies if possible).

The initial reaction of most people to this concept is that the antennas will be too large. They are large, but the weight penalty for the spacecraft is not too bad if you are willing to make the transmitting antenna large. For example: A 10 km transmitting array at 30 GHz can send power to a 100 m collecting array at geostationary orbit distances. These antennas are large, but the concept should not be rejected out of hand if good microwave powered thrusters exist. A factor that might make this concept more viable would be the construction of a large solar

power satellite (SPS) with the microwave transmitter array on the SPS designed for propulsion applications as well as prime power. By making the transmitting array large and giving it a multiple electronic beam steering capability, then the power that isn't needed on earth could be used by microwave powered tugs moving between LEO to GEO and the moon.

Recommendation:

If studies are going to be done on beamed laser propulsion, then similar studies should be done on beamed microwave propulsion.

LASER PUSHED LIGHTSAILS

The concept of pushing a lightsail with a laser was invented the year that the first laser was demonstrated [Forward 1962]. The basic formula that determines the acceleration a of a sail of mass m for a given incident power P is

$$a = 2P/mc,$$

where the factor 2 comes from the double momentum transfer of the reflected photons and c is the velocity of light. From this formula it is easy to calculate that 1.5 gigawatts of laser power are needed to accelerate one kilogram of payload and sail at one earth gravity. This is not much push for that amount of power and reflects the high specific impulse of the concept. Laser pushed lightsails seem to be best suited to light payloads and relativistic mission speeds.

A recent survey of this concept for interstellar missions [Forward 1983] concluded that if you design the system to use a very large transmitter lens (1000 kilometers minimum) and have sufficient laser power available (an array of solar-pumped lasers in orbit around Mercury), then a number of interesting interstellar missions can be performed.

Recommendation:

Because of the high (infinite) specific impulse of the photons and the low thrust per kilowatt of laser power, this concept seems to be limited to interstellar missions. Although interstellar travel is not of direct interest to the Air Force, it is of interest to NASA and the nation. Some thought should be given to the design of a minimum-weight precursor interstellar probe using the laser-pushed light sail concept.

References:

R.L. Forward, "Pluto - the gateway to the stars", Missiles and Rockets 10, 26 (2 April 1962).

R.L. Forward, "Roundtrip interstellar travel using laser pushed lightsails", (accepted for publication in J. Spacecraft and Rockets, 1983).

MICROWAVE PUSHED SAILS

One of the more exotic concepts uncovered during the contract is the idea of a microwave pushed sail [Dyson 1982]. This is an extreme version of a perforated sail where the wires in the mesh are kept small while the mass per unit area is lowered by increasing the hole size and increasing the wavelength of the microwave power proportionately. This concept uses the same acceleration versus power equation as the laser pushed lightsail: 1.5 megawatts can push one gram at one earth gravity. Like the laser pushed sail, the maser pushed sail is probably limited to interstellar missions because of the high exhaust velocity.

I added my ideas of interstellar probes made of wire mesh with imbedded microcircuits [Forward 1964, 1976] to the Dyson maser pushed sail idea to produce the "Starwisp" concept for a high-speed interstellar probe. A journal paper based on the concept is presented in Appendix C. The abstract of the paper follows:

Starwisp is a light-weight, high-speed interstellar fly-by probe pushed by beamed microwaves. The basic structure is a wire mesh sail with microcircuits at each intersection. The mesh sail is driven at high acceleration using a microwave beam formed by a large fresnel-zone-plate transmitter lens made of alternating sparse metal mesh rings and blank rings. The high acceleration allows Starwisp to reach a coast velocity near that of light while still close to the transmitting lens. Upon arrival at the target star, the transmitter floods the star system with microwave energy. Using the wires as microwave antennas, the microcircuits collect energy to power their optical detectors and logic circuits to form images of the planets in the system. The phase of the microwaves at each point of the mesh is sensed and the information used to form the mesh into a retrodirective phased array microwave antenna that beams a signal back to earth. A minimal Starwisp would be a 1 km mesh sail weighing 16 grams and carrying 4 grams of microcircuits. It would be accelerated at 115 gravities by a 10 GW microwave beam, reaching one-fifth of the speed of light in a few days. Upon arrival at Alpha Centauri 21 years later, Starwisp would collect enough microwave power to send back a high resolution picture every three minutes during its fly-through of the system.

References:

F.J. Dyson, "Maser-driven sail," unpublished notes (1982).

R.L. Forward, "Zero thrust velocity vector control for interstellar probes: Lorentz force navigation and circling," AIAA J. 2, 885-889 (1964).

R. L. Forward, "A programme for interstellar exploration," J. Brit. Interplanetary Soc. 29, 610-632 (1976).

TETHERS

In 1987 NASA is planning to fly the first space tether experiment. It will be a joint program with Italy. A 500 kg satellite designed to probe the characteristics of the upper atmosphere will be lowered 100 kilometers down from the normal 250 kilometer Shuttle altitude to 150 kilometers. At this altitude the atmospheric probe would normally return to earth in a fraction of an orbit because of the atmospheric drag, but the tether is acting as a "propulsion system" to transfer energy from the Space Shuttle to the smaller satellite.

Once the NASA planners have become comfortable with the tether concept, the Shuttle tether system can be used to transfer the Shuttle momentum to the payload, launching the payload into a transfer orbit while the Shuttle returns to earth [Bekey 1982]. Later, more advanced systems operating from large platforms can transfer payloads from LEO to GEO and back. This can be done with no expenditure of fuel as long as the amount of mass dropped inward down the earth's gravitational potential well equals or exceeds the amount of mass sent upwards.

The tethered satellite system also offers a new means for extracting energy from the ionosphere. The basic idea [Utah 1980] is to launch a satellite upward on an electrically insulated conductive tether. The motion of the conductive tether through the earth's magnetic field lines will generate voltage differences between the two ends of the tether of several thousand volts. In a normal eastward orbit, the placement of the satellite above the orbiter results in electron collection by the satellite and a need for electron emission from the Shuttle which can be supplied by the electron gun tested on one of the earlier flights. Power levels of 10 kilowatts are expected from the prototype system.

Recommendation:

The idea of using tethers to transfer energy and momentum has not received much attention in the propulsion research community. It is recommended that those involved in the more traditional forms of propulsion take a serious look at this concept since the engineering problems of deploying and using tethers will have been solved by 1987. If there are potential propulsion applications for this concept, the mission planners should be ready to take advantage of the developed technology.

References:

Utah State University, "The Tethered Satellite System - Facility Requirements Definition Team Report", Report under NASA Contract NAS8-33383, Center for Atmospheric and Space Sciences, Utah State University, Logan, Utah 84311 (May 1980).

I. Bekey, "Tethers Open New Space Options", *Astronautics & Aeronautics*, 32 (April 1983).

FREE-RADICAL HYDROGEN

Free radicals are single atoms of elements that normally form molecules. Atomic hydrogen is a free-radical form of hydrogen that releases energy when the hydrogen atoms combine to form hydrogen molecules. The ideal specific impulse from this reaction is 2130 sec. Although it is easy to produce large quantities of atomic hydrogen by electron bombardment, it has proven difficult to store it in high concentrations. Rosen [1973] did a complete survey of the work up to 1973, and showed [Rosen 1974] how to use it as a propellant. The FY81 JPL study [JPL 1981] covers the work since then.

Because of the recent interest in using spin-polarized atoms for fuel in fusion reactors, the research on this field has increased, especially at Princeton and MIT. MIT recently reported storing 0.8×10^{17} atoms/cc for four hours at 0.3 K using a 10 T magnetic field trap [Cline, et al. 1980], but the lifetime was inversely proportional to the storage density. The highest density achieved to date was 2×10^{18} atoms/cc using hydrostatic compression of a bubble of spin-polarized hydrogen gas by liquid helium [Sprik, Walraven, Silvera 1983, Hess, et al., 1983], but the lifetimes attained were only a few minutes. Proof that the material would be a good energy source was demonstrated in a few of the experiments when they terminated in a "spontaneous explosion".

Recommendation:

This work is receiving support from the fusion field. Propulsion oriented funding should wait for better ideas to attain high density storage.

References:

- G. Rosen, "Current status of free radicals and electronically excited metastable species as high energy propellants", Final Report on JPL Contract 953623, Drexel University, Philadelphia, PA (December 1973 revision of August 1973 report).
- G. Rosen, "Manufacture and deflagration of an atomic hydrogen Propellant", AIAA Journal 12, 1325 (1974).
- R.W. Cline, et al., "Magnetic confinement of spin-polarized atomic hydrogen", Phys. Rev. Lett. 45, 2117 (1980).
- R. Sprik, J.T.M. Walraven, and I.F. Silvera, "Compression of spin-polarized hydrogen to high density", Phys. Rev. Lett. 51, 479-482 (1983).
- H.F. Hess, et al., "Observation of three-body recombination in spin-polarized hydrogen", Phys. Rev. Lett. 51, 483-486 (1983).

METALLIC HYDROGEN

Metallic hydrogen is a postulated high energy propellant that releases its energy when the atomic metal is converted into gas molecules. It is estimated to have a specific impulse of 1700 sec and a specific density of 1.15 (solid molecular hydrogen has a specific density of 0.076). Very high pressures will be needed to produce the metal form of hydrogen. The present estimates [van Straaten, et al. 1982] are pressures of 1.9 to 5.6 Mbars.

Theoretical studies [MacDonald and Burgess 1982] indicate that the metal will be a liquid at all pressures. There has been theoretical speculation that once formed, the metal state may be metastable and remain in the metal form after the pressure is released. Other theoretical estimates seem to cast doubt on any metastable state.

Most of the experimental research on producing metallic hydrogen has ceased. The only active work seems to be at the University of Amsterdam [Straaten, et al. 1982] using a diamond-anvil cell. Their maximum pressure seems to be 0.5 Mbar.

With little active research on producing metallic hydrogen, and with the theoretical estimates of the required pressures being almost an order of magnitude more than the presently achievable pressures, it seems that the last assessment of the status of metallic hydrogen [JPL 1982] still stands: Metallic hydrogen would be a good fuel, IF it can be made and IF it will remain stable when the pressure is removed.

Recommendation:

Wait for the development of new high pressure machines that can produce steady megabar pressures.

References:

J. van Straaten, R.J. Wijngaarden, and Isaac F. Silvera, "Low-temperature equation of state of molecular hydrogen and deuterium to 0.37 Mbar: Implications for metallic hydrogen", Phys. Rev. Lett. 48, 97 (1982)

A.H. MacDonald and C.P. Burgess, "Absence of crystallization in metallic hydrogen", Phys. Rev. B26, 2849 (1982)

UNCONVENTIONAL NUCLEAR PROPULSION CONCEPTS

When nuclear fission was first demonstrated, it was hoped by the propulsion community that this new energy source would be the long-sought-for replacement for chemical fuels. Unfortunately, the physics and politics of nuclear reactors prevented that dream from being realized. Even the most optimistic designs failed to achieve an increase in specific impulse that was an order of magnitude larger than the best chemical launch systems. Although fission reactors have not produced a new propulsion system, and were deliberately not studied on the contract, there may be other techniques for releasing or utilizing nuclear energy. The most promising new unconventional nuclear propulsion concept was antiproton annihilation propulsion which is discussed in Section 1. In addition I have found a few other concepts that I think deserve further study.

Quark Catalyzed Fusion

Quarks are hypothetical particles predicted by some of the theories of quantum electrodynamics. They have charges that are multiples of 1/3 of an electronic charge. Negatively charged quarks can replace an electron in a deuterium molecule and catalyze D-D fusion which can be used for propulsion. Fractionally charged particles have been reported to have been observed on a number of occasions on small niobium balls levitated in a specially constructed superconducting chamber that is capable of measuring forces due to the electric field effects of a small fraction of a charge [LaRue, Phillips, and Fairbank 1980]. DOE is presently funding two experiments [Hendricks and Zweig 1982] based on ink-jet techniques to process multi-kilogram amounts of finely ground material to extract large quantities of fractionally charged particles.

Recommendation:

If and only if significant quantities of fractionally charged particles are found, then it is recommended that further studies of this concept be given high priority.

References:

G.S. LaRue, J.D. Philips, and W.M. Fairbank, Phys. Rev. Lett. 46, 967 (1981).

C.D. Hendricks, and G. Zweig, "Detection and Enrichment of Fractionally Charged Particles in Matter", DOE Advanced Energy Projects 24 and 25, DOE/ER-0150, U.S. Department of Energy, Division of Advanced Energy Projects, Office of Energy Research, Washington, DC 20545.

Imploded Micropellet Fusion Propulsion

The original Orion concept obtained propulsion by dropping small fission bombs out the back of the rocket where they were exploded behind a "pusher plate" to obtain thrust. The Orion concept was/is technically feasible, but environmentally undesirable and politically unthinkable. The solution is to switch to "clean" micropellet fusion bombs.

Fusion is being attempted in two ways. One is by containment of the deuterium-tritium fusion fuel in the form of a hot plasma in some kind of magnetic bottle. The other is to compress the cold D-T fusion fuel to high densities and pressures by impacting a tiny pellet of the fuel with either laser beams, electron beams, ion beams, or high speed BBs. To date, none of these approaches have worked, although some neutrons have been released. If imploded micropellet fusion is found to be feasible in the laboratory, then, even if it never becomes commercially viable as a prime power source, it still may be viable as an advanced propulsion concept.

Although laser imploded D-T micropellet fusion has not been demonstrated in the laboratory, we already have detailed engineering designs [Hyde, Wood, and Nuckolls 1972] for a rocket engine that can convert those isotropic miniature explosions into directed thrust. The rocket engine uses a magnetic nozzle formed by two superconducting magnetic rings. The magnetic fields from the two coils contain the plasma coming from the microexplosion point, then direct it rearward to provide thrust. The paper also discusses the design of the shielding for the superconducting magnetic coils. The shield not only stops the gamma rays and neutrons, but uses the neutrons to breed the tritium needed for future pellets. The spacecraft design also includes mass and size estimates for the lasers, mirrors, auxiliary systems, and heat-pipe radiators.

Recommendation:

The Department of Energy is funding the research to develop the implosion technology. It is recommended that the propulsion community fund further research on those areas specifically related to the propulsion application. These would be detailed design studies for the magnetic nozzle, lightweight radiators, lightweight tritium breeders, and lightweight versions of the implosion method that finally works.

References:

R. Hyde, L. Wood, and J. Nuckolls, "Prospects for Rocket Propulsion with Laser Induced Fusion Microexplosions," AIAA Paper 72-1063 (Dec 1972).

Muon Catalyzed Fusion

Muons are elementary particles with a mass of 106 MeV and a lifetime of 2.2 microseconds. Sometimes called "heavy electrons", they carry one unit of electronic charge. They can act as a fusion catalyst by replacing an electron in a hydrogen molecule. Because of their large mass, the muon orbits are so tight that the two nuclei come close enough together that the nuclei have a finite probability of fusing. Despite their short lifetime, the muons can catalyze many reactions.

The catalytic capability of the muon has been known for decades, but dismissed since elementary calculations showed that the muon could not catalyze enough reactions to compensate for the energy cost of creating it. During this contract it was learned that DOE is funding experiments to measure the actual (rather than the calculated) efficiency of muon-catalyzed fusion reactions [Jones 1983]. The experiments are still in progress. The reaction is not simple. "Enhancements" have been observed in the D-T-muon reaction, while He^3 , a natural byproduct of tritium decay, has been observed to scavenge muons and remove them from the reaction chain. The experiments have been carried out at high temperatures and pressures and it has been observed that high temperature increases the reaction yield by factors of 3 or more.

Recommendation:

Considering the difficulty of obtaining muons (they have to be obtained from decaying pions), and the difficulty of obtaining the fusion fuel (tritium is radioactive), and the marginal ideal efficiency, it is doubtful if this line of research will lead to an alternate propulsion energy source. The research effort is still young, however, and should be encouraged. In addition to the present DOE research, studies should be done on the effect of using He^3 filters in the target, using magnetically polarized muons and targets, and developing more efficient muon generators. If a breakthrough occurs in any of these areas then it is recommended that further study on this concept be given high priority.

References:

S.E. Jones, "Status and prospects of muon-catalyzed fusion research", EGG-SE-6290, prepared under DOE contract DE-AC07-76ID01570, Idaho National Engineering Lab (May 1983).

S.E. Jones, et al., "Experimental investigation of muon-catalyzed fusion in high-density deuterium-tritium mixtures", Third Int. Conference on Emerging Nuclear Energy Systems, Helsinki, Finland (6-9 June 1983).

Ultracold Neutron Fission

Neutrons that have a very low kinetic energy are moving very slowly and consequently have a very large quantum mechanical wavelength. For example a neutron with a velocity of 1 meter per second has a wavelength of 0.4 microns, about that of light. This quantum-nuclear wave can interact coherently with all nuclei within a wavelength. If the nuclei in a nearby wall are repulsive, the neutron will find itself repelled without approaching the wall. If the nuclei are reactive, the reaction will have a very large cross section. Thus, very slow (ultracold) neutrons can be used to initiate a nuclear fission reaction at will, just by pumping them into some neutron sensitive material such as uranium or lithium when the reaction is desired. No "critical mass" is required.

Ultracold neutrons were first made in quantities by using a cold neutron moderator made of cryogenically cooled hydrogen. Later, other techniques such as rapidly moving turbines and vibrators were proposed [Forward 1964], and later used [Luschikov 1977, Golub, et al. 1979] to create significant amounts of ultracold neutrons. Both magnetic bottles (which work on the nuclear magnetic moment of the neutron) and total internal reflection bottles (which interact with the coherent quantum wavelength of the neutron) have been used to contain a neutron longer than its 15 minute beta decay lifetime (it decays into an electron and a proton).

Recommendation:

The finite lifetime of the neutron limits this concept as a propulsion energy source. There are theoretical indications that the dineutron (a two neutron deuteron) or a tetraneutron (a four neutron alpha particle) may be stable against beta decay. If any evidence for these particles is discovered, then it is recommended that further study on this concept be given high priority.

References:

- R.L. Forward, "Ultracold neutrons and their potential value in gravitational research", RR-267A, Hughes Research Labs, Malibu, CA 90265 (Oct 1964).
- R. Golub, et al., "Ultracold neutrons", Sci. Am., 240, 134 (June 1979).
- V.I. Luschikov, "Ultracold Neutrons", Physics Today, 42-51 (June 1977).

Magnetic Monopole Catalytic Fusion

Magnetic monopoles are hypothetical particles that have only one magnetic pole, either north or south, not both as magnets do. They were first predicted by Dirac to explain the quantization of charge. Later theories not only predict their existence but also predict they are extremely heavy. A very recent, very complete bibliography [Craven and Trower 1983] was uncovered in the literature survey.

Magnetic monopoles could have a significant effect on future propulsion since they can catalyze proton decay, releasing most of the proton energy. Once one magnetic monopole has been trapped, then it can be used in a magnetic accelerator to produce more magnetic monopoles. One experiment to detect magnetic monopoles has produced a positive result [Cabrera 1982] but no further events have been seen to date.

Recommendation:

If and only if more magnetic monopole events are found or a magnetic monopole is captured, then it is recommended that further study of this concept be given high priority.

References:

R.E. Craven and W.P. Trower, "Magnetic monopole bibliography 1981-1982 (and previous versions)" Fermilab-82/96 (March 1983).

Blas Cabrera, "First results from a superconductive detector for moving magnetic monopoles", Phys. Rev. Lett. **48**, 1378 (1982).

APPENDIX A

**EXTRACTING ELECTRICAL ENERGY FROM THE VACUUM
BY COHESION OF CHARGED FOLIATED CONDUCTORS**

Dr. Robert L. Forward*
Forward Unlimited
34 Carriage Square
Oxnard, California 93030 USA

(805) 983-7652
(805) 983-7617

28 September 1983

Work supported in part by
Air Force Rocket Propulsion Laboratory
Contract F04611-83-C-0013.

*On leave from Hughes Research Laboratories,
3011 Malibu Canyon Road, Malibu, California 90265 USA

ABSTRACT

Any pair of conducting plates at close distances ($< 1 \mu\text{m}$) experience an attractive Casimir force that is due to the electromagnetic zero point fluctuations of the vacuum. A "vacuum fluctuation battery" can be constructed by using the Casimir force to do work on a stack of charged conducting plates. By applying a charge of the same polarity to each conducting plate we obtain a repulsive electrostatic force that opposes the Casimir force. If the applied electrostatic force is adjusted to always be slightly less than the Casimir force, the plates will move toward each other and the Casimir force will add energy to the electric field between the plates. A vacuum fluctuation battery made of a multitude of 20-nm-thick metal films brought to 20 nm spacing will have an electrical energy per kilogram equal to that of a good chemical battery. The battery can be recharged by making electrical forces slightly stronger than the Casimir force to re-expand the foliated conductor.

THE CASIMIR FORCE

In 1948 Casimir predicted that the electromagnetic zero point energy fluctuations of the vacuum should have observable effects on macroscopic objects. Specifically, he predicted that there would be an attractive force between two conducting plates [Casimir, 1948; Harris, 1972].

The Casimir interaction-energy-per-unit-area, u , between two conducting plates separated by a distance a , and the resulting force-per-unit-area or pressure, P , is

$$u = \frac{U}{A} = -\frac{\pi^2}{720} \frac{\hbar c}{a^3}, \quad (1)$$

$$P = \frac{F}{A} = -\frac{du}{da} = \frac{\pi^2}{240} \frac{\hbar c}{a^4}, \quad (2)$$

where $\hbar = 1.054 \times 10^{-34}$ J-sec and $c = 3 \times 10^8$ m/sec.

It is interesting to note that this attractive force is independent of the value of the electronic charge, e , and does not depend on the type of material in the conducting plates. This indicates that it is a fundamental force that exists in the vacuum between any pair of conductors that "may be interpreted as a zero point pressure of electromagnetic waves" [Casimir, 1948, p. 795].

Casimir's results were later expanded by Lifshitz to include forces between dielectrics. Lifshitz found that for dielectrics the Casimir force depends upon the dielectric constant of the material in the plates. The force per unit area between two dielectric plates of dielectric constants, ϵ_1 and ϵ_2 , when separated by a distance, a , is [Lifshitz, 1956]

$$P_{dd} = \frac{F}{A} = -\frac{\pi^2}{240} \frac{\hbar c}{a^4} \frac{(\epsilon_1 - 1)(\epsilon_2 - 1)}{(\epsilon_1 + 1)(\epsilon_2 + 1)} f(\epsilon) , \quad (3)$$

where $f(\epsilon)$ is a function that tends to 1.0 when ϵ is very large, and 0.35 when $\epsilon < 4$.

The Casimir equation (2) for two conducting plates can be obtained from the Lifshitz equation (3) by letting the dielectric constant go to infinity. The force between dielectric plates is always smaller than that between conducting plates, and if a plate has dielectric constant near unity, the Casimir force goes to zero.

Note that the energy given by Equation (1) becomes infinite at zero separation. If we use a cutoff distance of the order of the diameter of an atom, then the energy is of the same order of magnitude as the measured surface energy of the material [Israelachvili, 1973; Mahanty and Ninham, 1976]. In general, the vacuum fluctuation interaction energy between two bodies is the difference between the surface energy of the system at a given separation distance and the sum of the surface energies of the two bodies taken separately [Mahanty and Ninham, 1976, section 4.8].

The Casimir equation (2) and the Lifshitz equation (3) take into account the retardation effects in the electromagnetic field. The equations hold down to separation distances corresponding to one radian of the shortest wavelength radiation, λ , that the conductor can reflect [Casimir and Polder, 1946, 1948, Lifshitz, 1955, p. 81, footnote +]:

$$a_{min} = \lambda_{min}/2\pi . \quad (4)$$

When the separation is less than a_{min} , then the equation for the pressure reverts to the nonretarded force previously calculated by van der Waals [1873] and London [1930] between atoms. For two conducting plates, the pressure due to the unretarded electromagnetic vacuum fluctuation forces is [Hamaker, 1937]

$$P = \frac{F}{A} = \frac{C}{6\pi a^3} . \quad (5)$$

where C is an empirical constant that depends upon the material in the plates.

EXPERIMENTAL VERIFICATION OF THE CASIMIR FORCE

The experimental measurement of the Casimir force has been attempted a number of times with varying degrees of success. Usually, the experiment is carried out between a curved dielectric lens and a flat dielectric plate. The separation distance is typically measured by observing the Newton rings. The first successful measurements were carried out on quartz, thallium halide, and chromium-plated quartz against quartz, with separation distance down to 100 nm [Deriagin and Abrikosova, 1956; Abrikosova and Deriagin, 1957, Deriagin and Abrikosova, 1958]. Chromium-quartz data was obtained to 150 nm, and followed the $1/a^4$ Lifshitz prediction for retarded fields.

Other dielectric plate experiments were carried out with slowly improving precision [Kitchener and Prosser, 1957; Black, et al., 1960; Tabor and Winterton, 1969; Wittmann et al., 1971; Israelachvili and Tabor, 1972; Israelachvili and Adams, 1976]. A typical data set is shown in Figure 1 [Whittmann et al., 1971]. The closest separation distance obtained was 1.4 nm with two crossed cylinders of mica [Israelachvili and Tabor, 1972]. Their data shows good agreement with the $1/a^4$ Lifshitz law from 30 nm to 20 nm, with a break in slope at 15 nm changing to a $1/a^3$ London-van der Waals law from 10 nm down to 1.4 nm.

At a separation distance of 1.4 nm, the measured force between the two mica cylinders was over 10 kN/m². Although high, this force level is significantly less than what we would expect for metal plates at these distances for two reasons. First the dielectric constant of mica is only $\epsilon_1 = 1.59$, so the force from the Lifshitz equation (4) is decreased by the factor

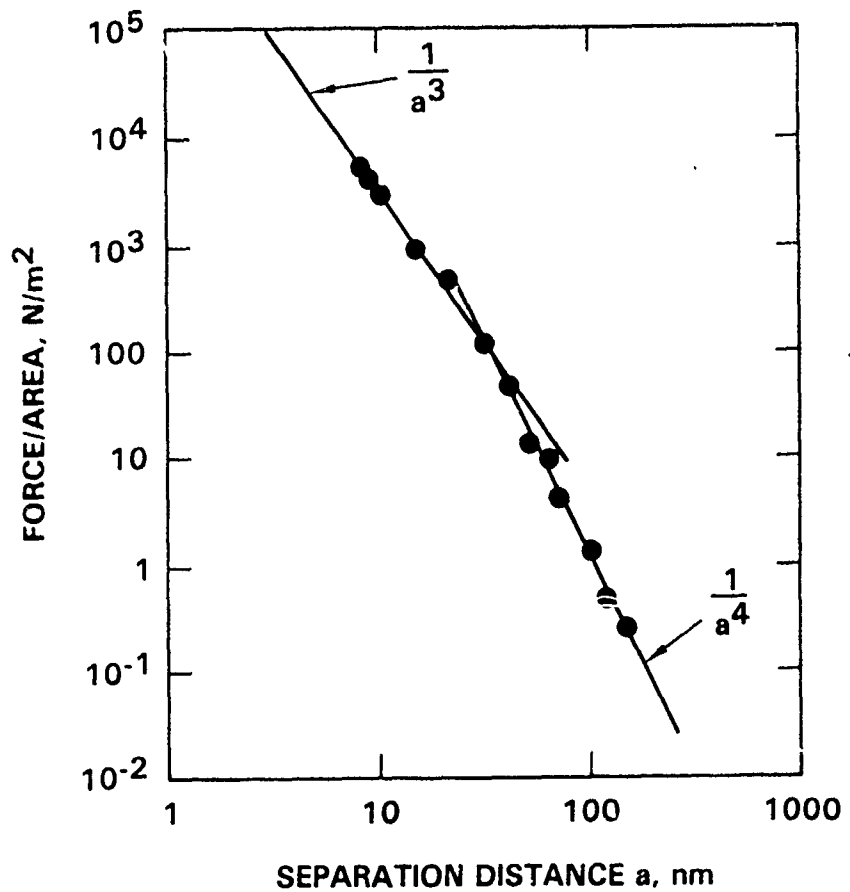


Figure 1 - Measurement of the forces between
two quartz plates

of $(\epsilon_1 - 1)^2 / (\epsilon_1 + 1)^2 = 0.14$. Second, the switchover from the $1/a^4$ retarded field behavior to the $1/a^3$ non-retarded field behavior takes place at larger distances than we would expect for a good ultraviolet reflecting metal like aluminum, leading to a lower force level.

Good experiments with conducting plates have proved to be extremely difficult. About the same time the first measurements on a curved chromium surface against a flat quartz plate were successfully made [Deriagin and Abrikosova, 1956, 1958], measurements were attempted on flat plates of chromium, chromium-steel, and aluminum [Sparnaay, 1957, 1958]. The closest distance obtained was 500 nm with chromium plates. The poor accuracy of the force measurement on chromium or chromium-steel would not allow the determination of the difference between a $1/a^4$ law and a $1/a^3$ law. The aluminum plate experiments were a failure. They were unpredictable and sometimes even gave a repulsion instead of an attraction. Later attempts on chromium-quartz interaction [Silfhout, 1966] gave good agreement with the Lifshitz law down to 100 nm, but experiments with chromium-chromium and aluminum-aluminum were erratic and of poor quality. Again, aluminum-aluminum often showed signs of repulsion, even at 700 nm distance [Silfhout, 196, p. 529].

Some recent experiments [Hunklinger, Geisselmann, and Arnold, 1972; Arnold Hunklinger, and Dransfeld, 1979] that should have had the benefit of years of technology were also unable to obtain good data between conducting plates at short distances. In this case, the conducting plates were silicon crystal and amorphous silicon over glass. The force showed a $1/a^4$ dependence down to 300 nm, then deviated strongly, almost flattening out at 200 nm. The closest spacing attained by this more modern apparatus was only 89 nm.

Thus although experiments on dielectric plates are in good agreement with theory, there are no good experiments to date on

metal plates down to the spacings (1 to 20 nm) that will show the deviation from the $1/a^4$ retarded field law to the $1/a^3$ non-retarded field law. With the advances in microcircuit technology, including the development of molecular beam epitaxy "atomic spray guns" that can lay down monolayers of atoms, it should now be possible to prepare samples of metals that are flat enough to carry out Casimir force experiments at separation distances of less than a nanometer.

EXTRACTION OF ENERGY FROM THE VACUUM FLUCTUATION FIELDS

The Casimir force has some of the properties of the gravity force since it is purely attractive, is independent of the material in the plates, and is a function of the inverse power of the separation distance, although the variation with separation distance goes as a higher power than the gravity force. Although there is no rigorous proof known that the vacuum fluctuation field is a conservative field like the gravity field, it is highly probable that it is. Otherwise, it would be possible to design machines using the Casimir force that would allow an infinite amount of energy to be extracted from the vacuum.

Even if the vacuum fluctuation field is a conservative field, that does not mean we cannot use it to obtain energy. The gravity field of the earth is a conservative field force and yet hydroelectric dams extract energy from the gravity field by using water coming from a region of high gravitational potential. In reality, of course, the energy extracted from a hydroelectric dam came originally from the sun, which evaporated the water from the oceans at a low gravitational potential and placed it in lakes at a high gravitational potential. The hydroelectric dam is then seen as a mechanism that uses the gravitational force of the earth as a "catalyst" to convert the gravitational potential energy of the water into kinetic energy that can, in turn, be converted into electricity by the turbines.

Hydroelectric dams are also used for energy storage. During times of low electrical demand, electricity can be used to pump water back up to a lake at high gravitational potential.

In the same manner, we can prepare a conductor in a foliated state which is in a "high" vacuum fluctuation potential energy state due to its large surface energy. We can then use the Casimir force as a means to convert the potential energy into kinetic energy as the foliated conductors cohere into a solid block of conductor that is in a "low" vacuum fluctuation potential energy state. The part of the hydroelectric turbines can be played by any mechanism that can convert kinetic energy into electricity; but for the example used in this paper, we will use the electrostatic repulsion force between two conducting plates with the same polarity of charge.

THE VACUUM FLUCTUATION BATTERY

We now propose a general concept for the construction of an aluminum foil "vacuum fluctuation battery." A large number of leaves of ultrathin aluminum foil are arranged in a stack with the leaves separated by a few microns. Each leaf is connected electrically to an active bidirectional power supply and the shape and position of the leaf is monitored by sensors. The power supply gives each leaf a small amount of positive charge. The positive charge will create an electrostatic repulsion between the plates that will keep the plates separated despite the attempt of the Casimir force to pull them together. This electrostatic suspension system is unstable, of course, so the position of each leaf will have to be electronically stabilized by the feedback from the position sensors through the active power supply. Stability may also be enhanced by unique geometries or partial mechanical support of the leaves using frames of insulating material such as aluminum oxide.

The voltages applied to the end leaf and the next-to-the-end leaf are then adjusted so that the electrostatic repulsion

between these two leaves is lowered until the electrostatic force is slightly less than the Casimir force at that distance. The Casimir force will draw the two leaves together, doing work against the repulsive electric field between the plates. By adjusting the electric field to always be slightly less than the Casimir force, the active bidirectional power supply can extract electrical energy out of the kinetic energy of the motion of the plates as they move from large separation distances (where the vacuum fluctuation potential energy given by Equation (1) is near zero) to the minimum separation distance where the vacuum fluctuation potential energy given by Equation (1) is large and negative. The process is repeated by the next leaf from the end until the foliated conductor is condensed into a solid block. Alternately, all the leaves could be brought together at the same time in a manner similar to compressing an accordion.

Thus, by cohering the multitude of aluminum leaves in a foliated conductor into a single block of aluminum under the careful control of an electronic servo system, it is possible to extract electrical energy from the vacuum.

If the collapse process is halted before the aluminum films cohere, then the vacuum fluctuation battery can be "recharged" by making the applied electrostatic force slightly larger than the Casimir force. The leaves will be pushed apart at the cost of supplying energy from the bidirectional power supply.

Another version of the vacuum fluctuation battery that might be easier to fabricate and have more stability would be a wide, flat spiral of foil (see Figure 2) built along the lines of a SlinkyTM toy. Here there would be only one conductor with which to make contact, and each turn of the spiral would act against the neighboring turns. The spiral configuration would allow a substantial compaction of the foil from large spacings to small spacings while maintaining uniform spacing.

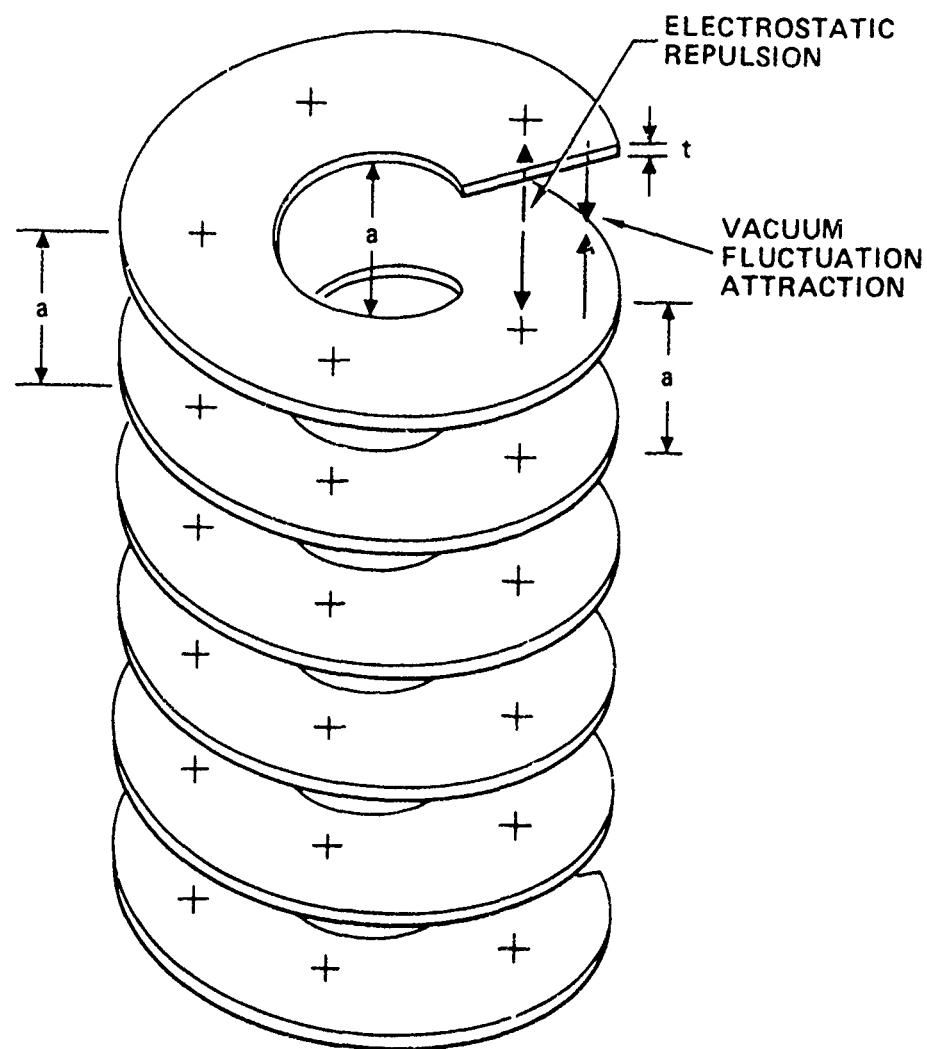


Figure 2 - Spiral design for a vacuum fluctuation battery.

ESTIMATES OF BATTERY PERFORMANCE

Aluminum has a reflectance of greater than 90% at the UV wavelength of 120 nm [AIP Handbook, 1972, p. 6-124], so it should have a Casimir force below 20 nm. At 20 nm spacing, Equation (2) predicts that two aluminum foils should experience a force per unit area of 8120 N/m^2 . The potential energy due to the vacuum fluctuation interaction at 20 nm spacing is given by Equation (1) as 5.4 J/m^2 .

The electrical voltages needed to counter this Casimir force are minimal, even at the closest distance. The force on the plates of a capacitor with an area A, capacitance C, voltage V, and charge Q, where the separation distance, a, is small compared to the dimensions of the plate is

$$F = Q^2/2\epsilon_v A = CV^2/2a = \epsilon_v AV^2/2a^2 , \quad (6)$$

where $\epsilon_v = 8.85 \times 10^{-12} \text{ F/m}$ is the capacititivity of the vacuum. To equal the Casimir force of $F = 8120 \text{ N}$ between a pair of conducting foils of area $A = 1 \text{ m}^2$ separated by a distance $a = 20 \text{ nm}$ only requires 0.86 V.

If we make the aluminum into ultrathin sheets, then the reflectance will drop with film thickness. There is no data available at 120 nm wavelength, but at 220 nm an aluminum film only 20 nm thick has a reflectance of 76% [AIP Handbook, 1972, p. 6-159]. If we assume that our aluminum foils are 20 nm thick, then their mass per unit area is easily shown to be 5.4 mg/m^2 .

Since the amount of energy we can extract from the contraction of one leaf is 5.4 J, that means that the contraction of a foliated array of 20-nm-thick aluminum films to a separation distance of 20 nm should produce an energy of 100 kJ/kg. In "battery" language this is 28 W-h/kg. The energy/mass performance of this vacuum is comparable to that of a good chemical battery.

REFERENCES

I.I. Abrikosova and B.V. Deriagin, "Direct measurement of molecular attraction of solid bodies. II. Method for measuring the gap. Results of experiments.," Soviet Physics JETP 4, 2-10 (1957) [Zu. Eksp. Teor. Fiz. 31, 3-13 (1957)].

American Institute of Physics Handbook, (McGraw Hill, 1972).

W. Arnold, S. Hunklinger, and K. Dransfeld, "Influence of optical absorption on the van der Waals interaction between solids," Phys. Rev. B19, 6049-6056 (1979); Erratum, Phys. Rev. B21, 1713 (1980).

W. Black, J.G.V. de Jongh, J.T.G. Overbeek, and M.J. Sparnaay, "Measurements of retarded van der Waals' forces," Trans. Farad. Soc. 56, 1597-1608 (1960).

H.B.G. Casimir and D. Polder, "Influence of retardation on the London-van der Waals forces," Nature 158, 787-788 (1946).

H.B.G. Casimir and D. Polder, "The influence of retardation on the London-van der Waals forces," Phys. Rev. 73, 360-372 (1948).

H.B.G. Casimir, "On the attraction between two perfectly conducting plates," Proceedings Koninklijke Nederlandse Akademie van Wetenschappen, Amsterdam 51, No. 7, 793-796 (1948) [in English] [This reference is hard to obtain. Casimir's result is re-derived in an easily readable form in Harris 1972].

B.V. Derigian and I.I. Abrikosova, "Direct measurement of the molecular attraction of solid bodies. I. Statement of the problem and method of measuring forces by using negative feedback," Soviet Physics JETP 3, 819-829 (1957) [Zh. Eksp. Teor. Fiz. 30, 993-1006 (1956)].

B.V. Deriagin and I.I. Abrikosova, "Direct measurements of molecular attraction of solids," J. Phys. Chem. Solids 5, 1-10 (1958).

H. Hamaker, Physics 4, 1058 (1937).

Edward G. Harris, A Pedestrian Approach to Quantum Field Theory, (Wiley-Interscience, NY, 1972.) [Harris gives the wrong volume number for the Casimir 1948 paper.]

S. Hunklinger, H. Geisselmann, and W. Arnold, "A dynamic method for measuring the van der Waals forces between macroscopic bodies," Rev. Sci. Instrum. 43, 584-587 (1972).

J.N. Israelachvili and D. Tabor, "Measurement of van der Waals dispersion forces in the range of 1.5 to 130 nm," Proc. Roy. Soc. A331, 19 (1972).

J.N. Israelachvili, "Van der Waals dispersion force contribution to works of adhesion and contact angles on th basis of macroscopic theory," J. Chem. Soc. Faraday II 69, 1729 (1973).

J.N. Israelachvili and G.E. Adams, "Direct measurement of long range forces between two mica surfaces in aqueous KNO_3 solutions," Nature 262, 774-776 (1976).

J.A. Kitchener and A.P. Prosser, "Direct measurement of the long-range van der Waals forces," Proc. Royal Soc. A242, 403-409 (1957).

E.M. Lifshitz, "The theory of molecular attractive forces between solids," Soviet Physics JETP 2, 73-83 (1956) [Zh. Eksp. Teor. Fiz. 29, 94 (1955)].

F. London, Z. Phys. 60, 491 (1930).

J. Mahanty and B.W. Ninham, Dispersion Forces (Academic Press, NY, 1976).

A. van Silfhout, "Dispersion forces between macroscopic objects," Proceedings Koninklijke Nederlandse Akademie van Wetenschappen B69, "Part I," 501-515; "Part II," 516-531; "Part III," 532-541 (1966).

M.J. Sparnaay, "Attractive forces between flat plates," Nature 180, 334-335 (1957).

M.J. Sparnaay, "Measurements of attractive forces between flat plates," Physica 24, 751-764 (1958).

D. Tabor and R.H.S. Winterton, "The direct measurement of normal and retarded van der Waals forces," Proc. Royal Soc. A312, 435-450 (1969).

J.H. van der Waals, Ph.D. Thesis, University of Leiden (1873).

F. Wittmann, H.J. Splitgerber, and K. Ebert, "Studium der van der Waals-Kraft im Bereich kleiner Abstände (A study of the van der Waals force at small distances)," Z. Phys. 245, 354-360 (1971) [in German].

APPENDIX B

**LIGHT-LEVITATED GEOSTATIONARY CYLINDRICAL ORBITS
USING PERFORATED LIGHT SAILS**

Dr. Robert L. Forward*
Forward Unlimited
34 Carriage Square
Oxnard, California 93030 USA

(805) 983-7652
(805) 983-7617

8 May 1983

Work supported in part by
Air Force Rocket Propulsion Laboratory
Contract F04611-83-C-0013.

*On leave from Hughes Research Laboratories,
3011 Malibu Canyon Road, Malibu, California 90265 USA

LIGHT-LEVITATED GEOSTATIONARY CYLINDRICAL ORBITS
USING PERFORATED LIGHT SAILS

Dr. Robert L. Forward

ABSTRACT

A perforated light sail is attached to a communication satellite in geostationary orbit and tilted toward the sun. The light pressure from the sun provides a component of force perpendicular to the orbital plane. This force "levitates" the satellite northward (or southward) of the nominal equatorial geostationary orbit plane by a distance determined by the mass-to-area ratio of the sail plus communication package. By using a light sail with perforations smaller than the wavelength of the sunlight, the mass of the sail can be decreased significantly without affecting the reflectivity. The distance of the levitated sail in the north-south direction can be many thousands of kilometers, and can even allow a satellite to operate in a geostationary "orbit" whose orbital "center" is outside the earth's surface. This concept will permit poleward "stacking" of communication satellites at the more desirable angular positions along the normal equatorial geostationary orbit, and for the first time will allow geostationary satellites to communicate directly with the polar regions.

BACKGROUND

This paper is an extension of a previous paper with a similar title¹ that first proposed the light-levitated cylindrical orbit concept. The maximum amount of north-south distance obtained in that paper was limited to a few thousand kilometers by the assumed minimum mass-to-reflective area ratio of any sail of 0.1 gm/m^2 . This mass to reflective area ratio is that of the lightest sail known at that time which was made of 30 nm aluminum film. Films thinner than this start to become transparent to light.

In this paper we introduce a new sail concept called the perforated light sail² that has a greatly reduced mass-to-reflective area ratio and consequently can be used to create a geostationary orbit that is at a distance that is north or south of the equatorial plane by more than the radius of the earth, thus allowing a direct line of sight to the polar regions.

PERFORATED LIGHTSAILS

It is well known to radar engineers that a reflector of radar waves does not have to be made of solid metal. The weight and wind resistance of the reflector can be reduced by orders of magnitude without affecting the reflectivity by making the reflector of "chicken wire" mesh, provided that the holes in the mesh are much smaller than a wavelength of the microwave radiation. In the same manner, we can lower the mass and reduce the upper atmospheric drag of any light sail by perforating the sail material with tiny holes that are smaller than a wavelength of light. This will allow the perforated lightsails to be launched at Shuttle altitudes (present solid sails cannot be launched below 1000 km altitude), and the performance of the perforated lightsails, whether they are made of aluminum-covered plastic film³ or aluminum film,⁴ will be significantly improved over an equivalent solid sail.

There are a number of techniques for making a perforated sail structure that have already been developed by those working on replication of submicron electronic microcircuits. Both electron beams and ion beams can make holes and lines smaller than a wavelength of light. Two ultraviolet laser beams directed at each other will create a holographic fringe pattern with spacings of 0.2 μm , and a crossed pair of holographic gratings on a photosensitive resist can create an array of square dots with 0.2 μm spacing that can be used as a mask to make a square mesh of aluminum wires with 0.2- μm spacings and thickness-to-hole-size ratio that can be varied by varying the resist exposure/development cycle. Samples of these perforated light sails have not been made and tested yet, but if the results in the microwave domain hold, we can expect that the mass-to-reflective area of these perforated sails can be improved by an order of magnitude over solid sails.

LEVITATED GEOSTATIONARY COMMUNICATION ORBIT

In the proposed system, a communication package designed for geostationary operation is launched and placed into an earth-synchronous equatorial orbit. Then a large reflective perforated lightsail is deployed and tilted so that it faces toward the sun at a tilt angle θ . At this angle, the light sail of area A will experience a force F due to the light flux of the sun, $S = 1.4 \text{ kW/m}^2$, of

$$F = \frac{2SA}{c} \sin \theta , \quad (1)$$

where c is the speed of light, and the factor 2 comes from the double transfer of photon momentum to the sail by the incoming and reflected photons. This force has a polar component that is given by

$$F_p = \frac{2SA}{c} \sin \theta \cos \beta , \quad (2)$$

where β is the angle of the sail with respect to the plane of the orbit. The angle β lies between $0 \pm 23.5^\circ$. It equals 0 at the time of the equinoxes and reaches its maximum excursions at the solstices. The angle β is greater than 0 when the sun and sail are both on the same side of the equatorial plane, and less than 0 when they are on opposite sides.

As is shown in Figure 1, the poleward component of the light pressure force will "levitate" the satellite into an orbit that is north (or south) of the equatorial synchronous orbit. The levitated orbit can still be earth-synchronous, but the center of these orbits will be north (or south) of the gravitational center of the earth. The set of possible levitated orbits has cylindrical symmetry along the north-south earth spin axis. The light pressure also produces an equatorial force in the plane of the orbit given by

$$F_e = \frac{2SA}{c} \sin \theta \sin \beta . \quad (3)$$

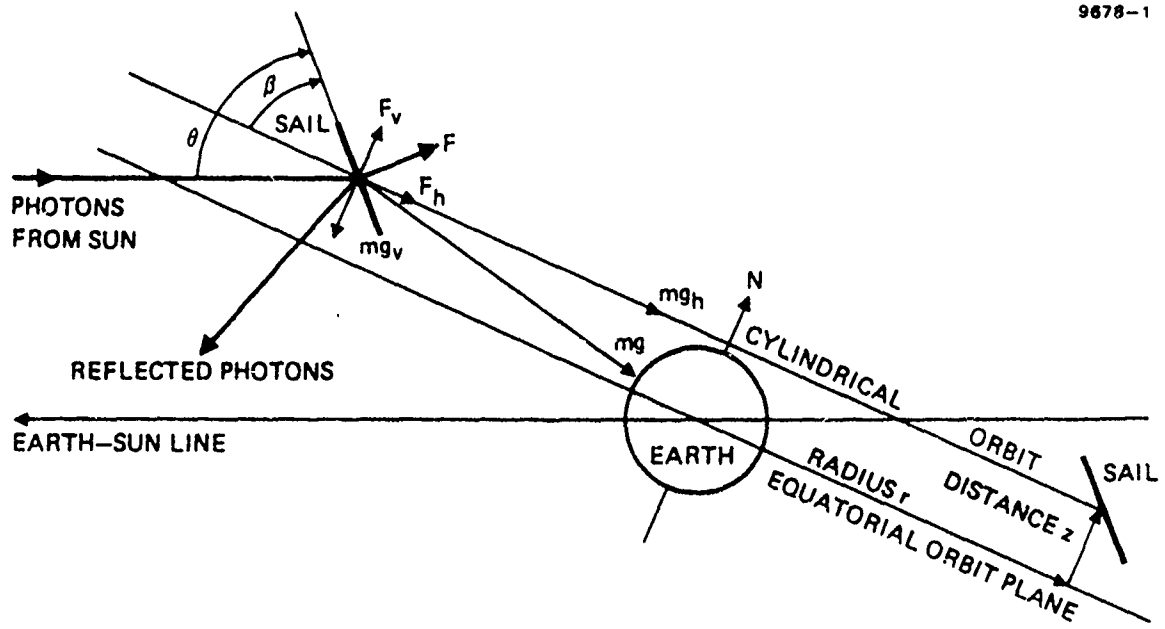


Figure 1. Light-levitated cylindrical orbit.

This constant equatorial thrust is many times weaker than the gravitational attraction of the earth so the shape of the orbit is still predominantly determined by the earth. The effect of this constant thrust is to leave the orbit essentially circular, but to displace the circular orbit to the side away from the sun. This effect was observed in the orbit of the early Echo balloon satellite.

The flux intensity and the angle to the sun are not exactly constant, but will, because of the finite distance of the sun, vary by a few parts in 10,000 during the day as the sail moves about in its orbit. The analyses below ignore these insignificant variations.

The maximum north-south distance obtainable at a given time of year is calculated by setting the derivative of F_p with respect to θ equal to zero. At the equinoxes, we find that the optimum angles for maximum distance are $\theta = \beta = 45^\circ$ ($\sin \theta = \cos \theta = \sin \beta = \cos \beta = 0.707$). The polar and equatorial forces are equal at this time and are given by

$$F_p = F_e = SA/c . \quad (4)$$

At one solstice, the sun and sail are on opposite sides of the equatorial plane, and the optimum angles for maximum vertical lift are $\theta=56.75^\circ$ and $\beta=\theta-23.5^\circ=33.25^\circ$. At this time we have $\sin \theta = \cos \beta = 0.836$, so that the polar force is 1.4 times the force at the equinoxes. At the other solstice, the sun and sail are on the same side and the sail angles are smaller, resulting in poorer coupling of the sunlight into polar force. The optimum angles at this time are $\theta=33.25^\circ$ and $\beta=\theta+23.5^\circ=56.75^\circ$. With these angles, $\sin \theta = \cos \beta = 0.548$. We will assume this worst case force level for the remainder of four calculations, since the sail angle can always be "trimmed" at other times of the year, or the extra thrust can be used to smooth out the slight orbital perturbations to achieve exact geosynchronism.

For the worst case solstice time, the polar force is found to be

$$F_p = 0.60 \text{ SA/c} , \quad (5)$$

while the equatorial force is

$$F_e = 0.92 \text{ SA/C} . \quad (6)$$

GRAVITY FORCE

A communications satellite and sail of mass m in an orbit of radius r levitated a distance z above the equatorial plane is at a distance

$$R = (r^2 + z^2)^{1/2} \quad (7)$$

from the center of the earth of mass M and experiences a gravitational force,

$$mg = GMm/R^2 , \quad (8)$$

where $G = 6.67 \times 10^{-11} \text{ m}^3/\text{kg}\cdot\text{s}^2$ is the Newtonian gravitational constant.

The polar component of this gravitational force is

$$mg_p = mgz/R = GMmz/R^3 , \quad (9)$$

while the equatorial component is

$$mg_e = mgr/R = GMmr/R^3 . \quad (10)$$

The centrifugal force of the motion of the satellite in the cylindrical orbit with angular velocity Ω and orbital radius r balances the equatorial component of the gravitational force (ignoring for now the horizontal component of the light pressure):

$$m\Omega^2 r = GMmr/R^3 . \quad (11)$$

Eliminating mr from both sides and solving for the radius of the orbit, we obtain

$$r = [(GM/\Omega^2)^{2/3} - z^2]^{1/2} . \quad (12)$$

If we assume that we want the levitated orbit to have the same period as a geostationary orbit, then the geostationary angular velocity Ω_g will be related to the radius R_g of the equatorial geostationary orbit by the usual relation:

$$\Omega_g^2 R_g^3 = GM . \quad (13)$$

Substituting this relation into Equation (12), we find that the locus of the levitated geostationary orbits form a sphere with a radius equal to the radius of the equatorial geostationary orbits:

$$r = [R_g^2 - z^2]^{1/2} . \quad (14)$$

(In reality, the locus of orbits will be pushed to one side at higher values of z by the equatorial component of the light pressure force.)

NORTH-SOUTH LEVITATION DISTANCE

The distance z that the perforated sail and payload will be levitated in the north-south direction is determined by the balance between the polar component of the gravitational force and the polar component of the light pressure force. Thus.

$$F_p = mg_p , \quad (15)$$

and

$$\frac{2SA}{c} \sin \theta \cos \beta = \frac{GMmz}{R_g^3} . \quad (16)$$

Solving for the levitation distance, we get

$$z = \frac{2 \sin \theta \cos \beta SR_g^3 g \frac{A}{m}}{GcM} , \quad (17)$$

where A/m is the reflective area to mass of the perforated sail. If we make the following substitutions for the constants in Equation (17):

$$\theta = 33.25^\circ$$

$$\beta = 56.75^\circ$$

$$S = 1.4 \text{ kW/m}^2$$

$$R_g = 42 \text{ Mm}$$

$$G = 6.67 \times 10^{-11} \text{ m}^3/\text{kg}\cdot\text{s}^2$$

$$c = 300 \text{ Mm/s}$$

$$M = 6 \times 10^{24} \text{ kg} ,$$

we obtain a relation giving the maximum north-south orbital distance obtainable from a perforated lightsail and payload of a given area to mass ratio:

$$z = (520 \text{ kg/m}) A/m . \quad (18)$$

Thus, for an orbital levitation distance equal to the radius of the earth (6400 km), the mass-to-reflective area of the sail plus payload needs to be less than 0.08 g/m². For the sail mass equal to the payload mass, the sail needs to have a mass-to-area ratio of 0.04 g/m², a value easily reached by a perforated aluminum film sail. For a one metric ton payload, the one ton sail will have diameter of 5.6 km.

The ratio of the light pressure force in the equatorial plane to the gravity force in the equatorial plane is a measure of the amount of offset of the orbit from the polar axis:

$$K = \frac{F_e}{mg_e} = \frac{2 \sin \theta \sin \beta SR_q^3}{GMcr} \frac{A}{m} . \quad (19)$$

Substituting Equation (17) for the area-to-mass ratio we find a simple relation for the ratio of the light force to the gravitational force in the equatorial plane:

$$K = z \sin \beta / r \cos \theta . \quad (20)$$

Since this ratio is proportional to the offset of the center of the levitated orbit from the polar axis, and since the orbital offset will cause the viewing angle from the earth to vary slightly during the day, we want to keep this combined effect at a minimum. Thus, it is obvious that we want to minimize the angle β , since we require that the polar component of light thrust remain sufficient to maintain the desired north (south) distance of the levitated orbit.

EXAMPLE OF A POLAR VIEWING LEVITATED ORBIT

In the example shown in Figure 2, we have chosen a levitated orbit with a north levitation distance of 13,000 km, or twice the radius of the earth. This puts the communication satellite at an angle of 9.3° above the horizon at the north pole. Normally, the sail will be trimmed during the orbit so that it will stay at the same position in the sky. The figure shows the situation at the summer solstice where we have the worst case sun angle. The angle of the sail with respect to the orbital plane is $\beta = 30^\circ$, and the angle of the sail with respect to the sun line is $\theta = 6.5^\circ$.

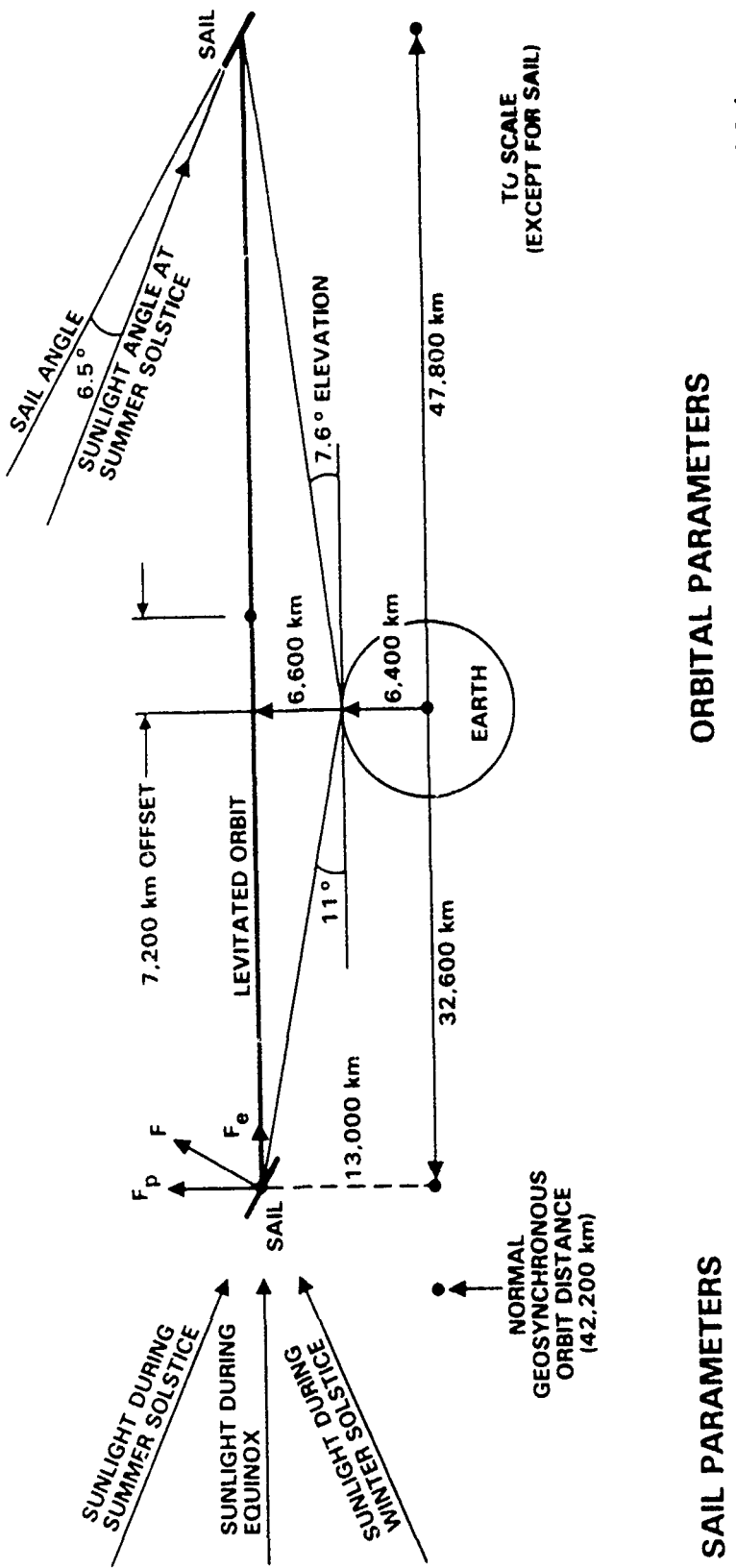
The mass-to-area ratio needed to achieve this levitation distance is 0.013 g/m^2 . This mass-to-area ratio is one-eighth the mass of an aluminum film sail. For a one metric ton sail supporting a one ton payload, the diameter of the perforated lightsail is 12 km.

The radius of the levitated orbit is 40,200 km, which is some 2000 km less than an equatorial geostationary orbit. At the worst case time of the season, there will be no trim capability left in the sail and the orbital offset due to the light pressure will be 7,200 km, creating a $\pm 1.7^\circ$ north-south variation of the communication satellite in the sky at the polar regions.

CONCLUSIONS

Perforated light sails can be used to create geostationary orbits that are not in the equatorial plane of the earth. This will alleviate crowding at the more desirable angular positions along the equatorial geostationary orbit, and for the first time will allow geostationary satellites to communicate directly with the polar regions.

FIGURE 6



ORBITAL PARAMETERS

ORBITAL RADIUS	— 40,200 km
ORBITAL OFFSET	— 7,200 km
ORBITAL LEVITATION	— 13,000 km
ORBITAL PERIOD	— 24 hours
POLAR ELEVATION	— $9.3^\circ \pm 1.7^\circ$ (WORST CASE)

Figure 2. Polar geostationary orbit using perforated light sails.

REFERENCES

1. R.L. Forward, "Light-levitated geostationary cylindrical orbits", *J. Astronaut. Sci.* 28, 73-80 (1981).
2. R.L. Forward, "Perforated microstructured lightsail", Patent Disclosure F-001, Contract F04611-83-C-0013, Air Force Rocket Propulsion Lab., Edwards AFB, CA (1983).
3. L.D. Friedman et al., "Solar sailing - the concept made realistic", AIAA paper 78-82, AIAA 16th Aerospace Sciences Meeting, Huntsville, Alabama (16-18 January 1978).
4. K.E. Drexler, "High performance solar sails and related reflecting devices," AIAA paper 79-1418, 4th Princeton/AIAA Conf. on Space Manufacturing Facilities, Princeton, NJ (14-17 May 1979).

APPENDIX C

STARWISP

Dr. Robert L. Forward*
Forward Unlimited
34 Carriage Square
Oxnard, California 93030 USA

(805) 983-7652
(805) 983-7617

1 June 1983

Work supported in part by
Air Force Rocket Propulsion Laboratory
Contract F04611-83-C-0013.

*On leave from Hughes Research Laboratories,
3011 Malibu Canyon Road, Malibu, California 90265 USA

STARWISP

Dr. Robert L. Forward

ABSTRACT

Starwisp is a light-weight, high-speed interstellar fly-by probe pushed by beamed microwaves. The basic structure is a wire mesh sail with microcircuits at each intersection. The mesh sail is driven at high acceleration using a microwave beam formed by a large fresnel-zone-plate transmitter lens made of alternating sparse metal mesh rings and blank rings. The high acceleration allows Starwisp to reach a coast velocity near that of light while still close to the transmitting lens. Upon arrival at the target star, the transmitter floods the star system with microwave energy. Using the wires as microwave antennas, the microcircuits collect energy to power their optical detectors and logic circuits to form images of the planets in the system. The phase of the microwaves at each point of the mesh is sensed and the information used to form the mesh into a retrodirective phased array microwave antenna that beams a signal back to earth. A minimal Starwisp would be a 1 km mesh sail weighing 16 grams and carrying 4 grams of microcircuits. It would be accelerated at 115 gravities by a 10 GW microwave beam, reaching one-fifth of the speed of light in a few days. Upon arrival at Alpha Centauri 21 years later, Starwisp would collect enough microwave power to send back a high resolution picture every three minutes during its fly-through of the system.

INTRODUCTION

Starwisp is a net of semi-intelligent wires that will be accelerated to near-relativistic speeds by modest amounts of beamed microwave power. During its fly-by through the nearer stellar systems, it will send back pictures that will allow us to count and size the planets and even obtain pictures of some of the planetary surfaces if we are lucky enough to have the probe pass within a few AU of the planets.

A source of microwave power that might be available in the near future would be a solar power satellite. One proposed solar power satellite design uses large arrays of solar cells to convert sunlight into electricity, which is then used to generate about 10 GW of microwaves. In normal use, these microwaves would be beamed to antennas on the earth's surface and converted into electrical power. During the testing phase of the solar power satellite, this microwave power could be used to launch one or more modest-sized Starwisp probes to the nearer star systems. For more distant journeys with more massive probes moving at higher velocities, it would be necessary to construct a special purpose source of microwave energy with a power level of 1-100 TW.

TRANSMISSION OF MICROWAVES

The normal transmitting antenna for a solar power satellite is not large enough to transmit a microwave beam over the distances that will be needed to send a Starwisp probe on its way. It will be necessary to construct a very large transmitter lens to relay the microwave power out to the Starwisp sail. The transmitter lens will be a microwave Fresnel zone plate with rings of wire mesh alternating with empty rings. The wire mesh will have holes larger than the microwave wavelength, but small enough to affect the phase of the microwaves passing through them so that the phase shift is exactly 180°. Thus, the

microwaves passing through the mesh portions will be a half-wavelength out of phase with the microwaves passing through the empty portions, causing all the different pathlengths to be in phase at the focal point.

A lens of diameter D can focus radiation of wavelength λ to a spot size of diameter d at a distance s given the relation,

$$Dd = 2.44 s\lambda , \quad (1)$$

where the factor 2.44 indicates that the diameter of the focal spot is not taken at the half-power point of the main beam, but at the diameter of the first null in the diffraction pattern of the circular lens. There is a maximum of 84% of the energy in this main lobe, which gives a beam efficiency of $\epsilon_b = 0.84$. There will be some loss in the transmitting antenna due to energy reflected and absorbed by the phase-shifting mesh and the fact that a Fresnel zone plate is not a perfect lens, so the transmitter lens will have a Fresnel lens efficiency, ϵ_f . Thus, of the transmitted power from the source, the maximum amount of incident microwave power, P_i , at the focal spot is:

$$P_i = \epsilon_b \epsilon_f P_t . \quad (2)$$

ACCELERATION OF SAIL

The mesh structure of the Starwisp sail will have a reflectance ϵ_r , a transmittance ϵ_t , and an absorptance ϵ_a , where, of course,

$$\epsilon_r + \epsilon_t + \epsilon_a = 1 . \quad (3)$$

The acceleration of a sail of mass M and microwave photon momentum transfer efficiency ϵ_m driven by an incident beam of microwave power P_i is

$$a = \frac{2\epsilon_m P_i}{Mc} , \quad (4)$$

where $c = 3 \times 10^8$ m/s is the velocity of light. The momentum transfer efficiency, ϵ_m , consists of two components. First, when the microwaves hit the sail, the sail receives an impulse from all the microwave flux except that which passes through the sail $(1 - \epsilon_t)$, including the portion of the microwaves absorbed by the resistive losses in the sail. Second, the sail receives another impulse from the portion of the microwaves reflected from the sail. Thus, the momentum transfer efficiency is given by

$$\epsilon_m = [(1 - \epsilon_t) + \epsilon_r]/2 = (2\epsilon_r + \epsilon_a)/2 \approx \epsilon_r . \quad (5)$$

There will be two phases of acceleration. First there will be a constant acceleration a_0 while the sail is still close to the transmitting lens and the lens can focus to a spot size smaller than the sail. If we include all the efficiencies in the power transmission system, then the initial acceleration in terms of the transmitted power, P_t , is

$$a_0 = \frac{2\epsilon_p P_t}{Mc} , \quad (6)$$

where the "propulsion" efficiency, ϵ_p , is the product of the Fresnel lens efficiency, the beam efficiency, and the momentum transfer efficiency,

$$\epsilon_p = \epsilon_f \epsilon_b \epsilon_m \approx \epsilon_f \epsilon_b \epsilon_r . \quad (7)$$

The distance s_0 over which the acceleration stays constant is determined by the wavelength λ , the transmitter lens diameter D , and the sail diameter d :

$$s_0 = \frac{D d}{2.44\lambda} . \quad (8)$$

At a constant acceleration a_o over the distance s_o the sail will have reached a velocity v of

$$v_o = (2a_o s_o)^{1/2} \quad , \quad (9)$$

in the time,

$$t_o = (2s_o/a_o)^{1/2} \quad . \quad (10)$$

The sail is now at the point where the beam diameter is greater than the sail diameter and the power on the sail drops off with distance. At a distance x from the transmitter lens, the minimum diameter of the beam B from the lens of diameter D is

$$B = 2.44 \lambda x/D \quad . \quad (11)$$

The amount of power collected by the sail of diameter d is then

$$P_c = \frac{d^2}{B^2} \epsilon_b \epsilon_f P_t \quad , \quad (12)$$

and the acceleration from that collected power is

$$\dot{v} = \frac{2\epsilon_m P_c}{M c} = \frac{2\epsilon P_t}{M c} \frac{d^2}{B^2} = a_o \frac{d^2}{B^2} \quad . \quad (13)$$

Substituting in Equation (11) for the beam diameter B , and using Equation (8) to simplify, we get the acceleration as a function of the square of the distance x from the lens:

$$\dot{v} = \frac{a_o s_o^2}{x^2} \quad . \quad (14)$$

This acceleration can be integrated from the point $x = s_0$ out to infinity to obtain the solution for the terminal velocity v_t of the sail. It is easily shown that the maximum terminal velocity obtainable is

$$v_t^2 = 2 v_o^2 = 4 a_o s_o . \quad (15)$$

Substituting in Equation (6) for a_o and Equation (8) for s_o , and rearranging, we can obtain an equation for the transmitted power needed to accelerate a given sail to a given terminal velocity, v_t :

$$P_t = \frac{2.44 M c v_t^2 \lambda}{8 \epsilon_p d D} . \quad (16)$$

SAIL PARAMETERS

The mass of a mesh sail depends predominantly upon the diameter d of the sail, the diameter b and density ρ of the wire used in the mesh, and the maximum diameter h of the holes in the mesh. There is also a slight variation that depends upon the geometry of the mesh. For a sail with an n by n square mesh with spacing r , the length of the wire is easily determined to be

$$L = 2n(n + 1)r = 2 n^2 r . \quad (17)$$

The mass of a square sail using wire of diameter b and density ρ is

$$m = \frac{\pi}{4} \rho b^2 L \quad (18)$$

The diameter of the sail (along the diagonal dimension) is

$$d = n h = 2^{1/2} n r , \quad (19)$$

and the area of the square sail is

$$A = n^2 r^2 = d^2 / 2 \quad . \quad (20)$$

Thus, the mass per unit area of the square sail is

$$u = \frac{m}{A} = \frac{\pi \rho b^2}{2 r} \quad . \quad (21)$$

The maximum hole size is along the diagonal of the square hole, or

$$h = 2^{1/2} r \quad . \quad (22)$$

If we assume the actual sail is circular in shape with a diameter d equal to the longest dimension of the square sail, but rounded out with square mesh elements with the same mass per unit area, then the mass of the circularized sail is found to be

$$M = \frac{\pi}{4} u d^2 = \epsilon_g \frac{\pi^2}{4} \frac{\rho b^2 d^2}{h} \quad , \quad (23)$$

where ϵ_g is a geometry factor that is 0.707 for a square sail. Similar analyses with hexagonal and triangular meshes give the same equation, provided that the maximum hole diameter h is kept the same. As is shown in Table 1 and Figure 1, the geometry factor varies slightly with the choice of mesh structure, with the heavier mesh structures being those having more wires meeting at each intersection.

TABLE I

Parameters of Various Mesh patterns		
Type of Mesh	Number of Intersecting Wires	Geometry Factor (eg)
Hexagonal	3	$3^{-1/2}$ (0.577)
Square	4	$2^{-1/2}$ (0.707)
Triangular	6	$3/4$ (0.750)

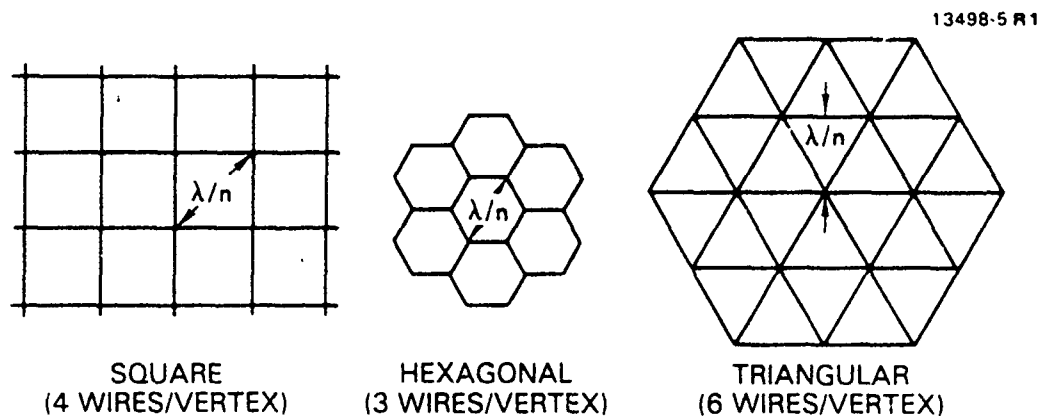


Figure 1. Basic types of mesh structures

If we make the assumption that the maximum hole diameter in the mesh is some fraction of the wavelength of the microwave radiation,

$$h = \epsilon_h \lambda , \quad (24)$$

and substitute Equation (24) into Equation (23), we find that the mass of the sail is inversely dependent on the microwave wavelength:

$$M = \frac{\pi^2}{4} \frac{\epsilon_p \rho b^2 d^2}{\epsilon_h g \lambda} . \quad (25)$$

Substituting this equation for the mass into Equation (6) we see that the initial acceleration increases with increasing wavelength.

$$a_0 = \frac{8 p \epsilon_h P_t \lambda}{\pi^2 \epsilon_p \rho b^2 d^2 g} . \quad (26)$$

If we assume that the transmitted power is fixed and the terminal velocity is fixed, then there is a fixed relationship between the ratio of the diameter of the sail and the diameter of the transmitting lens. Substituting Equation (25) for the mass in Equation (16) and solving for the ratio D/d, we find that the ratio of the lens diameter to the sail diameter is independent of the wavelength of microwave radiation and depends only on the parameters of the mesh wires, the transmitted power, and the terminal velocity desired:

$$\frac{D}{d} = \frac{2.44 \pi^2}{32} \frac{\epsilon_q c \rho b^2 v_t^2}{\epsilon_p \epsilon_h P_t} \quad (27)$$

In actuality, the propulsion efficiency ϵ_p is a function of the wavelength and the size of the mesh through the reflectance efficiency, ϵ_r . But parametric studies of the possible variations of the propulsive efficiency ϵ_p with wire size and spacing have shown that the combination of the two efficiency factors $\epsilon_p \epsilon_h$ is roughly a constant with the value 0.04.

REFLECTANCE OF A WIRE MESH

The reflectance of a wire mesh for microwaves has received some study since a wire mesh makes a good ground plane for an antenna. The complete theory for arbitrary relative orientation and polarization is complicated, but does seem to agree with experiment.¹ The reflectance efficiency ϵ_r of a perfectly conducting square bonded wire mesh at normal incidence is a function of a mesh parameter K that not only depends upon the ratio of the mesh spacing to the microwave wavelength h/λ , but also logarithmically on the ratio of the mesh spacing to the wire diameter h/b :

$$K = \frac{2h}{\lambda} \ln(h/\pi b) . \quad (28)$$

The reflectance as a function of the mesh parameter is shown in Figure 2, which is derived from Figure 4(a)1 of Astrakhan.¹

The reflectance of the mesh also depends upon the electrical conductivity of the wires.¹ Aluminum has a room-temperature resistivity of 28 nohm-m. An aluminum wire one micron in diameter and one centimeter long will have a resistance of 360 ohms. This is almost perfectly matched to the free space impedance of 377 ohms, which would make the wire an absorber rather than a reflector. Fortunately, Starwisp will be bathed in the 2.7 K temperature of deep space and hence will be quite cold. The resistivity of pure aluminum, like most metals, drops rapidly with temperature.² At 40 K, for example, the resistivity is down to 1% of the room temperature value and is decreasing as

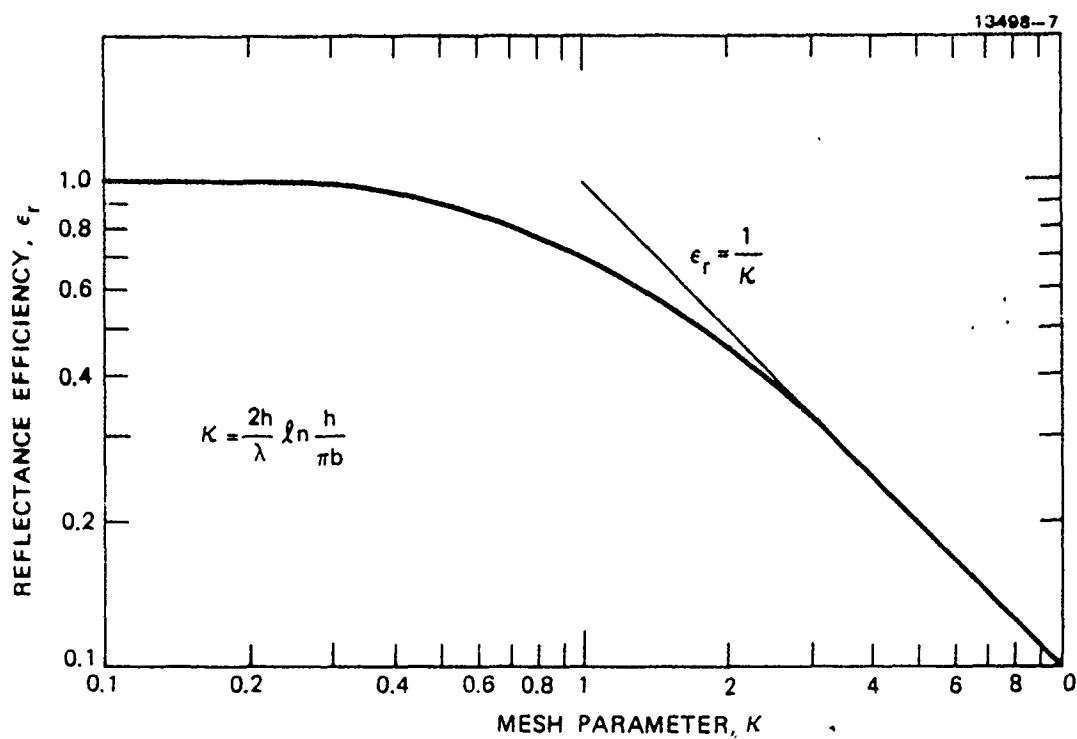


Figure 2. Mesh reflectance vs. wire size and spacing

the fifth power of the absolute temperature. Because of the high conductivity at low temperatures, we will assume that the effect of wire resistance on the microwave reflectance can be neglected, even for submicron wires. This assumption must be re-evaluated in any detailed engineering study.

INFORMATION RETURN FROM THE STARWISP PROBE

The Starwisp interstellar probe consists of more than fine aluminum wire. At each intersection of the wires there is a tiny microcircuit that controls the currents and voltages across the intersection. The microcircuits can assist in adjusting the microwave impedance at each intersection to maximize the reflected power during the acceleration period and to keep the sail centered about the main microwave beam. Later, on arrival at the target star system, the microcircuits can be rearranged to select certain pairs of wires to act as a good retroresponder antenna to an interrogating microwave signal beamed from the solar system. The microcircuits would be bigger than a wavelength of light in at least one dimension so they could be used to provide directional sensitivity to photo, IR, and UV detectors built into them, yet would be small in the other dimensions to reduce weight.

For a sail with a diameter d and a mesh spacing of h , the number of mesh intersections is approximately

$$n = \frac{\pi d^2}{4 h^2} , \quad (29)$$

which for typical mesh spacings of millimeters to centimeters results in the order of 10^{11} intersections per square kilometer. If each intersection contains a microcircuit chip 5 microns square by a half-micron thick with the density of silicon carbide (3200 kg/m^3), then the mass of each chip would be about $4 \times 10^{-14} \text{ kg}$.

As the Starwisp probe approaches a stellar system, the microwave beam will be turned on to flood the stellar system with microwave energy. At the distance s_* of the stellar system, the microwave beam from the transmitter lens with a diameter D will have spread out until the beam has the diameter,

$$B_* = 2.44 s_* \lambda/D \quad . \quad (30)$$

The power collected by the sail of diameter d is then proportional to the ratio of the area of the sail to the area of the beam, the transmitter efficiencies, and the transmitted power:

$$\frac{P_*}{B_*^2} = \frac{d^2}{B_*^2} \epsilon_b \epsilon_f P_t \quad . \quad (31)$$

The microcircuits at each intersection of the Starwisp mesh will collect that energy using the wires in the mesh as microwave antennas. In the process, each circuit will phase-lock its internal clock to the microwave phase it is receiving. In this manner the circuits can determine their relative position on the phase front of the microwave beam and compensate for any variation in position of their portion of the sail. Working in coordination, the circuits will analyze the light, IR, and UV signals each is receiving through its detectors. The detectors will be designed so that each has a limited field of view, with different microcircuits having detectors that look in different directions. By using the known background stars as reference point sources in a form of speckle interferometry, the microcircuits can unscramble the responses from the individual detectors to produce an image. That image will be inserted as modulation on a return microwave beam that is sent back to earth in the same direction as the incident beam by the microcircuits using the wires in the mesh as a phased array antenna.

The Starwisp probe, acting as a phased array antenna with a diameter d , will produce a beam back at the earth with a diameter B_e of

$$B_e = 2.44 s_* \lambda / d . \quad (32)$$

If we assume a collection-computation-retrodirection power efficiency of the sail of ϵ_c (≈ 0.2), then the amount of power received back at earth P_e through the large transmitter lens with D is

$$P_e = \frac{D^2}{B_e^2} \epsilon_c P_a . \quad (33)$$

Shannon has shown³ that the amount of energy needed to transmit a bit of information when limited by thermal noise of temperature T is

$$E = kT \ln 2 = 0.69 kT , \quad (34)$$

where $k = 1.38 \times 10^{-16}$ J/K is Boltzmann's constant. If we assume a sky temperature of $T_s = 2.7$ K, then the minimum amount of energy E_i needed to transmit a bit of information is

$$E_i = 0.69 kT_s = 2.6 \times 10^{-16} \text{ J/bit} . \quad (35)$$

If we assume that to provide adequate signal-to-noise ratio we would require a signal energy that is a factor of $1/\epsilon_i$ (≈ 10) times this minimum energy, then the received power P_e at earth will be able to carry a bit rate of

$$\dot{N} = \frac{\epsilon_i P_e}{E_i} . \quad (36)$$

A high resolution picture (1000 by 1000 pixels) with a good gray scale (256 shades of gray or 8 bits per pixel) requires N_p bits per picture (~ 8 million bits). Thus, the time T_p it takes to transmit one picture is

$$T_p = N_p / \dot{N} \quad . \quad (37)$$

INTERSTELLAR MISSIONS

Now that we have the basic equations for a Starwisp probe mission, let us look at a couple of examples. In the first example we will assume that the amount of microwave power available will be limited to that from a typical solar power satellite. This means that the weight of the sail and the terminal velocity must be kept low, which results in a long mission and minimal data return. Also, the diameter of the transmitter lens needed begins to boggle the imagination (although the mass is not that large for the size of the object). In the second example we assume that we have the microwave power needed to do fast missions with good data return to more star systems than just the nearest ones. In this case, the size and mass of the sail and lens are more reasonable and the mission times are more reasonable. The only thing that begins to boggle the imagination is the amount of microwave power needed.

POWER-LIMITED MISSION TO ALPHA CENTAURI

We will want to transport a Starwisp probe over the 4.3 lightyears to the nearest star system, Alpha Centauri, and get the information back well within the active lifetime of the generation that sent it. To accomplish this, we will assume that the Starwisp probe will be accelerated to one-fifth the speed of light ($v_t = 6 \times 10^7 \text{ m/sec}$). At this speed Starwisp will cross the gulf to the nearest stars in 21.5 years and the information will return to the earth 25.8 years after launch.

The plans for the first solar power satellite may seem grand to those that plan them, but they are marginal for an interstellar probe. Starwisp would prefer more power at longer wavelength, but it will make do with a solar satellite design that produces a transmitted power of $P_t = 10$ GW at a wavelength of $\lambda = 3$ cm (X-band). The Starwisp sail will be a square mesh with a geometry factor of $\epsilon_g = 0.707$ made of aluminum wire with a density of $\rho = 2700$ kg/m³, a diameter of $b = 0.1$ micron, and mesh spacing of $h = 0.3$ cm ($\epsilon_h = 0.1$). This gives a mesh parameter:

$$K = \frac{2h}{\lambda} \ln(h/\pi b) = 1.83 \quad (28a)$$

Looking up this value in Figure 2, we find that the reflectance of the sail is $\epsilon_r = 0.50$. If we estimate the Fresnel lens efficiency to be $\epsilon_f = 0.80$ and the beam efficiency to be $\epsilon_b = 0.84$, then the "propulsion" efficiency of the microwaves on the sail is

$$\epsilon_p = \epsilon_f \epsilon_b \epsilon_r = 0.34 \quad . \quad (7a)$$

The ratio of the transmitter lens diameter to the sail diameter is then calculated to be

$$\frac{D}{d} = \frac{2.44\pi^2 \epsilon_g c \rho b^2 v_t^2}{32 \epsilon_p \epsilon_h P_t} = 50,000 \quad (27a)$$

If we choose the sail diameter to be $d = 1$ km, then the transmitter lens diameter needs to be 50,000 km or 4 times the diameter of the earth. Since half of the lens is empty and half is a sparse mesh with spacing larger than a microwave wavelength, the mass of the lens is estimated to be only 50,000 tons.

The mass of the Starwisp sail is easily calculated from Equation (25) and is only 16 grams of wire. For a sail with

diameter $d = 1$ km and a mesh spacing of 3 mm, the number of mesh intersections is about 10^{11} . The mass of the 10^{11} chips would be four grams, bringing the total weight of Starwisp up to 20 grams.

The initial acceleration of a sail of 20 grams driven by a microwave beam of 10 GW is quite high:

$$a_0 = \frac{2\epsilon_p P_t}{M c} = 1130 \text{ m/s} = 115 \text{ gees} , \quad (6a)$$

although the microwave flux level is reasonable:

$$F = \frac{P_i}{A} = 8.6 \text{ kW } (\approx 6 \text{ suns}) . \quad (38)$$

The constant acceleration period lasts until Starwisp exceeds the reach of the transmitter lens at the distance,

$$s_0 = \frac{D d}{2.44\lambda} = 6.8 \times 10^{11} \text{ m} = 4.5 \text{ AU} , \quad (8a)$$

in the time,

$$t_0 = (2s_0 a_0)^{1/2} = 35000 \text{ sec} = 10 \text{ hours} . \quad (10a)$$

After a week of acceleration at a slowly decreasing rate, Starwisp will have reached its maximum velocity of $c/5$ and left the solar system on its 270,000 AU journey to our nearest neighbors.

As Starwisp approaches Alpha Centauri at one-fifth the speed of light, it will travel from -30 AU to +30 AU on the other side (about the distance across the Pluto/Neptune orbits) in about 40 hours. During that time (as well as periodically during the mission for calibration and update) the transmitter system on the earth will have sent a beam of microwave power to interrogate the microcircuit transponders built into the Starwisp mesh. The microwave beam will also supply the power needed to operate the transponders.

The distance s_* to Alpha Centauri is

$$s_* = 4.3 \text{ lightyears} = 4.1 \times 10^{16} \text{ m} . \quad (36)$$

At this distance, the beam from the transmitter lens with lens diameter $D = 50,000 \text{ km}$ has spread out until the beam diameter B_* at Alpha Centauri is

$$B_* = 2.44 s_a \lambda / D = 6 \times 10^7 \text{ m} . \quad (30a)$$

The power P_* collected by the sail of diameter $d = 1 \text{ km}$ is then

$$P_* = \frac{d^2}{B_*^2} \epsilon_f \epsilon_b P_t = 2 \text{ W} . \quad (31a)$$

The Starwisp probe, acting as a phased array antenna with a diameter d will produce a beam back at the earth with a diameter B_e of

$$B_e = 2.44 s_a \lambda / d = 3 \times 10^{12} \text{ m} = 20 \text{ AU} . \quad (32a)$$

If we assume a collection-computation-retrodirection power efficiency of the sail, ϵ_c (≈ 0.2), then the amount of power received back at earth P_e through the large transmitter lens with diameter D is

$$P_e = \frac{D^2}{B_o^2} \epsilon_c P_* = 100 \text{ pW} . \quad (33a)$$

If we assume an information signal-to-noise efficiency of $\epsilon_i = 0.1$, then this amount of power will allow the transmission of

$$N = \frac{\epsilon_i P_o}{E_i} = 40,000 \text{ bits/sec} , \quad (36a)$$

or a high resolution picture every

$$T_p = N_p / N = 200 \text{ sec} = 3 \text{ min} . \quad (37a)$$

HIGH-POWER HIGH-SPEED MISSION TO EPSILON ERIDANI

Let us now look at a mission that is not limited by the amount of microwave power available. If we leave all the parameters the same as in the power limited mission, but increase the microwave power level to 10 TW and the terminal velocity to half the speed of light, then the ratio of the lens diameter to the sail diameter becomes

$$D/d = 300 . \quad (27b)$$

We can now choose a sail diameter of 30 km, which gives us a more realistic sail mass of 14 kg, including a number of kilograms of payload more sophisticated than small detectors. The diameter of the transmitter lens is now a more reasonable 9000 km, only three-quarters the diameter of the earth. The microwave flux on the sail and the sail acceleration will stay about the same, but with the new sail and lens dimensions, the constant acceleration period will last 18 hours and reach out to 23 AU.

With the higher terminal velocity of half the speed of light, we can consider missions to more distant stellar systems, such as Epsilon Eridani at 10.8 lightyears. The high speed Starwisp will reach Epsilon Eridani in 21 years, and the data will return after 32 years. At Epsilon Eridani, the higher transmitted power and the larger size of the sail gives the sensors and processors on the Starwisp 9 kW of power to use. This higher power level and the larger diameter of the sail acting as a phased transmitting array will allow the Starwisp to send back to earth a continuous series of high resolution color pictures at standard television frame rates during the flythrough of the Epsilon Eridani system.

ACKNOWLEDGMENT

This paper is the result of a serendipitous conversation with Freeman Dyson on the subject of interstellar transport. While discussing the idea of a perforated lightsail⁴ with holes smaller than the wavelength of light to decrease the mass without decreasing the reflectivity, Dyson reached into his files and pulled out some notes⁵ on an interstellar perforated sail pushed by microwaves. The Dyson maser-driven sail is an extreme version of the perforated lightsail, with the area of the holes very much larger than the area of the wires. Dyson had found that for a given amount of microwave power, the acceleration of the sail increased in direct proportion to the wavelength of the microwaves. By combining the Dyson maser-driven sail concept with some previous ideas on communicating over interstellar distances with thin wire mesh spacecraft carrying microcircuits,^{6,7} I was able to produce the Starwisp concept for a light-weight, high-speed interstellar probe capable of returning useful information from the nearest stars.

REFERENCES

1. M.I. Astrakhan, "Reflecting and screening properties of plane wire grids," *Radio Eng.* 23, 76-83 (1968). [It should be noted that Figures 2 and 3 of Astrakhan seem to be for mesh spacings of $\lambda/4$, and not $\lambda/2$ as stated in the text.]
2. J. Bardeen, "Electrical conductivity of metals," *J. Appl. Physics* 11, 88-111 (1940).
3. C.E. Shannon, "A Mathematical Theory of Communication," *Bell System Tech. J.* 27, No. 3, 379-423; No. 4, 623-656 (1948).
4. R.L. Forward, "Perforated microstructured lightsail," Patent Disclosure F-001, AF Contract F04611-83-C-0013, Edwards AFB, CA (1983).
5. F.J. Dyson, "Maser-driven sail," unpublished notes.
6. R.L. Forward, "Zero thrust velocity vector control for interstellar probes: Lorentz force navigation and circling," *AIAA J.* 2, 885-889 (1964) [last paragraph of conclusion section].
7. R.L. Forward, "A programme for interstellar exploration," *J. Brit. Interplanetary Soc.* 29, 611-632 (1976). [See also figure and caption on page 610.]